DEVELOPMENTAL SIGNALING AND ACUTE LUNG INJURY

By

YUJIE GUO

Bachelor of Science in Biosciences
University of Science and Technology of China
Hefei, Anhui, China
2006

Bachelor of Laws
Southwestern University of Science and Technology
Mianyang, Sichuan, China
2013

Submitted to the Faculty of the
Graduate College of the
Oklahoma State University
in partial fulfillment of
the requirements for
the Degree of
DOCTOR OF PHILISOPHY
May, 2014

DEVELOPMENTAL SIGNALING AND ACUTE

LUNG INJURY

Dissertation Approved:

Dr. Lin Liu

Dissertation Adviser

Dr. Jerry Malayer

Dr. Tom Oomens

Dr. Myron Hinsdale

Dr. Jeff Hadwiger

Name: Yujie Guo

Date of Degree: May, 2014

Title of Study: DEVELOPMENTAL SIGNALING AND ACUTE LUNG INJURY

Major Field: Veterinary Biomedical Sciences (Physiology)

Abstract:

The present study is initiated to explore the potential implication of developmental signaling in AEC I injury, acute inflammatory response, and host defense against pathogen invasion during the pathogenesis of ALI/ARDS.

We demonstrated that P2X7R induced AEC I death by suppressing Wnt/β-catenin signaling through activating GSK-3β and proteasome. On the other hand, Wn3a overrides the effect of P2X7R on inhibiting Wnt/β-catenin signaling to prevent the AEC I death and restricts the severity of ALI/ARDS. Our study on Wnt/β-catenin signaling and P2X7R-mediated purinergic signaling provides insights for future drug development and new therapeutic strategies to limit AEC I damage in ALI/ARDS patients.

Furthermore, we identified platelet-derived Dkk1 as the major Wnt antagonist, contributing to the depression of Wnt/β-catenin signaling during ALI/ARDS. Intratracheal administration of Wnt3a or neutralization of Dkk1 inhibited neutrophil influx into alveolar airspace of the injured lungs potentially through the attenuated ICAM-1/VCAM-1 mediated adhesion of inflammatory cells. We reported for the first time a role of Wnt/β-catenin signaling in modulating inflammatory response, and a functional communication between platelets and AEC during ALI/ARDS. Targeting Wnt/β-catenin signaling and this communication therefore represents a potential therapeutic strategy to reduce acute inflammation in ALI/ARDS patients.

Lastly, we discovered that Axin1, a scaffold protein, was degraded during influenza virus infection of mice. More importantly, we found that Axin1 boosted type I IFN response to influenza virus infection through the stimulation of JNK/c-Jun and Smad3 signaling. Axin1 also interacted with IFIT1/2/3, a viral RNA sensor complex. In addition, Axin1 specifically promoted the degradation of hnRNP M, a nucleoprotein required for efficient activity of influenza virus polymerases, and sequentially EZH2. Axin1 and its chemical stabilizer, XAV939, successfully reduced influenza virus and respiratory syncytial virus replication, and protected the mice from influenza virus infection. Thus, our study provides new mechanistic insights into the regulation of type I IFN response and presents a new potential therapeutics of targeting Axin1 against influenza virus infection and reducing the incidence of viral pneumonia.

TABLE OF CONTENTS

Chapter Page

LIST OF TABLES

Table Page

LIST OF FIGURES

Figure Page

Figure Page

LIST OF ABBREVIATIONS

5' ppp-dsRNA	5' triphosphate double stranded RNA
ABC	Activated β-catenin
AEC	Alveolar epithelial cells
AEC I	Type I alveolar epithelial cells
AEC II	Type II alveolar epithelial cells
ALI	Acute lung injury
AMC	7-amido-4-methylcoumarin
AMØ	Alveolar macrophage
ARDS	Acute respiratory distress syndrome
ATF2	Activating transcription factor 2
ATP	Adenosine triphosphate
Axin	Axis inhibition protein
BAL	Bronchoalveolar Lavage
Bcl-2	B-cell lymphoma 2
Bmp4	Bone morphogenetic protein 4
BzATP	2'(3')-*O*-(4-Benzoylbenzoyl)adenosine-5'-triphosphate
CCL2	Chemokine (C-C motif) ligand 2
CCL5	Chemokine (C-C motif) ligand 5
CCN	CCN family of extracellular matrix-associated signaling proteins
CCND1	G1/S-specific cyclin-D1
CCNE1	G1/S-specific cyclin-E1
CD40L	CD40 ligand
CD62P	P-Selectin
CFU	Colony-forming units
Con_CM	Control conditional medium
COPD	Chronic obstructive pulmonary disease
COX-2	Cyclooxygenase 2
DAPI	4',6-diamidino-2-phenylindole
Dkk1	Dickkopf-1
DMEM	Dulbecco's Modified Eagle's Medium
DMSO	Dimethyl sulfoxide
dpi	Days post infection
E.coli	Escherichia coli
EDTA	Ethylenediaminetetraacetic acid
ELISA	The enzyme-linked immunosorbent assay

EMEM	Eagle's Minimum Essential Medium
EZH2	Histone-lysine N-methyltransferase
FACS	Fluorescence-activated cell sorting
FBS	Fetal bovine serum
FIO_2	Fraction of inspired oxygen
GFP	Green fluorescent protein
GSK-3β	Glycogen synthase kinase-3β
HA	Hemagglutinin
HEK293	Human Embryonic Kidney 293 cells
HIPK2	Homeodomain-interacting protein kinase 2
HIV	Human immunodeficiency virus
hnRNP M	Heterogeneous nuclear ribonucleoprotein M
HRP	Horseradish peroxidase
IACUC	Institutional animal care and use committee
ICAM-1	Intercellular Adhesion Molecule 1
IFIT	Interferon -induced protein with tetratricopeptide repeats 1
IFN	Interferon
IFNAR1/2	Interferon-α/β receptor 1/2
IGF-1	Insulin-like growth factor 1
IgG	Immunoglobulin G
IL-18	Interleukin-18
IL1RN	Interleukin 1 receptor antagonist
IL-1β	Interleukin-1 beta
IL-6	Interleukin-6
IL-8	Interleukin-8
IPF	Idiopathic pulmonary fibrosis
IRF3/7	Interferon regulatory factor 3/7
ISGs	Interferon Stimulated Genes
ISRE	Interferon-sensitive response element
JAMs	Junctional adhesion molecule
JNK	c-Jun N-terminal kinases
KC	Chemokine (C-X-C motif) ligand 1
KGF	Keratinocyte growth factor
KRM1/2	Kremen1/2
LARU	Laboratory animal rescource unit
LDH	Lactate dehydrogenase
LEF	Lymphoid enhancer factor
LIX	Chemokine (C-X-C motif) ligand 5
LPS	lipopolysaccharide
LRP5/6	Low-density lipoprotein receptor-related protein 5/6

LRRFIP1	Leucine-rich repeat flightless-interacting protein 1
MAPK	Mitogen-activated protein kinase
MCP-1	Monocyte chemoattractant protein-1
MDA5	Melanoma Differentiation-Associated protein 5
MDCK	Madin-Darby canine kidney
MIP-2	Macrophage inflammatory protein 2
M-MLV	Moloney murine leukemia virus
MP	Matrix protein
MPO	Myeloperoxidase
mRNA	Messenger RNA
MSC	Mesenchymal stem cell
MV	Mechanical Ventilation
Mx	Myxovirus resistance
NFAT	Nuclear factor of activated T-cells
NFκB	Nuclear factor kappa-light-chain-enhancer of activated B cells
NOD	Nucleotide-binding oligomerization domain
nonO/p54(nrb)	Non-POU domain-containing octamer-binding protein
NOS2	Nitric oxide synthase 2
NP	Nucleoprotein
NS1	Non-structural protein 1
OAS1	2',5'-oligoadenylate synthetase 1
oATP	Oxidized ATP
P2X7R	P2X purinoceptor 7
PAGE	Polyacrylamide gel electrophoresis
PaO_2	Partial pressure of oxygen in arterial blood
PARylation	Poly(ADP-ribosyl)ation
PBS	Phosphate buffered saline
PCNA	Proliferating cell nuclear antigen
PEEP	Positive end-expiratory pressure
PF4	Platelet factor 4
PFA	Polyunsaturated Fatty Acid
pfu	Plaque-forming unit
PKR	Protein kinase R
PR	Platelet releasate
PRP	Platelets-rich plasma
PRRs	Pattern recognition receptors
RANTES	Regulated on activation, normal T cell expressed and secreted
RIG-1	Retinoic acid-inducible gene 1
ROS	Reactive oxygen species

RSV	Respiratory Syncytial Virus
SDS	Sodium Dodecyl Sulfate
Ser	Serine
SFPQ	Splicing factor, proline- and glutamine-rich
sFRP1	Secreted frizzled-related protein 1
Smad3	Mothers against decapentaplegic homolog 3
SPC	Surfactant protein C
STAT1/2	Signal Transducers and Activators of Transcription 1/2
SUMO	Small Ubiquitin-like Modifier
T1α	Podoplanin
TBS	Tris-buffered saline
TC1	Uncharacterized protein C8orf4
TCF	T-cell factor
$TCID_{50}$	Median tissue culture infective dose
TFs	Transcription factors
TGF-β	Transforming growth factor beta
TLR-4	Toll-like receptor 4
TMB	Tetramethylbenzidine
TNF-α	Tumor necrosis factor alpha
TNKS1/2	Tankyrase-1/2
TPCK	L-(tosylamido-2-phenyl) ethyl chloromethyl ketone
TRAIL	TNF-related apoptosis-inducing ligand
Tyr	Tyrosine
VCAM-1	Vascular cell adhesion protein 1
Wnt3a_CM	Wnt3a conditional medium
Wnt5a_CM	Wnt5a conditional medium

CHAPTER I

INTRODUCTION

1.1 Acute lung injury

Acute lung injury (ALI) and its severe form, acute respiratory distress syndrome (ARDS), are life-threatening diseases caused by a variety of reasons including sepsis, trauma, drug overdose, multiple transfusions, and viral or bacterial pneumonia (1). ALI/ARDS is characterized by damage the of capillary-alveolar interface, initiation of proinflammatory cytokine and chemokine storm, and infiltration of inflammatory cells (2). It is clearly recognized as a syndrome of acute respiratory failure and acute inflammation with up to 40% mortality in human patients (3). Clinically, ALI/ARDS is defined as acute respiratory distress with severe hypoxemia ($PaO_2/FIO_2<300$ for ALI, and $PaO_2/FIO_2<200$ for ARDS) and diffuse alveolar infiltrates on chest X-ray (4).

The alveolar epithelium plays prominent roles in the pathogenesis of ALI by serving as a primary barrier of defense against various insults and regulating immune response (5). It consists of two different types of cells: the terminally differentiated squamous alveolar epithelial type I cells (AEC I), which covers around 95% of the total lung surface area, and the surfactant producing cuboidal alveolar epithelial type II cells (AEC II), which participates in host defense (6). AEC I are more sensitive to injury than other lung cells (7). Damage of AEC I is observed in

all forms of ALI, leading to the deficiency of gas exchange and disruption of fluid clearance. The molecular mechanisms of AEC I death during ALI have been studied to some extent involving the regulation of several signaling pathways, such as TGF-β pathway, NFκB pathway, and Fas/FasL-mediated pathway (8). It will be significantly beneficial if novel signaling pathways regulating AEC I death can be identified.

The neutrophil is an essential component of the innate immune system and vital to our lives. However, inflammatory damage caused by activated neutrophils also contributes to the progression of ALI/ARDS (9). Activation and transmigration of neutrophils through endothelium, interstitium, and epithelium is the central event in the development of ALI/ARDS. Activated neutrophils release cytotoxic compounds (proteolytic enzymes, cationic peptides, and ROS) that can injure host cells (10). The depletion of neutrophils is protective in some animal models of ALI (11-13). Lung edema and endothelial and epithelial cells injuries accompanied by infiltration of neutrophils are broadly accepted as the classic paradigms in this acute lung inflammation scenario (14).

Adhesion molecules such as inter-cellular adhesion molecule 1 (ICAM-1 or CD54) and vascular adhesion molecules (VCAM-1 or CD106) are involved in the sequestration, adhesion, and subsequent transendothelial/epithelial migration of neutrophils mediated by β2 (CD18/CD11) and α4β1 (CD49d/CD29), α4β7 (CD49d/CD103) integrins during ALI (10). What is not clear is the relative contribution of selectins (P, E, and L-selectins) and adhesion molecules (VCAM-1, ICAM-1, and JAMs) to the whole infiltration process (capture, rolling, adhesion, and transmigration) of inflammatory cells during ALI (9). There is evidence that up-regulation of ICAM-1 and VCAM-1 in pulmonary vascular endothelium promotes neutrophil sequestration and mediates strong adhesion of neutrophils to endothelial cells (9). ICAM-1 and VCAM-1 are also expressed in AEC and mediates the adhesion of neutrophils and macrophages, and facilitates the transepithelial migration of monocytes (15-17). Up-regulation of both ICAM-1 and VCAM-1

occurs as a result of increased gene transcription in response to inflammatory cytokines such as TNF-α and IL-1β (18). The promoter regions of ICAM-1 and VCAM-1 genes contain several NFκB (P50/P60) binding sites. Mutation of either of these elements abolishes its cytokine responsiveness (18). Considering the critical role of ICAM-1 and VCAM-1 in the progression of acute lung inflammation, it is important to perform more detailed studies on the mechanisms which control their expression.

Platelets are the central mediators in hemostasis of circulatory system and also contribute to acute pulmonary inflammation by regulating inflammatory response of endothelial cells and activation of leukocytes (19-21). There is emerging evidence that acute pulmonary inflammation is associated with the activation of aggressive platelets in the blood and sequestration in pulmonary vascular beds (22,23). Platelet activation following the onset of thrombocytopenia leads to the release of cytokines (IL-1β and CD40L), chemokines (PF4, CCL5 and RANTES), and other soluble factors (PFA and Dkk1), and aggregation of platelets with neutrophils or monocytes via cell surface P-selectin (CD62P) (22,24,25). Platelets also interact with endothelial cells, resulting in the increase of vascular permeability, and promoting the release of proinflammatory cytokines (IL-6) or chemokines (IL-8) (26). Blocking of platelet-leukocyte interaction (27), platelet depletion (28), and anti-platelets therapy (19,29) have all been proved to be protective in the animal model of ALI/ARDS. Platelet components are found in the bronchoalveolar fluid (BAL) in ALI (30). However, it is not clear whether platelets can directly affect the functions of alveolar epithelium (22). Novel functions of platelets in regulating ALI/ARDS need to be explored.

1.2 Purinergic P2X7 receptor (P2X7R) and lung diseases

The purinergic receptor P2X7R, a transmembrane ligand-gated ion channel receptor activated by extracellular ATP, is widely expressed in a variety of cells including endothelial

cells, epithelial cells, fibroblasts, monocytes, lymphocytes and dendritic cells (31). It shares, in common with other P2X receptors, the ability to form nonselective cation channels. On the other hand, the unusually long C terminus of P2X7R seems to allow it couple to a spectrum of downstream targets responsible for its cytotoxic properties (32).

Stimulation of P2X7R with low concentrations of ATP opens a membrane channel within millisecond, and causes the influx of small cations (Na^+, $Ca^{2+,}$ and K^+) (33). However, high concentrations of ATP or sustained stimulations lead to membrane blebbing and apoptotic or necrotic cell death in P2X7R-expressing cells including epithelial cells, endothelial cells, stem cells and macrophages (34-37). Extracellular ATP-induced cell death has been observed in colitis (38), spinal cord injury (39), and glomerulonephritis (40). However, the contribution of ATP and its receptors to AEC I death during ALI/ARDS is not well understood.

P2X7R is required for mature IL-1β and IL-18 production and release from immune cells because of its essential role in inflammasome-mediated cytokine signaling cascade and caspase activation (32,41). In the lung, P2X7R deficient mice have a protective phenotype in LPS-induced ALI (42) and bleomycin-induced lung fibrosis (43) with attenuated inflammation. P2X7R is also involved in the pathogenesis of several other chronic lung inflammatory diseases such as asthma and emphysema, in which it functions as an inflammatory mediator (44,45). P2X7R has previously been found to be expressed specifically in AEC I and regulating lung surfactant secretion in a paracrine manner (46,47). Together with its ability to modulate pulmonary inflammatory response, P2X7R could act as a potential regulator of AEC I cell death in response to pathological insults.

1.3 Wnt/β-catenin signaling and lung diseases

Wnt is a family of secreted glycoproteins and plays an important role in development, tissue regeneration, and cell fate determination (48). In the absence of Wnt ligands, the

intracellular β-catenin is phosphorylated by glycogen synthase kinase-3β (GSK-3β) and degraded in proteasome. The binding of Wnt ligands with frizzled receptors leads to the disruption of GSK-3β-mediated phosphorylation of β-catenin and thus attenuation of proteasome-mediated degradation. The stabilized β-catenin then translocates into the nucleus, where it binds to T-cell factor (TCF)/Lymphoid enhancer factor (LEF) transcription factor to increase the transcription of its downstream genes (49).

Wnt/β-catenin signaling is instrumental in orchestrating proper lung development in embryos (50) and regeneration of lung epithelium after injury in adults (51-54). Activating Wnt/β-catenin signaling inhibits apoptosis induced by activating the intrinsic or mitochondrial pathway, such as starvation or hydrogen peroxide, or the extracellular or receptor pathway, such as TRAIL and TNFα (55). Blocking the Wnt/β-catenin signaling prevents cell proliferation and results in apoptosis or necrosis (56,57). In the lung, activation of Wnt/β-catenin signaling promotes AEC II survival (52) while depletion of β-catenin in AEC results in an increased AEC death in bleomycin-induced lung injury model (58). β-catenin-regulated CCN extracellular matrix-associated signaling proteins also promote epithelial repair after inflammatory lung injury (59). The direct effect of Wnt/β- signaling in AEC I injury during ALI is unknown.

In inflammatory lung diseases, depression of Wnt/β-catenin signaling is observed in COPD (60,61) and asthma patients (62,63), and contributes to their dysfunctional epithelial repair. Wnt/β-catenin signaling is also inhibited in mechanical ventilation (MV)-insulted and S. pneumoniae-infected lungs (64,65). On the other hand, up-regulation of Wnt/β-catenin signaling has also been demonstrated in resolution of acute lung injury and alveolar epithelium repair following acute injury (66,67). Interestingly, transepithelial migration of neutrophils also activates Wnt/β-catenin signaling in AEC II and accelerates the process of repair (54). All of these studies reveal a dynamic, complicated, and subtle response of Wnt/β-catenin signaling in inflammatory lung diseases. Considering a great number of Wnt/β-catenin signaling agonists and

antagonists are in the pre-clinical development stage (68), characterizing the role of Wnt/β-catenin signaling will open a new window to amplify our potential to control these diseases.

It has been reported that Wnt/β-catenin signaling can inhibit the endothelial and epithelial inflammatory response by suppressing proinflammatory cytokines (62,69), chemokines (70,71), adhesion molecule (70,72), and other inflammatory regulators (70,73) potentially through interacting with NFκB signaling under different inflammatory conditions (71,73,74). Although the importance of Wnt/β-catenin signaling in regulating inflammatory response is emerging, limited evidence is available for its implication in acute lung inflammation. Recent studies reveal essential roles of Wnt/β-catenin signaling in the pathogenesis of several adult lung diseases including pulmonary fibrosis (58,75), asthma (76), and chronic obstructive pulmonary disease (COPD) (77,78). Wnt antagonist sFRP1 was recently shown to be largely responsible for the inhibition of Wnt/β-catenin signaling in experimental emphysema (79). Considering the reduced capacity of BAL from ARDS patients to activate Wnt/β-catenin signaling in fibroblast [118], it is particularly important to identify the potential elevation of Wnt antagonists and investigate the emerging importance of Wnt/β-catenin signaling in progression of acute lung inflammation.

Recent evidence also points to important roles of Wnt antagonist Dkk1 in several inflammatory conditions such as atherosclerosis, arthritis, and osteoporosis by regulating inflammatory response of endothelial cells and homeostasis of epithelial cells (25,80,81). As a potential therapeutic target to limit the damage of inflammation, Dkk1 is also developed as a serum biomarker of inflammatory diseases and cancer patients (82-84). Neutralization therapy targeting Dkk1 has also shed light on osteolytic disease patients (81,85). Interestingly, Dkk1, as an important product of activated platelets (25), also accumulates in alveolar epithelium and BAL of idiopathic pulmonary fibrosis (IPF), in which Wnt/β-catenin signaling is aberrantly activated and modulates cell proliferation (86). However, the role of Dkk1 in development of ALI has not been studied.

1.4 Influenza virus and Type I IFN response

The mortality rate of pneumonia and influenza virus infection continually declined through the 20th century because of the improvement of anteceded medical strategies for prevention of lung infections (87,88). However, acute pulmonary infection remains a substantial concern because acute lower respiratory infections still cause the most deaths and are the largest economic burden among all infectious diseases worldwide (87-89). Unlike respiratory syncytial virus (RSV), which is the major cause of respiratory illness (bronchiolitis or pneumonia) in young children (90) and occasionally in adults (118), influenza virus has the ability to span on patients of all ages even adults (91).

The influenza virus belongs to the *Orthomyxoviriade* family and is classified into three types: A, B, and C according to their internal protein sequences (92). In the U.S., up to 20% of the population gets the flu each year, resulting in more than 200,000 hospitalizations, 36,000 deaths, and $87 billion in healthcare costs from seasonal flu-related complications (89). There is a risk that new strains of influenza can emerge and spread globally, causing pandemic-scale illness (14). The current treatment for influenza virus infection is to use antiviral drugs that target the viral proteins (neuraminidase and M2 channel), which only works if no new strains of influenza virus emerge (93). However, influenza viral proteins change due to a high mutation rate; As a result the virus can become resistant to these drugs. Thus, there is a critical need to develop improved anti-influenza medicines that are effective regardless of virus changes.

Interferon (IFN) was discovered in 1957 as an agent that can inhibit (interfere) the replication of influenza virus (94). The IFN family of cytokines is now recognized as the most potent vertebrate-derived signals for mobilizing antimicrobial effector functions against intracellular pathogens (95). Type I IFN (IFNβ, 12 IFNαs, IFNδ, IFNε, IFNκ, IFNo, and IFNτ), best known for their antiviral properties, mediate the induction of both innate immune response

and subsequent adaptive immunity to virus infection (96). It is widely accepted that viral attachment and viral dsRNA intermediates accumulating during virus replication are the primary mediators triggering IFNs production, which ultimately results in expression of thousands of IFN-stimulated genes (ISGs) (PKR, Mx proteins, OAS1, and etc.) and interrupts virus life cycle (97).

In the early phase of infection, Toll-like receptors, cytosolic RIG-1-like receptors (RIG-1 and MDA5), NOD-like receptors and C-type lectin receptors are major viral sensors involved in innate recognition of influenza virus (98). Recently, the novel IFN-regulated viral RNA sensor, interferon-induced protein with tetratricopeptide repeats 1 (IFIT1) was also implicated in antiviral activity (99). Activation of type I IFN expression by these pattern recognition receptors (PRRs) is highly controlled by several transcription factors (TFs) including *c-Jun*/ATF2 (AP1), interferon regulatory factor 3/7 (IRF3/7), and p50/p65 (NFκB) (100). In the later phase of infection, secreted type I IFN signal stimulates type I IFN receptor (IFNAR1/2) in both autocrine and paracrine fashion, and finally turns on cellular antiviral status (101).

Influenza virus is very effective at taking advantage of host cellular signaling to support its viral replication. However, this dependency can also be utilized to develop novel antiviral approaches by targeting these host factors (102,103). Genome-wide screening has been utilized to identify hundreds of host factors involved in influenza virus replication (104-107). Proteomics approaches and yeast two-hybrid analyses have also been used to identify numerous host molecules that interact with influenza virus components, especially involvement of non-structural protein 1 (NS1)-associated proteins in immune response (108-110) and Wnt/β-catenin signaling components (111). These functional genomics and proteomics have provided broad views of host response in virus-host interactions. However, they have been less effective in pinpointing the specific host factors in antiviral response.

Axin, which was identified from analysis of the mouse-Fused locus, is a negative regulator of Axis formation in the development of mouse embryos (112). Axin protein is present in two isoform (Axin1 and Axin2), and acts as an architectural platform for the degradation of the oncogenic protein β-catenin (113,114). Axin1 has, in fact, emerged as a multidomain scaffolding protein for many other signaling pathways, including C-Jun-NH2-kinase (JNK) mitogen-activated protein kinase (MAPK) signaling, p53 signaling, and transformation growth factor β (TGF-β) signaling (115). These intriguing roles of Axin1 in β-catenin-independent manner open the door to its function in multiple physiological and pathological processes. In the infectious diseases, Axin1 shows a preventive effect on bacterial Salmonella invasiveness and modulates inflammatory response during the infection (116). On the other hand, silencing of Axin1 up-regulates type I human immunodeficiency virus (HIV-1) gene expression and viral replication (117). However, there is no report on the involvement of Axin1 in the influenza virus infection and type I IFN response.

1.5 Specific aims and significances

In spite of the great strides made to understand the pathogenesis of ALI/ARDS, unacceptable morbidity and mortality remain, and formidable challenges persist. The treatment approach to ALI/ARDS is still relying on ventilatory and cardiovascular support because of the limited knowledge about the fundamental mechanisms that initiate and propagate the lung injury. Thus, the present study is designed to better understand the molecular mechanism behind AEC I injury, acute inflammatory response, and host defense against pathogen invasion during development of ALI/ARDS. To this end, we have laid down three specific objectives:

Specific Aim I: Investigate the roles of P2X7R and Wnt/β-catenin signaling in regulating AEC I death during ALI/ARDS

Specific Aim II: Explore the function of platelet-derived Wnt antagonist Dkk1 in ICAM-1/VCAM-1 mediated neutrophilic acute lung inflammation

Specific Aim III: Study the potential antiviral function of Axin1 as a type I IFN stimulator against influenza virus infection

Significance: A novel functional crosstalk between P2X7R-mediated purinergic signaling and Wnt/β-catenin signaling in regulating AEC I injury during ALI/ARDS is identified. Important roles of Wnt/β-catenin signaling in mitigating acute inflammatory response, and a Dkk1-mediated communication between platelets and AEC during ALI/ARDS are reported for the first time as well. Targeting Wnt/β-catenin signaling and this paracrine communication therefore represent a potential therapeutic strategy to limit the damage of ALI/ARDS. Our study also provides new mechanistic insights into the regulation of type I IFN response and presents a potential new broad-spectrum antiviral therapy by targeting Axin1 for the first time.

1.6 Reference

1. Matthay, M. A. and Zemans, R. L. (2011) *The Acute Respiratory Distress Syndrome: Pathogenesis and Treatment*, ANNUAL REVIEWS, PALO ALTO
2. Bhargava, M. and Wendt, C. H. (2012) *Translational Research* **159,** 205-217
3. Martin, T. R. and Matute-Bello, G. (2011) *Crit. Care Clin.* **27,** 735-752
4. Matthay, M. A. and Zimmerman, G. A. (2005) *Am. J. Respir. Cell Mol. Biol.* **33,** 319-327
5. Chen, J. W., Chen, Z. M., Chintagari, N. R., Bhaskaran, M., Jin, N. L., Narasaraju, T., and Liu, L. (2006) *J. Physiol.* **572,** 625-638
6. Manzer, R., Wang, J. R., Nishina, K., McConville, G., and Mason, R. J. (2006) *American Journal of Respiratory Cell and Molecular Biology* **34,** 158-166
7. Dobbs, L. G., Johnson, M. D., Vanderbilt, J., Allen, L., and Gonzalez, R. (2010) *Cell. Physiol. Biochem.* **25,** 55-62
8. Tang, P. S., Mura, M., Seth, R., and Liu, M. (2008) *Am. J. Respir. Cell Mol. Biol.* **294,** L632-L641
9. Grommes, J. and Soehnlein, O. (2011) *Molecular Medicine* **17,** 293-307

10. Segel, G. B., Halterman, M. W., and Lichtman, M. A. (2011) *Journal of Leukocyte Biology* **89,** 359-372

11. Grommes, J., Vijayan, S., Drechsler, M., Hartwig, H., Morgelin, M., Dembinski, R., Jacobs, M., Koeppel, T. A., Binnebosel, M., Weber, C., and Soehnlein, O. (2012) *Plos One* **7,**

12. Narasaraju, T., Yang, E., Samy, R. P., Ng, H. H., Poh, W. P., Liew, A. A., Phoon, M. C., van Rooijen, N., and Chow, V. T. (2011) *American Journal of Pathology* **179,** 199-210

13. Tate, M. D., Deng, Y. M., Jones, J. E., Anderson, G. P., Brooks, A. G., and Reading, P. C. (2009) *Journal of Immunology* **183,** 7441-7450

14. Short, K. R., Kroeze, E. J. B. V., Fouchier, R. A. M., and Kuiken, T. (2014) *Lancet Infectious Diseases* **14,** 57-69

15. Beck-Schimmer, B., Madjdpour, C., Kneller, S., Ziegler, U., Pasch, T., Wuthrich, R. P., Ward, P. A., and Schimmer, R. C. (2002) *European Respiratory Journal* **19,** 1142-1150

16. Herold, S., von Wulffen, W., Steinmueller, M., Pleschka, S., Kuziel, W. A., Mack, M., Srivastava, M., Seeger, W., Maus, U. A., and Lohmeyer, J. (2006) *Journal of Immunology* **177,** 1817-1824

17. Rosseau, S., Selhorst, J., Wiechmann, K., Leissner, K., Maus, U. R., Mayer, K., Grimminger, F., Seeger, W., and Lohmeyer, J. (2000) *Journal of Immunology* **164,** 427-435

18. Collins, T., Read, M. A., Neish, A. S., Whitley, M. Z., Thanos, D., and Maniatis, T. (1995) *Faseb Journal* **9,** 899-909

19. Caudrillier, A. and Looney, M. R. (2012) *Current Pharmaceutical Design* **18,** 3260-3266

20. Kornerup, K. N., Salmon, G. P., Pitchford, S. C., Liu, W. L., and Page, C. P. (2010) *Journal of Applied Physiology* **109,** 758-767

21. Weyrich, A. S. and Zimmerman, G. A. (2012) *Annu. Rev. Physiol.*

22. Bozza, F. A., Shah, A. M., Weyrich, A. S., and Zimmerman, G. A. (2009) *American Journal of Respiratory Cell and Molecular Biology* **40,** 123-134

23. Zarbock, A. and Ley, K. (2009) *Frontiers in Bioscience* **14,** 150-158

24. Danese, S., Katz, J. A., Saibeni, S., Papa, A., Gasbarrini, A., Vecchi, M., and Fiocchi, C. (2003) *Gut* **52,** 1435-1441

25. Ueland, T., Otterdal, K., Lekva, T., Halvorsen, B., Gabrielsen, A., Sandberg, W. J., Paulsson-Berne, G., Pedersen, T. M., Folkersen, L., Gullestad, L., Oie, E., Hansson, G. K., and Aukrust, P. (2009) *Arteriosclerosis Thrombosis and Vascular Biology* **29,** 1228-1234

26. Dixon, J. T., Gozal, E., and Roberts, A. M. (2012) *Archives of Physiology and Biochemistry* **118,** 72-82

27. Zarbock, A., Singbartl, K., and Ley, K. (2006) *Journal of Clinical Investigation* **116,** 3211-3219

28. Looney, M. R., Nguyen, J. X., Hu, Y. M., Van Ziffle, J. A., Lowell, C. A., and Matthay, M. A. (2009) *Journal of Clinical Investigation* **119,** 3450-3461

29. Erlich, J. M., Talmor, D. S., Cartin-Ceba, R., Gajic, O., and Kor, D. J. (2011) *Chest* **139,** 289-295

30. Pittet, J. F., Mackersie, R. C., Martin, T. R., and Matthay, M. A. (1997) *American Journal of Respiratory and Critical Care Medicine* **155,** 1187-1205

31. Khakh, B. S. and North, R. A. (2006) *Nature* **442,** 527-532

32. Ferrari, D., Pizzirani, C., Adinolfi, E., Lemoli, R. M., Curti, A., Idzko, M., Panther, E., and Di Virgilio, F. (2006) *J. Immunol.* **176,** 3877-3883

33. Ferrari, D., Los, M., Bauer, M. K. A., Vandenabeele, P., Wesselborg, S., and Schulze-Osthoff, K. (1999) *FEBS Lett.* **447,** 71-75

34. Ferrari, D., Chiozzi, P., Falzoni, S., DalSusino, M., Collo, G., Buell, G., and DiVirgilio, F. (1997) *Neuropharmacology* **36,** 1295-1301

35. Hanley, P. J., Kronlage, M., Kirschning, C., del Rey, A., Di Virgilio, F., Leipziger, J., Chessell, I. P., Sargin, S., Filippov, M. A., Lindemann, O., Mohr, S., Koenigs, V., Schillers, H., Baehler, M., and Schwab, A. (2012) *J. Biol. Chem.* **287,** 10650-10663

36. Kawano, A., Tsukimoto, M., Noguchi, T., Hotta, N., Harada, H., Takenouchi, T., Kitani, H., and Kojima, S. (2012) *Biochem. Biophys. Res. Commun.* **419,** 374-380

37. Lammas, D. A., Stober, C., Harvey, C. J., Kendrick, N., Panchalingam, S., and Kumararatne, D. S. (1997) *Immunity* **7,** 433-444

38. Gulbransen, B. D., Bashashati, M., Hirota, S. A., Gui, X., Roberts, J. A., MacDonald, J. A., Muruve, D. A., Mckay, D. M., Beck, P. L., Mawe, G. M., Thompson, R. J., and Sharkey, K. A. (2012) *Nat. Med.* **18,** 600-604

39. Wang, X. H., Arcuino, G., Takano, T., Lin, J., Peng, W. G., Wan, P. L., Li, P. J., Xu, Q. W., Liu, Q. S., Goldman, S. A., and Nedergaard, M. (2004) *Nat. Med.* **10,** 821-827

40. Taylor, S. R. J., Turner, C. M., Elliott, J. I., McDaid, J., Hewitt, R., Smith, J., Pickering, M. C., Whitehouse, D. L., Cook, H. T., Burnstock, G., Pusey, C. D., Unwin, R. J., and Tam, F. W. K. (2009) *J. Am. Soc. Nephrol.* **20,** 1275-1281

41. Ferrari, D., Chiozzi, P., Falzoni, S., DalSusino, M., Melchiorri, L., Baricordi, O. R., and DiVirgilio, F. (1997) *J. Immunol.* **159,** 1451-1458

42. Moncao-Ribeiro, L. C., Cagido, V. R., Lima-Murad, G., Santana, P. T., Riva, D. R., Borojevic, R., Zin, W. A., Cavalcante, M. C. M., Rica, I., Brando-Lima, A. C., Takiya, C. M., Faffe, D. S., and Coutinho-Silva, R. (2011) *Resp. Physiol. Neurobi.* **179,** 314-325

43. Riteau, N., Gasse, P., Fauconnier, L., Gombault, A., Couegnat, M., Fick, L., Kanellopoulos, J., Quesniaux, V. F. J., Marchand-Adam, S., Crestani, B., Ryffel, B., and Couillin, I. (2010) *Am. J. Respir. Crit. Care Med.* **182,** 774-783

44. Lucattelli, M., Cicko, S., Muller, T., Lommatzsch, M., De Cunto, G., Cardini, S., Sundas, W., Grimm, M., Zeiser, R., Durk, T., Zissel, G., Sorichter, S., Ferrari, D., Di Virgilio, F., Virchow, J. C., Lungarella, G., and Idzko, M. (2011) *Am. J. Respir. Cell Mol. Biol.* **44,** 423-429

45. Muller, T., Vieira, R. P., Grimm, M., Durk, T., Cicko, S., Zeiser, R., Jakob, T., Martin, S. F., Blumenthal, B., Sorichter, S., Ferrari, D., Di Virgillio, F., and Idzko, M. (2011) *Am. J. Respir. Cell Mol. Biol.* **44,** 456-464

46. Chen, Z. M., Jin, N. L., Narasaraju, T., Chen, J. W., McFarland, L. R., Scott, M., and Liu, L. (2004) *Biochem. Biophys. Res. Commun.* **319,** 774-780

47. Mishra, A., Chintagari, N. R., Guo, Y. J., Weng, T. T., Su, L. J., and Liu, L. (2011) *J. Cell Sci.* **124,** 657-668

48. Clevers, H. and Nusse, R. (2012) *Cell* **149,** 1192-1205

49. Clevers, H. (2006) *Cell* **127,** 469-480

50. Weng, T. T. and Liu, L. (2010) *Respiratory Research* **11,**

51. Crosby, L. M. and Waters, C. M. (2010) *American Journal of Physiology-Lung Cellular and Molecular Physiology* **298,** L715-L731

52. Flozak, A. S., Lam, A. P., Russell, S., Jain, M., Peled, O. N., Sheppard, K. A., Beri, R., Mutlu, G. M., Budinger, G. R. S., and Gottardi, C. J. (2010) *Journal of Biological Chemistry* **285,** 3157-3167

53. Volckaert, T., Dill, E., Campbell, A., Tiozzo, C., Majka, S., Bellusci, S., and Langhe, S. P. (2011) *Journal of Clinical Investigation* **121,** 4409-4419

54. Zemans, R. L., Briones, N., Campbell, M., McClendon, J., Young, S. K., Suzuki, T., Yang, I. V., De Langhe, S., Reynolds, S. D., Mason, R. J., Kahn, M., Henson, P. M., Colgan, S. P., and Downey, G. P. (2011) *Proceedings of the National Academy of Sciences of the United States of America* **108,** 15990-15995

55. Doubravska, L., Simova, S., Cermak, L., Valenta, T., Korinek, V., and Andera, L. (2008) *Apoptosis* **13,** 573-587

56. You, L., He, B., Xu, Z. D., Uematsu, K., Mazieres, J., Fujii, N., Mikami, I., Reguart, N., McIntosh, J. K., Kashani-Sabet, M., McCormick, F., and Jablons, D. M. (2004) *Cancer Res.* **64,** 5385-5389

57. You, L., He, B., Uematsu, K., Xu, Z. D., Mazieres, J., Lee, A., McCormick, F., and Jablons, D. M. (2004) *Cancer Res.* **64,** 3474-3478

58. Tanjore, H., Degryse, A. L., Crossno, P. F., Xu, X. C. C., McConaha, M. E., Jones, B. R., Polosukhin, V. V., Bryant, A. J., Cheng, D. S., Newcomb, D. C., McMahon, F. B., Gleaves, L. A., Blackwell, T. S., and Lawson, W. E. (2013) *Am. J. Respir. Crit. Care Med.* **187,** 630-639

59. Zemans, R. L., McClendon, J., Aschner, Y., Briones, N., Young, S. K., Lau, L. F., Kahn, M., and Downey, G. P. (2013) *American Journal of Physiology-Lung Cellular and Molecular Physiology* **304,** L415-L427

60. Heijink, I. H., de Bruin, H. G., van den Berge, M., Bennink, L. J. C., Brandenburg, S. M., Gosens, R., van Oosterhout, A. J., and Postma, D. S. (2013) *Thorax* **68,** 709-716

61. Wang, R., Ahmed, J., Wang, G. Q., Hassan, I., Strulovici-Barel, Y., Hackett, N. R., and Crystal, R. G. (2011) *Plos One* **6,**

62. Lee, H., Bae, S., Choi, B. W., and Yoon, Y. (2012) *Immunopharmacology and Immunotoxicology* **34,** 56-65

63. Sharma, S., Tantisira, K., Carey, V., Murphy, A. J., Lasky-Su, J., Celedon, J. C., Lazarus, R., Klanderman, B., Rogers, A., Soto-Quiros, M., Avila, L., Mariani, T., Gaedigk, R., Leeders, S., Torday, J., Warburton, D., Raby, B., and Weiss, S. T. (2010) *American Journal of Respiratory and Critical Care Medicine* **181,** 328-336

64. Hoogendijk, A. J., Diks, S. H., van der Poll, T., Peppelenbosch, M. P., and Wieland, C. W. (2011) *Plos One* **6,**

65. Villar, J., Cabrera, N. E., Casula, M., Valladares, F., Flores, C., Lopez-Aguilar, J., Blanch, L., Zhang, H. B., Kacmarek, R. M., and Slutsky, A. S. (2011) *Intensive Care Medicine* **37,** 1201-1209

66. Douglas, I. S., del Valle, F. D., Winn, R. A., and Voelkel, N. F. (2006) *American Journal of Respiratory Cell and Molecular Biology* **34,** 274-285

67. Villar, J., Cabrera, N. E., Valladares, F., Casula, M., Flores, C., Blanch, L., Quilez, M. E., Santana-Rodriguez, N., Kacmarek, R. M., and Slutsky, A. S. (2011) *Plos One* **6,**

68. Rey, J. P. and Ellies, D. L. (2010) *Developmental Dynamics* **239,** 102-114

69. Neumann, J., Schaale, K., Farhat, K., Endermann, T., Ulmer, A. J., Ehlers, S., and Reiling, N. (2010) *Faseb Journal* **24,** 4599-4612

70. Kim, J., Kim, J., Kim, D. W., Ha, Y., Ihm, M. H., Kim, H., Song, K., and Lee, I. (2010) *Journal of Immunology* **185,** 1274-1282

71. Sun, J., Hobert, M. E., Duan, Y. L., Rao, A. S., He, T. C., Chang, E. B., and Madara, J. L. (2005) *American Journal of Physiology-Gastrointestinal and Liver Physiology* **289,** G129-G137

72. Malhotra, S. and Kincade, P. W. (2009) *Experimental Hematology* **37,** 19-30

73. Du, Q., Zhang, X. L., Cardinal, J., Cao, Z. X., Guo, Z., Shao, L. F., and Geller, D. A. (2009) *Cancer Research* **69,** 3764-3771

74. Deng, J. O., Miller, S. A., Wang, H. Y., Xia, W. Y., Wen, Y., Zhou, B. H. P., Li, Y., Lin, S. Y., and Hung, M. C. (2002) *Cancer Cell* **2,** 323-334

75. Konigshoff, M., Kramer, M., Balsara, N., Wilhelm, J., Amarie, O. V., Jahn, A., Rose, F., Fink, L., Seeger, W., Schaefer, L., Gunther, A., and Eickelberg, O. (2009) *J. Clin. Invest.* **119,** 772-787

76. Sharma, S., Tantisira, K., Carey, V., Murphy, A. J., Lasky-Su, J., Celedon, J. C., Lazarus, R., Klanderman, B., Rogers, A., Soto-Quiros, M., Avila, L., Mariani, T., Gaedigk, R., Leeders, S., Torday, J., Warburton, D., Raby, B., and Weiss, S. T. (2010) *Am. J. Respir. Crit. Care Med.* **181,** 328-336

77. Kneidinger, N., Yildirim, A. O., Callegari, L., Takenaka, S., Stein, M. M., Dumitrascu, R., Bohla, A., Bracke, K. R., Morty, R. E., Brusselle, G. G., Schermuly, R. T., Eickelberg, O., and Konigshoff, M. (2011) *Am. J. Respir. Crit. Care Med.* **183,** 723-733

78. Wang, R., Ahmed, J., Wang, G. Q., Hassan, I., Strulovici-Barel, Y., Hackett, N. R., and Crystal, R. G. (2011) *Plos One* **6,**

79. Foronjy, R., Imai, K., Shiomi, T., Mercer, B., Sklepkiewicz, P., Thankachen, J., Bodine, P., and D'Armiento, J. (2010) *American Journal of Pathology* **177,** 598-607

80. Diarra, D., Stolina, M., Polzer, K., Zwerina, J., Ominsky, M. S., Dwyer, D., Korb, A., Smolen, J., Hoffmann, M., Scheinecker, C., van der Heide, D., Landewe, R., Lacey, D., Richards, W. G., and Schett, G. (2007) *Nature Medicine* **13,** 156-163

81. Ke, H. Z., Richards, W. G., Li, X. D., and Ominsky, M. S. (2012) *Endocrine Reviews* **33,** 747-783

82. Kim, K. I., Park, K. U., Chun, E. J., Choi, S. I., Cho, Y. S., Youn, T. J., Cho, G. Y., Chae, I. H., Song, J., Choi, D. J., and Kim, C. H. (2011) *Journal of Korean Medical Science* **26,** 1178-1184

83. Seifert-Held, T., Pekar, T., Gattringer, T., Simmet, N. E., Scharnagl, H., Stojakovic, T., Fazekas, F., and Storch, M. K. (2011) *Atherosclerosis* **218,** 233-237

84. Shen, Q. J., Fan, J., Yang, X. R., Tan, Y. X., Zhao, W. F., Xu, Y., Wang, N., Niu, Y. D., Wu, Z., Zhou, J., Qiu, S. J., Shi, Y. H., Yu, B., Tang, N., Chu, W., Wang, M., Wu, J. H., Zhang, Z. G., Yang, S. L., Gu, J. R., Wang, H. Y., and Qin, W. X. (2012) *Lancet Oncology* **13,** 817-826

85. Heiland, G. R., Zwerina, K., Baum, W., Kireva, T., Distler, J. H., Grisanti, M., Asuncion, F., Li, X. D., Ominsky, M., Richards, W., Schett, G., and Zwerina, J. (2010) *Annals of the Rheumatic Diseases* **69,** 2152-2159

86. Pfaff, E. M., Becker, S., Gunther, A., and Konigshoff, M. (2011) *European Respiratory Journal* **37,** 79-87

87. Fauci, A. S. and Morens, D. M. (2012) *New England Journal of Medicine* **366,** 454-461

88. Mizgerd, J. P. (2008) *New England Journal of Medicine* **358,** 716-727

89. Mizgerd, J. P. (2012) *American Journal of Respiratory and Critical Care Medicine* **186,** 824-829

90. Thompson, W. W., Shay, D. K., Weintraub, E., Brammer, L., Cox, N., Anderson, L. J., and Fukuda, K. (2003) *Jama-Journal of the American Medical Association* **289,** 179-186

91. Webster, R. G., Bean, W. J., Gorman, O. T., Chambers, T. M., and Kawaoka, Y. (1992) *Microbiological Reviews* **56,** 152-179

92. Medina, R. A. and Garcia-Sastre, A. (2011) *Nature Reviews Microbiology* **9,** 590-603

93. Muller, K. H., Kakkola, L., Nagaraj, A. S., Cheltsov, A. V., Anastasina, M., and Kainov, D. E. (2012) *Trends in Pharmacological Sciences* **33,** 89-99

94. Isaacs, A. and Lindenmann, J. (1957) *Proceedings of the Royal Society B-Biological Sciences* **147,** 258-267

95. Borden, E. C., Sen, G. C., Uze, G., Silverman, R. H., Ransohoff, R. M., Foster, G. R., and Stark, G. R. (2007) *Nature Reviews Drug Discovery* **6,** 975-990

96. Sadler, A. J. and Williams, B. R. G. (2008) *Nature Reviews Immunology* **8,** 559-568

97. Bowie, A. G. and Unterholzner, L. (2008) *Nature Reviews Immunology* **8,** 911-922

98. Barbalat, R., Ewald, S. E., Mouchess, M. L., and Barton, G. M. (2011) *Nucleic Acid Recognition by the Innate Immune System*, ANNUAL REVIEWS, PALO ALTO

99. Pichlmair, A., Lassnig, C., Eberle, C. A., Gorna, M. W., Baumann, C. L., Burkard, T. R., Burckstummer, T., Stefanovic, A., Krieger, S., Bennett, K. L., Rulicke, T., Weber, F., Colinge, J., Muller, M., and Superti-Furga, G. (2011) *Nature Immunology* **12,** 624-U177

100. Honda, K., Takaoka, A., and Taniguchi, T. (2006) *Immunity* **25,** 349-360

101. Kawai, T. and Akira, S. (2006) *Nature Immunology* **7,** 131-137

102. Medina, R. A. and Garcia-Sastre, A. (2011) *Nature Reviews Microbiology* **9,** 590-603

103. Shaw, M. L. (2011) *Reviews in Medical Virology* **21,** 358-369

104. Hao, L. H., Sakurai, A., Watanabe, T., Sorensen, E., Nidom, C. A., Newton, M. A., Ahlquist, P., and Kawaoka, Y. (2008) *Nature* **454,** 890-U46

105. Brass, A. L., Huang, I. C., Benita, Y., John, S. P., Krishnan, M. N., Feeley, E. M., Ryan, B. J., Weyer, J. L., van der Weyden, L., Fikrig, E., Adams, D. J., Xavier, R. J., Farzan, M., and Elledge, S. J. (2009) *Cell* **139,** 1243-1254

106. Konig, R., Stertz, S., Zhou, Y., Inoue, A., Hoffmann, H. H., Bhattacharyya, S., Alamares, J. G., Tscherne, D. M., Ortigoza, M. B., Liang, Y. H., Gao, Q. S., Andrews, S. E.,

Bandyopadhyay, S., De Jesus, P., Tu, B. P., Pache, L., Shih, C., Orth, A., Bonamy, G., Miraglia, L., Ideker, T., Garcia-Sastre, A., Young, J. A. T., Palese, P., Shaw, M. L., and Chanda, S. K. (2010) *Nature* **463,** 813-817

107. Karlas, A., Machuy, N., Shin, Y., Pleissner, K. P., Artarini, A., Heuer, D., Becker, D., Khalil, H., Ogilvie, L. A., Hess, S., Maurer, A. P., Muller, E., Wolff, T., Rudel, T., and Meyer, T. F. (2010) *Nature* **463,** 818-U132

108. Tafforeau, L., Chantier, T., Pradezynski, F., Pellet, J., Mangeot, P. E., Vidalain, P. O., Andre, P., Rabourdin-Combe, C., and Lotteau, V. (2011) *Journal of Virology* **85,** 13010-13018

109. Sui, B. Q., Bamba, D., Weng, K., Ung, H., Chang, S. J., Van Dyke, J., Goldblatt, M., Duan, R., Kinch, M. S., and Li, W. B. (2009) *Virology* **387,** 473-481

110. Hale, B. G., Randall, R. E., Ortin, J., and Jackson, D. (2008) *Journal of General Virology* **89,** 2359-2376

111. Shapira, S. D., Gat-Viks, I., Shum, B. O. V., Dricot, A., de Grace, M. M., Wu, L. G., Gupta, P. B., Hao, T., Silver, S. J., Root, D. E., Hill, D. E., Regev, A., and Hacohen, N. (2009) *Cell* **139,** 1255-1267

112. Zeng, L., Fagotto, F., Zhang, T., Hsu, W., Vasicek, T. J., Perry, W. L., Lee, J. J., Tilghman, S. M., Gumbiner, B. M., and Costantini, F. (1997) *Cell* **90,** 181-192

113. Jho, E. H., Zhang, T., Domon, C., Joo, C. K., Freund, J. N., and Costantini, F. (2002) *Molecular and Cellular Biology* **22,** 1172-1183

114. Li, V. S. W., Ng, S. S., Boersema, P. J., Low, T. Y., Karthaus, W. R., Gerlach, J. P., Mohammed, S., Heck, A. J. R., Maurice, M. M., Mahmoudi, T., and Clevers, H. (2012) *Cell* **149,** 1245-1256

115. Cortese, M. S., Uversky, V. N., and Dunker, A. K. (2008) *Progress in Biophysics & Molecular Biology* **98,** 85-106

116. Zhang, Y. G., Wu, S. P., Xia, Y. L., Chen, D., Petrof, E. O., Claud, E. C., Hsu, W., and Sun, J. (2012) *Plos One* **7,**

117. Kameoka, M., Kameoka, Y., Utachee, P., Kurosu, T., Sawanpanyalert, P., Ikuta, K., and Auwanit, W. (2009) *Aids Research and Human Retroviruses* **25,** 1005-1011

118. Linda L. Han, James P. Alexander and Larry J. Anderson. (1999) *J Infect Dis.* 179 (1): 25-30.

CHAPTER II

WNT3A MITIGATES ACUTE LUNG INJURY BY REDUCING P2X7 RECEPTOR-MEDIATED ALVEOLAR EPITHELIAL TYPE I CELL DEATH

2.1 Abstract

Acute lung injury (ALI) is characterized by pulmonary endothelial and epithelial cell damage, and loss of alveolar-capillary barrier. We have previously shown that P2X7 receptor (P2X7R), a cell death receptor, is specifically expressed in alveolar epithelial type I cells (AEC I). In this study, we hypothesized that P2X7R-mediated purinergic signaling and its interaction with Wnt/β-catenin signaling contributes to AEC I death. We examined the effect of P2X7R agonist 2'-3'-O-(4-benzoylbenzoyl)-ATP (BzATP) and Wnt agonist Wnt3a on AEC I death in vitro and in vivo. We also assessed the therapeutic potential of Wnt3a in a clinically relevant ALI model of intratracheal lipopolysaccharide (LPS) exposure in ventilated mice. We found that the activation of P2X7R by BzATP caused the death of AEC I by suppressing Wnt/β-catenin signaling through stimulating glycogen synthase kinase-3β (GSK-3β) and proteasome. On the other hand, the activation of Wnt/β-catenin signaling by Wnt3a, GSK-3β inhibitor, or proteasome inhibitor blocked the P2X7R-mediated cell death. More importantly, Wnt3a attenuated the AEC I damage caused by intratracheal instillation of BzATP in rats or LPS in ventilated mice. Our results suggest that Wnt3a overrides the effect of P2X7R on the Wnt/β-catenin signaling to prevent the AEC I death and restrict the severity of ALI.

Key words: Wnt/β-catenin signaling; P2X7R; Cell death; Acute lung injury

2.2 Introduction

Acute lung injury (ALI) and its severe form, acute respiratory distress syndrome (ARDS), are life-threatening diseases caused by a variety of reasons, including sepsis, trauma, and pneumonia (1). The alveolar epithelium consists of alveolar epithelial type I cells (AEC I) and alveolar epithelial type II cells (AEC II) and is believed to play an important role in the pathogenesis of ALI. AEC I cover most of the alveolar surface area and are the primary barrier of defense against the variety of insults (2,3). They are more sensitive to injury in comparison with other lung cells. Damage of AEC I can be observed in all types of ALI, leading to the deficiency of gas exchange, disruption of fluid clearance, and amplification of acute inflammation. Several molecular signaling pathways, such as TGF-β pathway, NFκB pathway, and Fas/FasL-mediated pathway, have been reported to regulate AEC I death during ALI (4).

Wnt is a family of highly conserved secreted signaling molecules and plays an important role in embryogenesis, tissue repair, and cell differentiation (5). Without the binding of Wnt ligands to the cells, the intracellular β-catenin is phosphorylated by glycogen synthase kinase-3β (GSK-3β) and degraded in proteasomes, and thus Wnt/β-catenin signaling is inactive. On the other hand, the binding of Wnt ligands with frizzled receptors on the cell surface leads to the disruption of GSK-3β-mediated phosphorylation of β-catenin and thus attenuation of its proteasome-mediated degradation. The stabilized intracellular β-catenin then translocates into the nucleus, where it binds to T-cell factor (TCF)/ Lymphoid enhancer factor (LEF) transcription factors to increase the transcription of its downstream genes.

We have previously shown that pleiotrophin and miR-375 regulate Wnt/β-catenin signaling during alveolar epithelial cell differentiation (6,7). Recent studies reveal essential roles of Wnt/β-catenin signaling in the pathogenesis of several lung diseases, including pulmonary

fibrosis (8,9), asthma (10), and chronic obstructive pulmonary disease (COPD) (11,12). Activation of Wnt/β-catenin signaling improves AEC II survival (13) while deletion of β-catenin in AEC results in an increased AEC death (8). Interestingly, transepithelial migration of neutrophils also activates Wnt/β-catenin signaling in AEC II and accelerates the epithelial repair (14). Thus, it is important to explore the potential contribution of Wnt/β-catenin to AEC I damage during ALI.

P2X7R is a transmembrane ligand-gated ion channel receptor activated by extracellular ATP (15). We have previously found that P2X7R is specifically expressed in AEC I and regulates lung surfactant secretion (16,17). However, high concentrations of ATP or sustained stimulations could lead to apoptosis or necrosis in P2X7R-expressing cells (18,19). P2X7R knockout mice have shown a protective phenotype in LPS-induced acute lung injury (20). Together with its ability to regulate pulmonary inflammatory response (21), P2X7R could act as a potential modulator of AEC I cell death in response to pathological insults.

In this study, we report for the first time the important integration of Wnt/β-catenin signaling and P2X7R-mediated purinergic signaling in AEC I death during ALI. The finding could be translated into a new therapeutic approach.

2.3 Materials and Methods

2.3.1 Cell culture

E10 cells, a gift from Dr. Mary Williams (Pulmonary Center, Boston University School of Medicine, MA, US), were cultured in CMRL 1066 supplemented with glutamax®, penicillin/streptomycin and 10% heat-inactivated fetal bovine serum (FBS) (Atlantic Biological, Miami, FL). R3/1, a gift from Dr. Roland Koslowski, Technische Universität Dresden, Germany, was maintained in RPMI 1640 complemented with 10 % FBS and penicillin/streptomycin. HEK 293 cells (ATCC, Manassas, VA) and HEK293 cells stably expressing rat P2X7R (HEK293-

P2X7R), a gift from Dr. Annmarie Surprenant (University of Manchester, Manchester, UK) were maintained in DMEM supplemented with 10% FBS and 100 μM non-essential amino acids. A549 cells (ATCC, Manassas, VA) were cultured in RPMI-1640 medium containing 10% FBS. H441 cells (ATCC, Manassas, VA) were maintained in F-12K Medium complemented with 10 % FBS. Cells were grown at 37 °C in a humidified atmosphere containing 5% CO_2.

2.3.2 Primary AEC I-like Cells

Primary AEC I-like cells were obtained by culturing primary AEC II on plastic plates for 7 days. To isolate AEC II, rat lung was perfused using solution II (0.9% NaCl, 0.1% glucose, 30 mM HEPES, 6 mM KCl, 0.1 mg/ml streptomycin sulfate, 0.07 mg/ml penicillin G, 0.07 mg/ml EGTA, 3 mM Na_2HPO_4, and 3 mM NaH_2PO_4, pH 7.4) to clear the red blood cells. Then the lung was lavaged with solution I (solution II plus 3 mM $MgSO_4$ and 1.5 mM $CaCl_2$), and digested with elastase (3 units/ml) for 3 X 12 min at 37°C. Then, the lung was chopped with a Mcllwain tissue chopper, and the cell suspension was digested with 100 ng/ml DNase I and filtered through 160- and 37-μm nylon mesh once and 15-μm nylon mesh twice. Then cells were seeded on rat IgG-coated polystyrene bacteriological plates twice for 45 min and 30 min to remove macrophages. The unattached cells were collected by centrifugation. The isolated AEC II had a purity of 90% and a viability of over 98%. To obtain AEC I-like cells, AEC II were seeded onto 96-well tissue culture plastic dishes at a density of 1 x 10^6 cells/plate in MEM with 10% FBS. After overnight culture, the culture media was changed to DMEM supplemented with 10% FBS. The medium was changed every 48 hours until day 7.

2.3.3 Preparation of conditioned medium

Overexpressing soluble murine Wnt3a/Wnt5a cell lines and control murine L cell line (ATCC) were maintained in DMEM supplemented with 10% FBS, 1% L-glutamine, and 0.4 mg/ml G418 (Invitrogen, Carlsbad, CA). To obtain Wnt3a-, Wnt5a- or control (Con)-conditioned

medium (CM), cells were cultured in fresh growth medium without G418 for 4 days and changed into fresh G418-free medium for additional 3 days. The cultured media were mixed, sterile-filtered, and stored at -80°C until use. The activity of Wnt3a_CM was determined by a TOPflash assay performed in 293T cells. Wnt3a_CM normally showed an approximately 7-fold increase of the reporter activity compared to Con_CM. To concentrate the soluble Wnt3a, 20 ml Wnt3a_CM was reduced into 2 ml 10X Wnt3a_CM by an ultra-filtration kit (Millipore, Billerica, MA).

2.3.4 Silencing of P2X7R in E10 cells

Two adenovirus-based shRNA vectors, si-P2X7R (1) and si-P2X7R (2), previously constructed in our lab were utilized to knockdown P2X7R (17). E10 cells were infected with virus control (si-control), si-P2X7R (1) and si-P2X7R (2) for 4 days at a multiplicity of infection (MOI) of 100 before BzATP treatment.

2.3.5 Cell viability and lactate dehydrogenase (LDH) assays

At the end of BzATP (Sigma-Aldrich, St. Louis, MO) treatment, cell viability was assessed by the Cell Viability Assay Kit (Millipore, Billerica, MA) which measured the activity of mitochondrial dehydrogenases. Data was normalized to the control without any treatment. The release of LDH was measured with a LDH assay kit (Diagnostic Chemicals Inc. CT). The values were expressed as a percentage of actual LDH in the medium to the maximal LDH released by freeze-thaw insults.

2.3.6 Western blot

The cells were lyzed in M-PER Mammalian Protein Extraction Reagent containing 1% Halt Protease Inhibitor Cocktail (Pierce, Rockford, IL) at 4°C, followed by sonication and freeze/thaw cycles. The proteins were separated in 10% SDS-PAGE and transferred to nitrocellulose membranes. The membranes were stained with Ponceau-S to view the transfer

quality. Then the membranes were blocked for 1 hour at room temperature with 5% dried milk in Tris-buffered saline (10 mM Tris/HCl, 100 mM NaCl and 0.05% Tween; pH 7.5) (TBS-T) and incubated overnight at 4°C with anti-P2X7R (1:500, SIGMA, St. Louis, MO), anti-activated β-catenin (1:1000, Millipore, Billerica, MA), anti-total β-catenin (1:2000, BD Transduction Laboratories, San Jose, CA), anti-Bcl2 (1:1000, Santa Cruz Biotechnology, Santa Cruz, CA), anti-PCNA (1:2000, Santa Cruz Biotechnology, Santa Cruz, CA), anti-GSK-3β (1:2000, BD Transduction Laboratories, San Jose, CA), anti-GSK-3β (*pY216*) (1:1000, BD Transduction Laboratories, San Jose, CA), anti-GSK-3β (*pS9*) (1:1000, Cell Signaling Technology, Danvers, MA), anti-β-actin (1:2000, SIGMA, St. Louis, MO), and anti-GAPDH (1:400, Santa Cruz Biotechnology, Santa Cruz, CA) antibodies. The blots were then rinsed in TBS-T, and incubated for 1 hour at room temperature with goat anti-rabbit, or goat anti-mouse secondary antibodies, coupled to horseradish peroxidase (1:2000, Jackson Immunoresearch, West Grove, PA). After being washed, the blots were developed by SuperSignal West Pico Chemiluminescent Substrate (Pierce, Rockford, IL).

2.3.7 Quantitative real-time PCR

Total RNA was extracted from cells or tissues using TRI-Reagent (Molecular Research Center, Cincinnati, OH) following the manufacturer's instructions. RNA was digested with TURBO DNase (Ambion, Austin, TX, USA) to remove the genomic DNA contamination. One μg of RNA was reverse-transcribed into cDNA using M-MLV reverse transcriptase (Invitrogen, Carlsbad, CA), random primers, and oligo dT (Promega, Madison, WI). Real-time PCR was carried out on 7900HT Fast Real-Time PCR System using SYBR Green I detection Master Mix (Eurogentec, CA). The primers were designed using Primer Express® software (Applied Biosystems, Foster City, CA), and listed in Table II.1. PCR involved an initial denaturation step at 94°C for 5 min, followed by 40 cycles of amplification (94°C for 30 s, 60°C for 1 min). A

dissociation curve was generated after each PCR to view the specificity of the amplification. All of the data was normalized to 18S rRNA.

Gene	Accession #	Forward primers	Reverse primers
18S	NR_003278.1	ATTGCTCAATCTCGGGTGGCTG	CGTTCTTAGTTGGTGGAGCGATTTG
Bmp4	NM_007554.2	TGGGATGCTGCTGAGGTTGAAG	CGAGCCAACACTGTGAGGAGTTTC
Axin2	NM_015732.4	GCGAGTGGCCAAAGCAATCTATAAG	GAGCCGATCTGTTGCTTCTTGATG
Cyclin D1	NM_007631.2	AGAAGTGCGAAGAGGAGG	TGTTCACCAGAAGCAGTTC
Cyclin E1	NM_007633.2	CACAACATCCAGACCCACACCAAC	ACCACACTCGGAGGAGGAGAAATC
P2X1R	NM_008771.3	TCAAGGACATTGTGCAGAGAAC	CAGTTGCCTGTGCGAATACCT
P2X2R	NM_153400.4	GCGTTCTGGGACTACGAGAC	ACGTACCACACGAAGTAAAGC
P2X3R	NM_145526.2	AAAGCTGGACCATTGGGATCA	CGTGTCCCGCACTTGGTAG
P2X4R	NM_011026.2	CTCGGGTCCTTCCTGTTCG	GTTTCCTGGTAGCCCTTTTCC
P2X5R	NM_033321.3	AGGGGGTGGCCTATACCAAC	GGTTAGGAGTCACGATCAGGTT
P2X6R	NM_011028.2	GTTAAGGAGCTGGAGAACCG	AGGATGCTCTGGACATCTGC
P2X7R	NM_011027.2	GACAAACAAAGTCACCCGGAT	CGCTCACCAAAGCAAAGCTAAT

Table II.1. PCR primer sequences for mouse genes

2.3.8 Immunofluorescence

E10 cells were cultured on 24-well plastic plates. Before collection, the cells were briefly washed with PBS and fixed with 4% paraformaldehyde for 15 min. After being washed with PBS, the cells were permeabilized with 0.3% Triton X-100 for 10 min and blocked with 10% FBS for 1 hour at room temperature. After rinse, the cells were incubated overnight with primary antibodies against β-catenin (1:200). Subsequently, cells were washed with PBS and incubated with Alexa 568-conjugated goat anti-mouse IgG (Invitrogen, Carlsbad, CA) for 1 hour. The nuclei were counterstained with 4',6-diamidino-2-phenylindole (DAPI, 1:1000, Invitrogen, Carlsbad, CA) for 2 min. Images were acquired using a Nikon Eclipse TE-2000 inverted fluorescence microscope.

2.3.9 TOPflash Assay

E10 cells were seeded in 96-well plastic plates. After reaching 85% confluence, the cells were transfected with 1 ng the *Renilla* luciferase control plasmid phRL-TK (Promega, WI) and 20

ng LEF/TCF reporter plasmid TOPflash (Millipore, MA) or FOPflash (a negative control plasmid for TOPflash, which has mutated LEF/TCF binding sites) using Lipofectamine 2000 (Invitrogen, Carlsbad, CA). After 24 hours, cells were treated with 400 μM BzATP for 0 - 12 hours. Dual-luciferase assay was performed using the Dual-Luciferase® Reporter Assay System (Promega, Madison, WI).

2.3.10 Proteasome activity assay

To measure proteasome activity, 100 μg of cell lysate was diluted with assay buffer (50 mM Tris [pH 7.4], 5 mM $MgCl_2$, 2 mM dithiothreitol, and 2 mM ATP) to a final volume of 1 ml and incubated with 50 μM fluorogenic proteasome substrate Suc-LLVY-AMC (AnaSpec, Fremont, CA). Proteolytic activities, reflected by the release of the fluorescent group, 7-amido-4-methylcoumarin (AMC), were continuously monitored in 30 min at 37°C by a fluorescence plate reader (Spectramax M2, Molecular Devices, Sunnyvale, CA) with excitation and emission wavelengths of 380 and 460 nm, respectively.

2.3.11 Animals

Male C57BL/6N mice (6 – 8 weeks old) were purchased from Jackson Laboratory (Bar Harbor, ME). Male Sprague-Dawley rats were purchased from Charles River Breeding Laboratories (Wilmington, MA). All the animals were housed and cared for by the Laboratory Animal Resource Unit, Oklahoma State University. Experimental protocols were reviewed and approved by the Institutional Animal Care and Use Committee of Oklahoma State University.

2.3.12 BzATP-induced acute lung injury in rat

Male Sprague-Dawley rats (275-300 g) were divided to four groups (n=8/group): 1) vehicle (200 μl PBS), 2) BzATP (10 mg/kg b.w. in 200 μl PBS), 3) BzATP and Wnt3a_CM (10 mg/kg b.w. BzATP in 100 μl PBS and 100 μl 10X Wnt3a_CM), and 4) BzATP and Con_CM (10

mg/kg b.w. BzATP in 100 µl PBS and 100 µl 10X Con_CM). Rats were anesthetized with intraperitoneal injection of ketamine (40 mg/kg b.w.) and xylazine (8 mg/kg b.w.). All of the reagents were intratracheally instilled. 24 hours after intratracheal instillation, a tracheotomy was performed. Bronchoalveolar lavage (BAL) was collected by lavaging the right lungs with 10 ml of normal saline. After centrifugation at 380 g for 10 min at 4°C, the cell pellets were resuspended in 1 ml of normal saline. Cell-free BAL and tissue samples of lavaged right lungs were immediately frozen in liquid nitrogen and stored at -80°C for subsequent analysis. Unlavaged left lungs were fixed in 4% paraformaldehyde for histological analysis.

2.3.13 LPS-induced acute lung injury in a ventilated mouse model

Male C57BL/6N mice (8 weeks) were divided into four groups (n=8/group): 1) lipopolysaccharides LPS from *Escherichia coli* 055:B5 (0.5 mg/kg b.w.) in 20 µl 10X Wnt3a conditional medium, 2) LPS 0.5 mg/kg b.w. in 20 µl 10X Con_CM, 3) LPS 0.5 mg/kg b.w. in 20 µl normal saline, 4) Control, without LPS and mechanical ventilation. LPS was intratracheally delivered into the lung. 1 hour after intratracheal instillation, mice were ventilated with a tidal volume of 12 ml/kg, a rate of 125 bpm, and 3 cm H_2O PEEP for 2.5 hours. At the end of ventilation, a tracheotomy was performed. The lungs were lavaged with 1 ml of normal saline three times. BAL was collected and centrifuged at 380 g for 10 min at 4°C. BAL cell pellets were resuspended in 200 µl of normal saline for subsequent analysis. Cell- free BAL fluid and lavaged lung tissue samples were frozen in liquid nitrogen and stored in −80°C freezer.

2.3.14 BAL analysis

Protein concentrations in the BAL fluid were determined by a Bio-Rad protein assay (Bio-Rad Laboratories, Hercules, CA). The total number of cells in BAL was counted with a hemocytometer. Differential cell count was performed on the BAL cells visualized by Wright-Giemsa staining. LDH activity in the BAL fluid was determined by a Cytotoxicity Detection kit

(Roche Applied Sciences, Indianapolis, IN) using type III L-lactic dehydrogenase (SIGMA, St. Louis, MO) as standards.

2.3.15 Western blot for T1α in BAL

For rat samples, BAL fluid (70 µl) was added with 7 µl SDS sample buffer (62.5 mM Tris HCl, pH 6.8, containing 5% 2-mercaptoethanol, 2% SDS, 10% glycerol, and 0.01% bromphenol blue) and heated at 95°C until 25 µl volume was reached. A monoclonal anti-T1α (1:2000, a gift from Dr. Mary C Williams, Boston University) antibody was used as a primary antibody. For mouse samples, BAL fluid (20 µl) was added with 4 µl SDS sample buffer and heated at 95 °C for 10 minutes. A hamster anti- T1α (1:2000, 8.1.1, DHSB, Iowa City, IO) was used as a primary antibody. Films were developed and scanned. The densities of bands were quantified by ImageJ software (National Institutes of Health, Bethesda, Maryland [http://rsb.info.nih.gov/ij/]).

2.3.16 Statistical analysis

The results were analyzed by one-way ANOVA with posthoc *Tukey's* test for multiple comparisons of control and treatment groups, or Student's *t*-test using GraphPad Prism (version 6). All results were reported as means ± s.e.m. (n=3-8 for each condition).

2.4 Results

2.4.1 P2X7R expression in lung cells

We have previously shown that P2X7R is specifically expressed in AEC I of the lung (16). Here we examined the expression of P2X7R in several lung cell lines by Western blot. HEK293-P2X7R cells, stably transfected cell line with P2X7R, were used as a positive control. P2X7R expression was observed in E10, an AEC I cell line and MLE15, a lung epithelial cell line. However, HEK293 (a human epithelial kidney cell line), R3/1 (a rat AEC I cell lines), A549

(a human carcinoma AEC II cell line), Pre-TII (a rat fetal AEC II cell line), H441 (a human lung papillary adenocarcinoma epithelial cell line), RLE-6TN (a rat lung AEC II cell line), and RFL-6 (a fetal lung fibroblast cell line), had no P2X7R expression (Fig. II.1A). The mRNA expression of mouse P2X subunits was further analyzed by PCR. P2X3R, P2X4R, P2X6R and P2X7R subunits were highly expressed in E10 cells. The expression of P2X1R and P2X5R subunits were barely detectable, and P2X2R had no expression in E10 cells. All of the P2X subunits were expressed in the lung tissue (Fig. II. 1B).

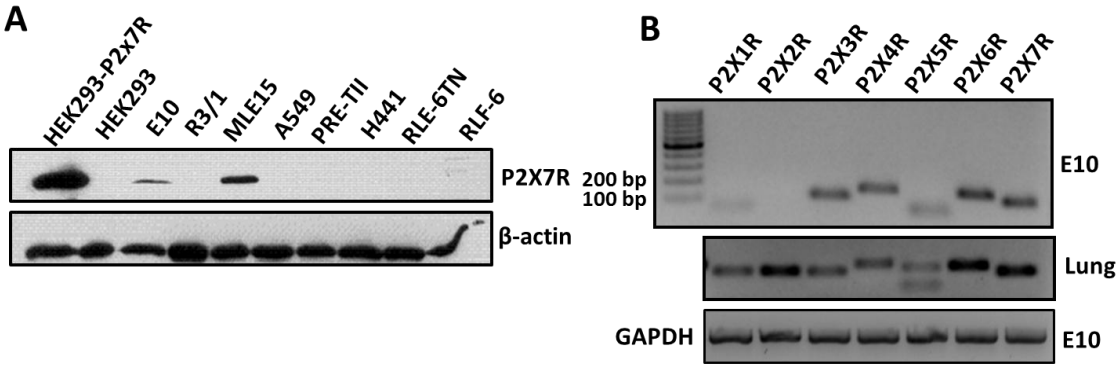

Fig. II.1. Expression of P2X receptors in the lung cells. (A) Protein expression of P2X7R in different lung cell lines (20 μg total protein) was analyzed by Western blot using β-actin as an internal control. (B) mRNA expression of P2XRs in E10 cells and normal mouse lung tissues was determined by electrophoresis using real-time PCR product with GAPDH as an loading control.

2.4.2 Prolonged activation of P2X7R causes cell death

Because P2X7R is well-known as a cell death receptor, we tested cell viability upon the activation of P2X7R in E10 cells. Treatment of E10 cells with BzATP, a potent P2X7R agonist, for 12 hours significantly decreased cell viability in a dose-dependent manner as measured by MTT assay and counting cell numbers (Fig. II. 2A and B). Direct cell lysis was monitored by LDH release. High doses (>200 μM) of BzATP dramatically increased LDH release from dead cells (Fig. II. 2C). To determine the specificity of BzATP, oxidized ATP (oATP, a P2X7R antagonist) was utilized to block P2X7R activity. Pre-incubation of E10 cells with 500 μM oATP totally attenuated the BzATP effect on cell viability (Fig. II. 2D) and LDH release (Fig. II. 2E).

Furthermore, silencing of P2X7R also significantly inhibited BzATP-induced reduction of cell viability (Fig. II. 3A) and increase of LDH release (Fig. II. 3B). In addition, BzATP did not induce cell death in the lung cells, A549 and H441, that do not express P2X7R (Fig. II. 3C and D). To determine whether BzATP-mediated cell death is reversible, E10 cells were treated with BzATP for various times and allowed them to recover in a normal medium without BzATP for 8 hours. The cells treated for up to 6 hours were reversible. However, if the cells were treated for longer than 8 hours, the cells cannot be recovered (Fig. II. 2F).

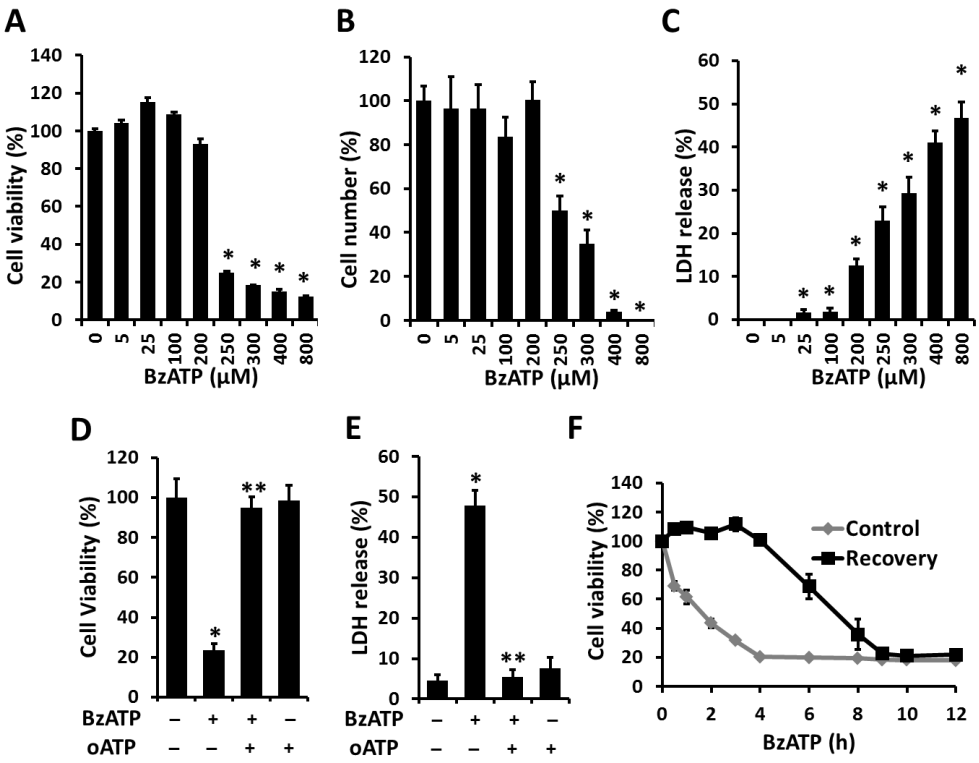

Fig. II. 2. Prolonged activation of P2X7R leads to E10 cell death. E10 cells were incubated with different concentrations of BzATP for 12 hours. Cell viability (A), viable cell numbers (B), and released LDH (C) were measured. E10 cells were treated with 400 μM BzATP in the absence or presence of 500 μM oATP for 12 hours. Cell viability (D) and released LDH (E) were measured. (F) E10 cells were treated with 400 μM BzATP for different times and recovered in a normal medium without BzATP for 6 hours, cell viability was determined. Data shown are means ± s.e.m. of three independent experiments, and statistical significance was determined by one-way ANOVA analysis with posthoc *Tukey's* test. *P<0.001 v.s. control without any treatment or 0 time, **P<0.001 v.s. 400 μM BzATP, and #P<0.005 v.s. si-control.

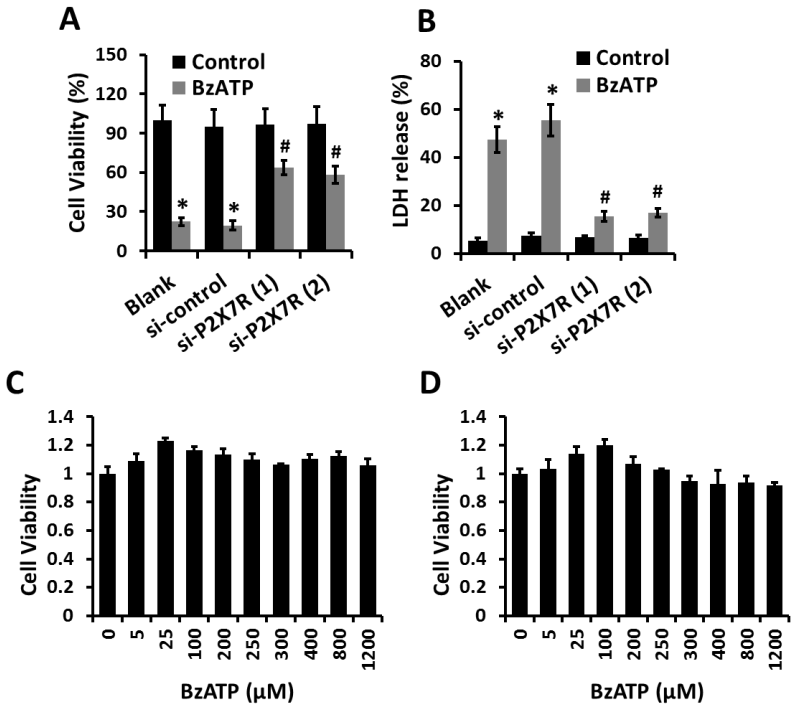

Fig. II. 3: Activation of P2X7R causes alveolar epithelial cell death. E10 cells were infected by adenovirus-based shRNA vectors (virus control (si-control), si-P2X7R (1) and si-P2X7R (2)) for 4 days and then treated with 400 μM BzATP for 12 hours. Cell viability (A) and Released LDH (B) were measured. A549 cells (C) and H441 cells (D) were incubated with different concentrations of BzATP for 12 hours. Cell viability was measured. Data shown are means ± s.e.m. of three independent experiments. Statistical significance was determined by one-way ANOVA analysis with posthoc Tukey's test. *P<0.001 v.s. control without any treatment or 0 time, **P<0.001 v.s. 400 μM BzATP, #P<0.005 v.s. si-control.

2.4.3 Activation of P2X7R suppresses Wnt/β-catenin signaling

Wnt/β-catenin signaling is important for cell proliferation and survival (5). We determined whether P2X7R-mediated cell death is due to down-regulation of the Wnt/β-catenin signaling. Several components of Wnt/β-catenin signaling were analyzed after BzATP treatment. Western analysis demonstrated that activated β-catenin and, to less extent, total β-catenin were down-regulated by BzATP treatment (Fig. II. 4A). Immunostaining confirmed that β-catenin level was significantly decreased (Fig. II. 4B). Proliferating cell nuclear antigen (PCNA) and B-cell lymphoma 2 (Bcl-2), classic cell survival proteins, were reduced as well (Fig. II. 4A). To further determine the effect of BzATP on β-catenin/TCF/LEF activity, dual-luciferase assay was

used to determine the activity of TOPflash, a TCF/LEF reporter plasmid expressing firefly luciferase. BzATP significantly decreased TOPflash activity (Fig. II. 4C). However, BzATP had no effect on FOPflash, a plasmid containing a mutated TCF/LEF binding site (Fig. II. 4C). Furthermore, we examined the mRNA expression of several Wnt/β-catenin downstream genes: Bmp4, Axin2, Cyclin D1, and Cyclin E1. Real-time PCR showed that expressions of all these four target genes were inhibited (Fig. II. 4D and E). Our results indicate that Wnt/β-catenin signaling is suppressed by BzATP treatment.

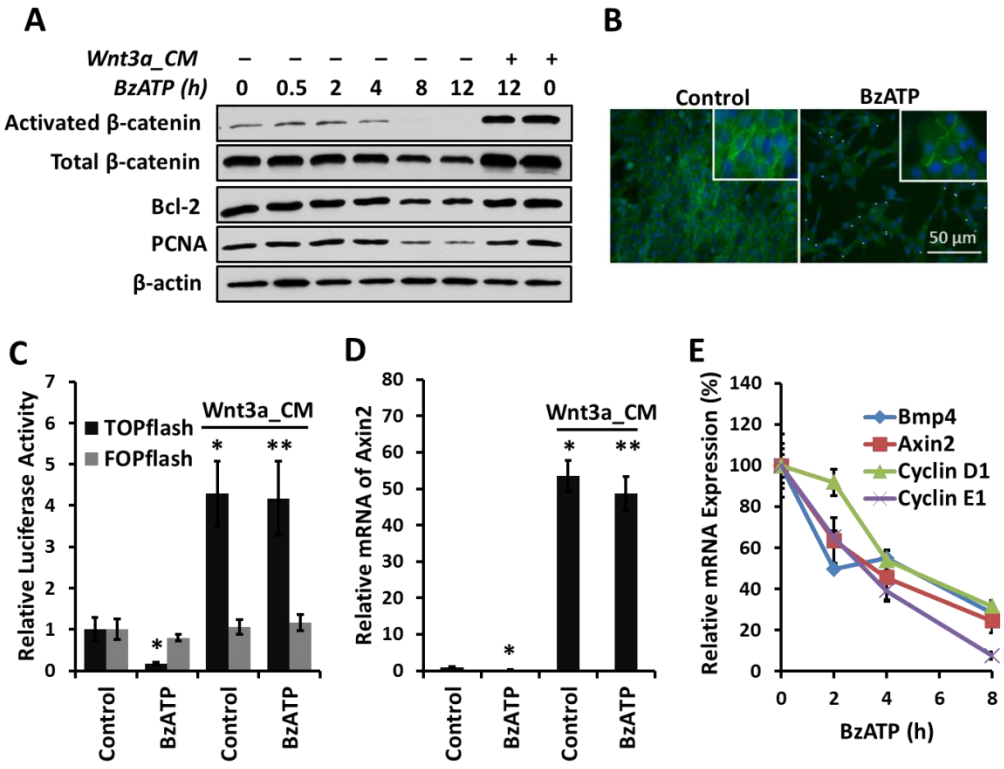

Fig. II. 4. Activation of P2X7R represses Wnt/β-catenin signaling. (A) E10 cells were treated with 400 μM BzATP for 0, 0.5, 2, 4, 8, and 12 hours with or without 50% Wnt3a_CM. Western blot was carried out to determine the protein expression of activated β-catenin, total β-catenin, Bcl-2, and PCNA. The expression of β-actin was used as an internal control. (B) Immunostaining was used to assess the β-catenin protein Expression in E10 cells treated with or without 400 μM BzATP for 6 hours. (C) Two hundred ng TOPflash/FOPflash and 1 ng pRL-TK, a control plasmid expressing a *Renilla* luciferase, were transfected into E10 cells. Two days after transfection, E10 cells were treated with 400 μM BzATP for 4 hours with or without 50% Wnt3a_CM. Dual-luciferase assay was performed and the results were expressed as the ratio of TOPflash/FOPflash luciferase activity to pRL-TK. (D) E10 cells were stimulated with 400 μM BzATP

for 8 hours with or without 50% Wnt3a_CM. The relative mRNA expression of Axin2 (fold changes) was determined using Real-time PCR and normalized to 18S rRNA. (E) The relative mRNA expression of Wnt/β-catenin downstream genes in E10 cells treated with 400 μM BzATP for various times were determined using Real-time PCR.Data. shown are means ± s.e.m. of three independent experiments. Statistical significance was determined by ANOVA analysis with posthoc *Tukey's* test. *P<0.001 v.s. control. **P<0.001 v.s. BzATP without Wnt3a_CM.

2.4.4 Wnt3a blocks P2X7R-mediated cell death

To evaluate the role of Wnt/β-catenin signaling in P2X7R-mediated cell death, we activated Wnt/β-catenin signaling with its nature ligand, Wnt3a and examined its effect on P2X7R-mediated depression of Wnt/β-catenin signaling and cell death. Wnt3a_CM and Wnt5a_CM were obtained from L-cells stably expressed Wnt3a or Wnt5a. The medium from L-cells (Con_CM) were used as a control. The pre-treatment of E10 cells with Wnt3a_CM prevented BzATP-mediated down-regulation of total β-catenin and activated β-catenin (Fig. II. 4A), inhibition of TOPflash activity (Fig. II. 4C) and decrease of Axin2 (Fig. II. 4D). As shown above, BzATP treatment caused a decrease in cell number of E10 cells. Wnt3a_CM, but not Wnt5a_CM or Con_CM prevented the BzATP-induced decrease in cell number (Fig. II. 7A). Immunstaining confirmed the activation of Wnt/β-catenin in E10 cells by Wnt3a as evidenced by nuclear translocation of β-catenin (Fig. II. 5A). Activation of Wnt/β-catenin signaling by Wnt3a_CM in E10 cells also blocked P2X7-mediated decrease in cell viability and increase in LDH release (Fig. II. 5B and C). Wnt3a_CM also protected primary AEC-I like cells from BzATP-induced cell death (Fig. II. 5D). YO-PRO dye uptake triggered by BzATP was not inhibited by Wnt3a_CM (Fig. II. 6), indicating that P2X7R activity itself is not affected by the activation of Wnt/β-catenin signaling.

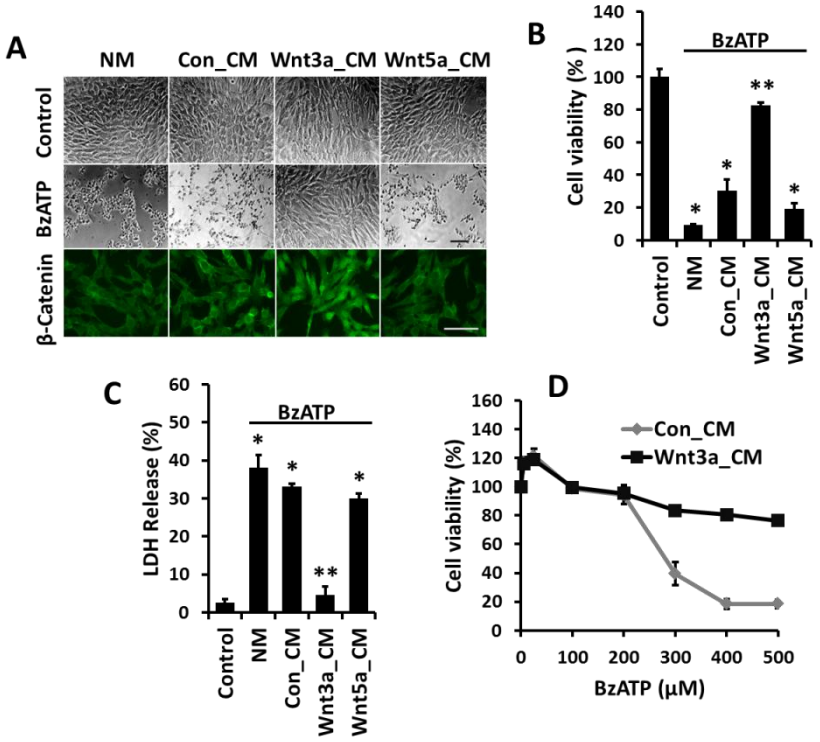

Fig. II. 5. Wnt3a blocks P2X7R-mediated cell death. E10 cells were treated with 400 μM BzATP for 8 hours together with 50% Control (Con), Wnt3a or Wnt5a conditioned medium (CM). (A) Immunostaining was carried out to determine β-catenin localization. (Scale bar: 50 μm). (B, C) Cell viability and LDH release were measured. Data shown are means ± s.e.m. Statistical significance was determined by ANOVA analysis with posthoc *Tukey's* test. *P< 0.001 v.s. control. **P<0.001 v.s. Con_CM. n=3. (D) Primary AEC I-like cells were treated with 0 - 500 μM BzATP for 12 hours with 50% Control (Con) or Wnt3a_CM, and Cell viability was measured.

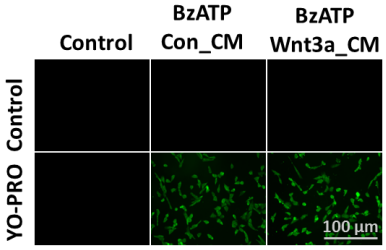

Fig. II. 6. Effect of Wnt3a on P2X7R activity. E10 cells were treated with 400 μM BzATP for 15 min and incubated with YO-PRO dye for 10 min. The fluorescence was observed using a Nikon TE-2000 inverted microscope.

2.4.5 Activation of P2X7R stimulates GSK-3β and proteasome activities

Since Wnt3a is known to inhibit GSK-3β, resulting in the activation of Wnt/ β-catenin signaling (5), we examined whether the down-regulation of Wnt/β-catenin pathway by P2X7R is through the stimulation of GSK-3β. We monitored the phosphorylation of Y216, an activated form of GSK-3β, and the phosphorylation of S9, an inactivated form of GSK-3β. The activation of P2X7R by BzATP increased the phosphorylation of Y216 and decreased the phosphorylation of S9 in GSK-3β without affecting the total GSK-3β expression (Fig. II. 7A). The result indicates that BzATP stimulates GSK-3β activity. As expected, LiCl, a selective inhibitor of GSK-3β, activated Wnt/β-catenin signaling as indicated by the translocation of β-catenin into nucleus (Fig. II. 7B) and reduced BzATP-mediated cell death (Fig. II. 7C and D).

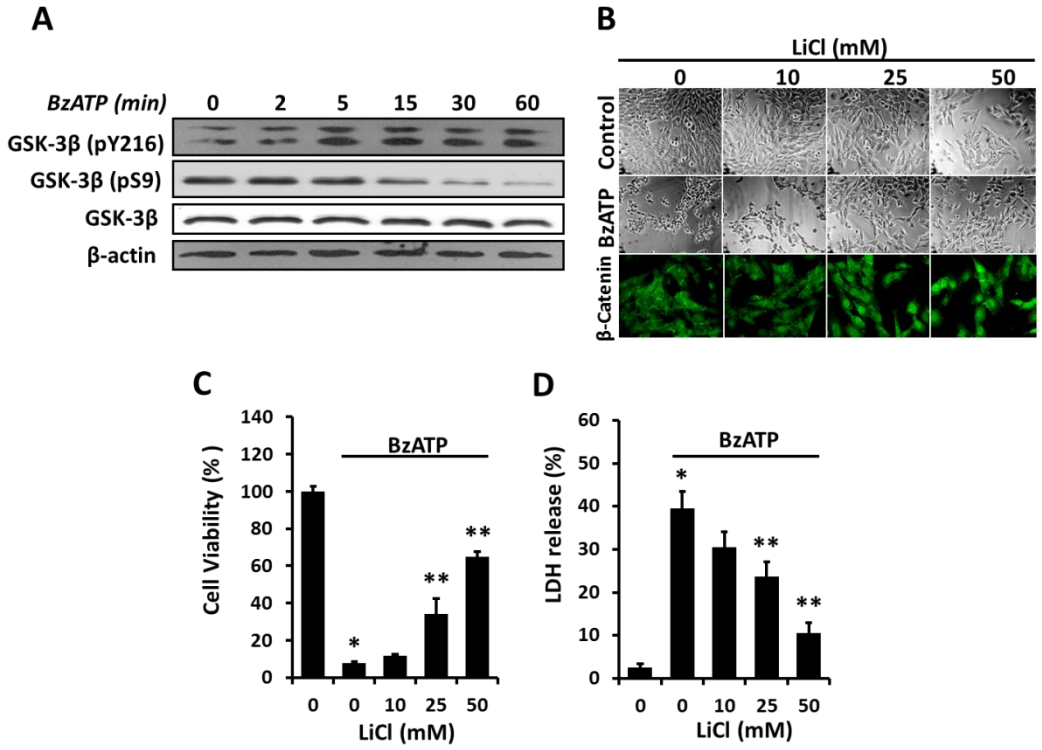

Fig. II. 7: GSK-3β mediates P2X7R-induced cell death. (A) E10 cells were incubated with 400 μM BzATP for different periods of time. The level of Tyr-216 *(pY216)* and Ser-9 *(pS9)* phosphorylated GSK-3β and total GSK-3β were determined by Western blot. (B) E10 cells were treated with 10, 25, and 50 mM LiCl in the presence or absence of 400 μM BzATP for 8 hours, and then immuo-stained with anti-β-catenin

antibodies. Scale bar: 50 μm. (C, D) E10 cells were treated with 400 uM BzATP together with different concentrations of LiCl for 8 hours. Cell viability and released LDH were measured. Data shown are means ± s.e.m. of three independent experiments. Statistical significance was deterined by ANOVA analysis with posthoc *Tukey's* test. *P<0.01 v.s. control (no BzATP). **P<0.01 v.s. BzATP only.

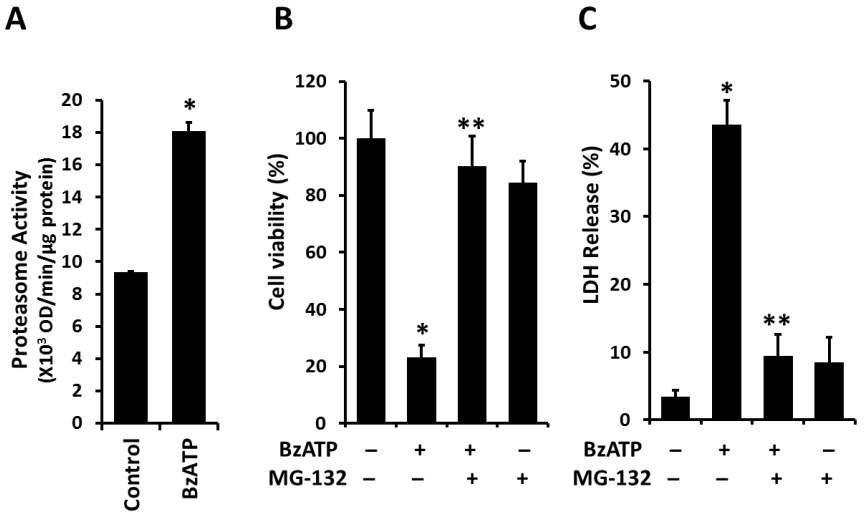

Fig. II. 8. Proteasome is involved in P2X7R-mediated cell death. (A) E10 cells were treated with 400 μM BzATP for 6 hours. Cell lysate was incubated with Suc-LLVY-AMC. Fluorescence was measured every 5 min for 30 min. The amount of AMC liberated per unit time was calculated as relative proteasome activity. (B, C) E10 cells were treated with 400 μM BzATP with or without 500 μM MG-132 for 8 hours. Cell viability and released LDH were measured. Values represent means ± s.e.m. of three independent experiments. Statistical significance was determined by ANOVA analysis with posthoc *Tukey's* test. *P<0.001 v.s. Control. **P<0.001 v.s. BzATP alone.

Because phosphorylated β-catenin by GSK-3β can be degraded through ubiquitin-proteasome system (5), we determined whether BzATP affected proteasome activity. The treatment of E10 cells with BzATP increased proteasome activity by one fold (Fig. II. 8A). Furthermore, MG-132, a proteasome inhibitor, blocked BzATP-mediated reduction of cell viability and increase in LDH release (Fig. II. 8B and C).

2.4.6 Wnt3a reduces AEC I death in BzATP-induced ALI in rats

To further investigate the role of P2X7R in AEC I death, BzATP was intratracheally instilled into the lung of rats. Histological examination of lung tissues showed evidence of diffuse lung injury with significant alveolar septal necrosis and edema formation seen in BzATP-treated mice (Fig. II. 9A). Bronchoalveolar lavage (BAL) cell analysis indicated that activation of P2X7R led to a 3.2-fold increase of alveolar macrophages. However, no significant neutrophil infiltrations were observed (Fig. II. 9B). BAL protein level was elevated by BzATP (Fig. II. 9C). LDH activity in BAL, representing necrotic cell death, was also increased by BzATP treatment (Fig. II. 9D). An increase of T1α, an AEC I marker, was observed in BAL of the BzATP-treated group, indicating AEC I damage (Fig. II. 9E). Instillation of Wnt3a_CM together with BzATP dramatically reduced the number of alveolar macrophages in BAL and BAL protein concentration in comparison with Con_CM (Fig. II. 9B and C). Wnt3a also significantly decreased LDH and T1α release caused by BzATP (Fig. II. 9D and E). It was noted that both protein concentration and LDH activity in BAL were higher in Con_CM than PBS group. This is likely due to existence of proteins and LDH in the conditioned medium. These results indicated that Wnt3a can limit AEC I death induced by activation of P2X7R in rats.

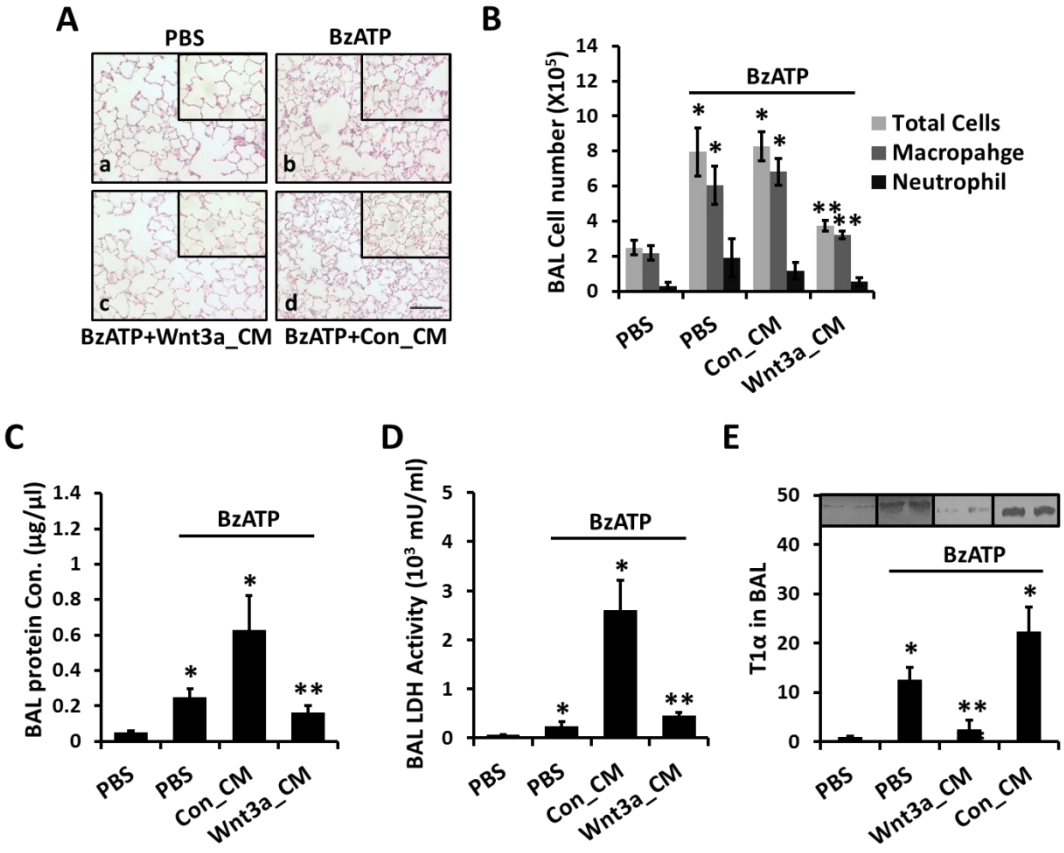

Fig. II. 9. Wnt3a reduces AEC I death in BzATP-treated rats. The rats were intratracheally instilled with BzATP with control (Con) or Wnt3a conditioned medium (CM) for 24 hours. (A) Histological analysis. Parafin sections (4 μm) of the lungs were stained with H&E. Control (a), BzATP (b), BzATP+Wnt3a_CM (c), and BzATP+Con_CM (d). Scale bar: 100 μm. (B) Total cell number and differential cell count in BAL. (C) BAL protein concentration. (D) LDH activity in BAL. (E) T1α protein in BAL. Representative bands of Western blots were shown. Values represent means ± s.e.m. (n=8/group). Statistical significance was determined by one-way ANOVA analysis with posthoc *Tukey's* test. *P<0.01 v.s. PBS alone group. **P<0.01 v.s. BzATP + Con_CM group.

2.4.7 Wnt3a reduces AEC I death during LPS-induced ALI in a ventilated mouse model

Because bacterial infection and mechanical ventilation are two major causes of ALI/ARDS in clinical situations, we further took use of a two-hit mouse model of ALI (22), which account for the impacts of both factors: LPS as bacterial infection and noninjurious mechanical ventilation (MV) as clinical mechanical ventilation support. In comparison with the

Con_CM group, Wnt3a_CM dramatically reduced the protein concentration in BAL fluid (Fig. II. 10A). LDH activity in BAL was also decreased 40% in Wnt3a_CM-treated group (Fig. II. 10B). Most importantly, T1α in BAL was 70% less in Wnt3a_CM -treated group than the control group (Fig. II. 10C). These results indicated that the activation of canonical Wnt/β-catenin signaling can significantly reduce AEC I death during ALI.

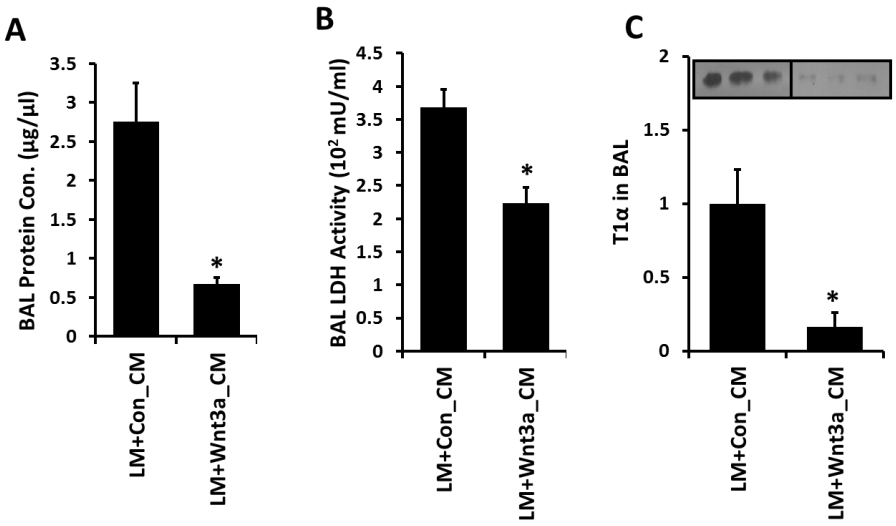

Fig. II. 10. Wnt3a reduces AEC I death in LPS and mechanical ventilation (LM)-induced ALI in mice. The mice were intratracheally instilled with LPS (0.5 mg/kg) for 1 hour and then ventilated for 2.5 hours (12 ml/kg, a respiratory rate of 125 bpm, and 3 cm H_2O PEEP). (A) Protein concentration in BAL. (B) LDH activity in BAL. (C) T1α protein in BAL. Values represent means ± s.e.m. (n=8/group). Statistical significance was determined by Student's *t*-test. *P<0.01 v.s. LM + Con_CM group.

2.5 Discussion

In this study, we investigated the mechanisms of P2X7R-mediated AEC I death during ALI. We found that the activation of P2X7R caused AEC I death at least partly by depressing the Wnt/β-catenin signaling pathway via GSK-3β and proteasome. The activation of the Wnt/β-catenin signaling or inhibition of GSK-3β or proteasome prevented P2X7R-mediated AEC I death. Furthermore, Wnt3a significantly reduced the AEC I damage caused by intratracheal instillation of BzATP in rats and LPS exposure in a ventilated mouse model.

ATP-induced cell death has been observed in P2X7R-expressing cells and can be blocked by P2X7R inhibitors (18,19). We have previously shown that P2X7R is highly expressed in AEC I in the lung (16). This gives us an idea that P2X7R might mediate AEC I death. This is supported by our current data showing that the treatment of E10 with BzATP, a specific P2X7R agonist, decreased cell viability in a dose-dependent manner, which was blocked by oATP, a P2X7R antagonist.

Activating Wnt/β-catenin signaling inhibits apoptosis induced by activating the intrinsic or mitochondrial pathway, such as starvation or hydrogen peroxide (23), or the extracellular or receptor pathway, such as TRAIL and TNF-α (23). Blocking the Wnt/β-catenin pathway prevents cell proliferation and results in apoptosis or necrosis (24). BzATP-induced AEC I death is likely through down-regulating Wnt/β-catenin signaling pathway since we observed BzATP activated GSK-3β and proteasome activity, and decreased β-catenin protein level.

The high level of extracellular ATP could be one major contributor to the pathogenesis of ALI (25). ATP-induced cell death has been observed in several inflammatory diseases, including colitis (26), spinal cord injury (27) and glomerulonephritis (28). P2X7R knockout mice have a protective phenotype of attenuated inflammation in models of LPS -induced acute lung injury (20) and bleomycin-induced lung fibrosis (25). P2X7R also functions as an inflammatory mediator and participates in the pathogenesis of several chronic lung inflammatory diseases such as asthma and emphysema (29). In our study, direct activation of P2X7R through intratracheal instillation of BzATP caused severe AEC I death and LDH release into the alveolar space, supporting the contribution of P2X7R to the pathogenesis of ALI.

There are no standard methods for activating Wnt/β-catenin signaling in the lung, an organ with more than 40 different types of cells. Wnt3a is one of the reported ligands constitutively present in the lung that can activate Wnt/β-catenin signaling in alveolar epithelium

(9). We demonstrated that the activation of Wnt/β-catenin in the lungs by Wnt3a reduced AEC I damage in two rodent models: BzATP-induced ALI in rat and a clinically relevant LPS and mechanical ventilation model in mice. GSK3β inhibitors are other compounds that are used to activate Wnt/β-catenin signaling in mice. These inhibitors attenuate the acute inflammation in blemocycin- and carrageenan-induced ALI (30). However, they also interfere with other signaling including NFκB and NFAT. Our current findings provide proof-of-concept to manipulate Wnt/β-catenin signaling as an efficient way to limit AEC I death during ALI.

Taken together, we demonstrate that P2X7R induces AEC I death by suppressing Wnt/β-catenin signaling via activating GSK-3β and proteasome. Wnt3a overcomes P2X7R-mediated down-regulation of Wnt/β-catenin signaling and prevents AEC I death during the acute phase of ALI/ARDS (Fig. II. 11). Our study on Wnt/β-catenin signaling and P2X7R-mediated purinergic signaling provides insights for future drug development and new therapeutic strategies of exploration.

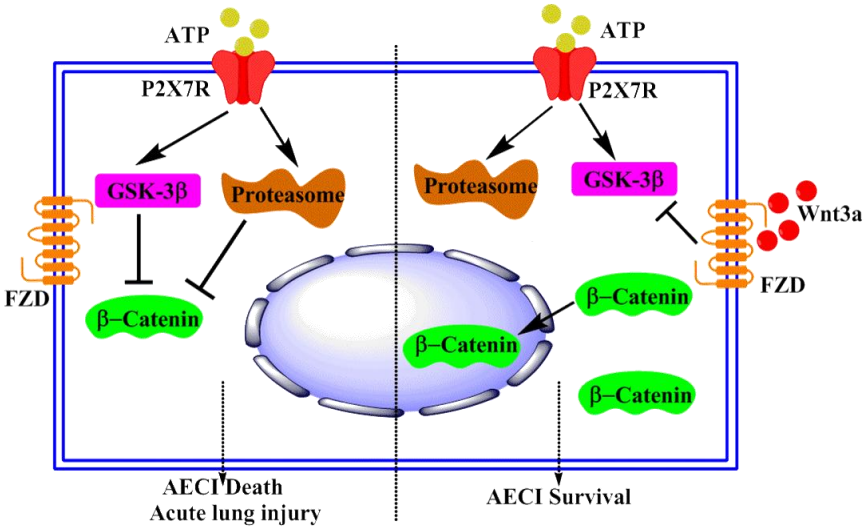

Fig. II. 11. A model of P2X7R-induced AEC I death and Wnt3a–mediated protection. Activation of P2X7R by ATP activates GSK-3β and proteasome and leads to degradation of β-catenin. This causes AEC I cell death. With the addition of Wnt3a, the activity of GSK-3β is inhibited. β-catenin is accumulated in the cytoplasmic and translocated into cell nucleus, which enhances AEC I cell survival.

2.6 Acknowledgements

We thank Dr. Mary Williams (Boston University) for providing anti-T1α antibody and E10 cells with the permission of Dr. Al Malkinson (University of Colorado), Dr. Annmarie Surprenant (University of Manchester) for HEK293-P2X7R cells, Dr. Roland Koslowski (Dresden University of Technology) for R3/1 cells, Dr. Joseph Alcorn (University of Texas Health Sciences Center at Houston) for MLE-15 cells, Dr. Rama Mallamaplli (University of Pittsburgh) for Pre-TII cells. Hamster anti-mouse T1α antibody developed by Dr. Andrew Farr (University of Washington) was obtained from the Developmental Studies Hybridoma Bank developed under the auspices of the NICHD and maintained by The University of Iowa, Department of Biology, Iowa City, IA 52242.

2.7 Reference

1. Matthay, M. A. and Zemans, R. L. (2011) *Annu. Rev. Pathol.* **6,** 147-163
2. Dobbs, L. G., Johnson, M. D., Vanderbilt, J., Allen, L., and Gonzalez, R. (2010) *Cell Physiol Biochem.* **25,** 55-62
3. Chen, J., Chen, Z., Chintagari, N. R., Bhaskaran, M., Jin, N., Narasaraju, T., and Liu, L. (2006) *J Physiol* **572,** 625-638
4. Tang, P. S., Mura, M., Seth, R., and Liu, M. (2008) *Am J Physiol Lung Cell Mol Physiol* **294,** L632-L641
5. Clevers, H. and Nusse, R. (2012) *Cell* **149,** 1192-1205
6. Weng, T., Gao, L., Bhaskaran, M., Guo, Y., Gou, D., Narayanaperumal, J., Chintagari, N. R., Zhang, K., and Liu, L. (2009) *J. Biol. Chem.* **284,** 28021-28032
7. Wang, Y., Huang, C., Reddy, C. N., Bhaskaran, M., Weng, T., Guo, Y., Xiao, X., and Liu, L. (2013) *Nucleic Acids Res.* **41,** 3833-3844
8. Tanjore, H., Degryse, A. L., Crossno, P. F., Xu, X. C., McConaha, M. E., Jones, B. R., Polosukhin, V. V., Bryant, A. J., Cheng, D. S., Newcomb, D. C., McMahon, F. B., Gleaves, L. A., Blackwell, T. S., and Lawson, W. E. (2013) *Am. J Respir. Crit Care Med.* **187,** 630-639
9. Konigshoff, M., Kramer, M., Balsara, N., Wilhelm, J., Amarie, O. V., Jahn, A., Rose, F., Fink, L., Seeger, W., Schaefer, L., Gunther, A., and Eickelberg, O. (2009) *J. Clin. Invest* **119,** 772-787

10. Sharma, S., Tantisira, K., Carey, V., Murphy, A. J., Lasky-Su, J., Celedon, J. C., Lazarus, R., Klanderman, B., Rogers, A., Soto-Quiros, M., Avila, L., Mariani, T., Gaedigk, R., Leeder, S., Torday, J., Warburton, D., Raby, B., and Weiss, S. T. (2009) *Am. J. Respir. Crit Care Med.* **181,** 328-336

11. Kneidinger, N., Yildirim, A. O., Callegari, J., Takenaka, S., Stein, M. M., Dumitrascu, R., Bohla, A., Bracke, K. R., Morty, R. E., Brusselle, G. G., Schermuly, R. T., Eickelberg, O., and Konigshoff, M. (2011) *Am. J Respir. Crit Care Med.* **183,** 723-733

12. Wang, R., Ahmed, J., Wang, G., Hassan, I., Strulovici-Barel, Y., Hackett, N. R., and Crystal, R. G. (2011) *PLoS. ONE.* **6,** e14793

13. Flozak, A. S., Lam, A. P., Russell, S., Jain, M., Peled, O. N., Sheppard, K. A., Beri, R., Mutlu, G. M., Budinger, G. S., and Gottardi, C. J. (2009) *J. Biol. Chem.* **285,** 3157-3167

14. Zemans, R. L., Briones, N., Campbell, M., McClendon, J., Young, S. K., Suzuki, T., Yang, I. V., De, L. S., Reynolds, S. D., Mason, R. J., Kahn, M., Henson, P. M., Colgan, S. P., and Downey, G. P. (2011) *Proc. Natl. Acad. Sci. U. S. A* **108,** 15990-15995

15. Khakh, B. S. and North, R. A. (2006) *Nature.* **442,** 527-532

16. Chen, Z., Jin, N., Narasaraju, T., Chen, J., McFarland, L. R., Scott, M., and Liu, L. (2004) *Biochem. Biophys. Res. Commun.* **319,** 774-780

17. Mishra, A., Chintagari, N. R., Guo, Y., Weng, T., Su, L., and Liu, L. (2011) *J. Cell Sci.* **124,** 657-668

18. Hanley, P. J., Kronlage, M., Kirschning, C., del, R. A., Di, V. F., Leipziger, J., Chessell, I. P., Sargin, S., Filippov, M. A., Lindemann, O., Mohr, S., Konigs, V., Schillers, H., Bahler, M., and Schwab, A. (2012) *J Biol. Chem.* **287,** 10650-10663

19. Jun, D. J., Kim, J., Jung, S. Y., Song, R., Noh, J. H., Park, Y. S., Ryu, S. H., Kim, J. H., Kong, Y. Y., Chung, J. M., and Kim, K. T. (2007) *J Biol. Chem.* **282,** 37350-37358

20. Moncao-Ribeiro, L. C., Cagido, V. R., Lima-Murad, G., Santana, P. T., Riva, D. R., Borojevic, R., Zin, W. A., Cavalcante, M. C., Rica, I., Brando-Lima, A. C., Takiya, C. M., Faffe, D. S., and Coutinho-Silva, R. (2011) *Respir. Physiol Neurobiol.* **179,** 314-325

21. Ferrari, D., Pizzirani, C., Adinolfi, E., Lemoli, R. M., Curti, A., Idzko, M., Panther, E., and Di Virgilio, F. (2006) *J. Immunol.* **176,** 3877-3883

22. Altemeier, W. A., Matute-Bello, G., Frevert, C. W., Kawata, Y., Kajikawa, O., Martin, T. R., and Glenny, R. W. (2004) *Am. J. Physiol Lung Cell Mol. Physiol* **287,** L533-L542

23. Doubravska, L., Simova, S., Cermak, L., Valenta, T., Korinek, V., and Andera, L. (2008) *Apoptosis.* **13,** 573-587

24. You, L., He, B., Xu, Z., Uematsu, K., Mazieres, J., Fujii, N., Mikami, I., Reguart, N., McIntosh, J. K., Kashani-Sabet, M., McCormick, F., and Jablons, D. M. (2004) *Cancer Res* **64,** 5385-5389

25. Riteau, N., Gasse, P., Fauconnier, L., Gombault, A., Couegnat, M., Fick, L., Kanellopoulos, J., Quesniaux, V. F., Marchand-Adam, S., Crestani, B., Ryffel, B., and Couillin, I. (2010) *Am. J. Respir. Crit Care Med.* **182,** 774-783

26. Gulbransen, B. D., Bashashati, M., Hirota, S. A., Gui, X., Roberts, J. A., MacDonald, J. A., Muruve, D. A., McKay, D. M., Beck, P. L., Mawe, G. M., Thompson, R. J., and Sharkey, K. A. (2012) *Nat. Med.* **18,** 600-604

27. Wang, X., Arcuino, G., Takano, T., Lin, J., Peng, W. G., Wan, P., Li, P., Xu, Q., Liu, Q. S., Goldman, S. A., and Nedergaard, M. (2004) *Nat. Med.* **10,** 821-827

28. Taylor, S. R., Turner, C. M., Elliott, J. I., McDaid, J., Hewitt, R., Smith, J., Pickering, M. C., Whitehouse, D. L., Cook, H. T., Burnstock, G., Pusey, C. D., Unwin, R. J., and Tam, F. W. (2009) *J Am Soc. Nephrol.* **20,** 1275-1281

29. Lucattelli, M., Cicko, S., Muller, T., Lommatzsch, M., de, C. G., Cardini, S., Sundas, W., Grimm, M., Zeiser, R., Durk, T., Zissel, G., Sorichter, S., Ferrari, D., Di, V. F., Virchow, J. C., Lungarella, G., and Idzko, M. (2011) *Am. J. Respir. Cell Mol. Biol.* **44,** 423-429

30. Cuzzocrea, S., Crisafulli, C., Mazzon, E., Esposito, E., Muia, C., Abdelrahman, M., Di, P. R., and Thiemermann, C. (2006) *Br. J Pharmacol.* **149,** 687-702

CHAPTER III

PLATELET-DERIVED WNT ANTAGONIST DICKKOPF-1 IS IMPLICATED IN ICAM-1/VCAM-1-MEDIATED NEUTROPHILIC ACUTE PULMONARY INFLAMMATION

3.1 Abstract

Neutrophil infiltration represents the early acute inflammatory response in acute lung injury. The recruitment of neutrophils from peripheral blood across endothelial/epithelial barrier into alveolar airspace is highly regulated by the adhesion molecules on alveolar epithelial cells (AEC). Wnt/β-catenin signaling is involved in the progression of inflammatory lung diseases including asthma, emphysema and pulmonary fibrosis. However, the function of Wnt/β-catenin signaling in acute lung inflammation is unknown. Here, we identified platelet-derived Dickkopf-1 (Dkk1) as the major Wnt antagonist contributing to the suppression of Wnt/β-catenin signaling in AEC during acute lung inflammation. Intratracheal administration of Wnt3a or neutralization of Dkk1 inhibited neutrophil influx into alveolar airspace of injured lungs. Activation of Wnt/β-catenin signaling in AEC attenuated ICAM-1/VCAM-1-mediated adhesion of both macrophages and neutrophils to AEC. We reported for the first time a role of Wnt/β-catenin signaling in modulating inflammatory response, and a functional communication between platelets and AEC during acute lung inflammation. Targeting Wnt/β-catenin signaling and the communication between platelets and AEC therefore represents a potential therapeutic strategy to limit acute pulmonary inflammation.

Keywords: Platelets, Dkk1, Wnt/β-catenin signaling, ICAM-1/VCAM-1, acute lung inflammation

3.2 Introduction

Activation and transmigration of neutrophils through endothelium, interstitium, and epithelium is the central event in the pathogenesis of ALI/ARDS (1). Activated neutrophils release cytotoxic compounds, including proteolytic enzymes, cationic peptides, and ROS, that can damage host cells. The depletion of neutrophils has been proven to be protective in multiple animal models of ALI (2-4). Adhesion molecules such as inter-cellular adhesion molecule 1 (ICAM-1 or CD54) and vascular adhesion molecular 1 (VCAM-1 or CD106) are extensively involved in the transendothelial/epithelial migration of neutrophils during ALI (1,5). Up-regulation of ICAM-1 and VCAM-1 expression in pulmonary vascular endothelium promotes neutrophil sequestration and mediates strong adhesion of neutrophils to endothelial cells (1). Both ICAM-1 and VCAM-1 are also expressed in AEC and mediates the adhesion of neutrophils and macrophages, and facilitates the transepithelial migration of monocytes (6-9). Shedding of sICAM-1 into alveolar airspace from AEC I is also reported in ALI (10). sICAM-1 is capable of activating alveolar macrophages, which play critical roles in host defense and is the major source of proinflammatory cytokines including tumor necrosis factor-alpha (TNF-α) and Interleukin-6 (IL-6) (11). Up-regulation of ICAM-1 and VCAM-1 is generally considered as a result of increased gene transcription upon stimulation by inflammatory cytokines such as TNF-α and interleukin-1β (IL-1β) (12). The promoter regions of ICAM-1 and VCAM-1 genes have been reported to contain several NFκB (P50/P65) binding sites. Mutations of these sites eliminate their responsiveness to TNFα (12).

Platelets are the central mediators in hemostasis of circulatory system and the major contributors to acute pulmonary inflammation by regulating inflammatory response of endothelial cells and activation of leukocytes (13-16). Acute pulmonary inflammation is always associated

with the activation of aggressive platelets in the blood and sequestration in pulmonary vascular beds (17,18). Platelet production following the onset thrombocytopenia are increased by up to 20-fold under the conditions of peripheral demand and inflammation (18). Activated platelets release cytokines (IL-1β and CD40L), chemokines (PF4, CCL5 and RANTES), and other soluble factors (PFA and Dkk1) to amplify the acute inflammatory response. Platelets also aggregate with neutrophils or monocytes via cell surface P-selectin (CD62P), which is considered as a molecular marker of platelet activation, and provides supportive juxtacrine and paracrine signals (18-20). By interacting with endothelial cells, activated platelets cause increases of vascular permeability, and promote the release of proinflammatory cytokines (IL-6) or chemokines (IL-8) from endothelial cells as well (19,21) . Platelet components are found in the broncheoalveolar fluid (BAL) from ARDS patients (22). However, it is still unclear whether platelets directly affect the functions of alveolar epithelium during the development of ALI (18).

Wnt/β-catenin signaling is essential in maintaining proper embryonic lung development (23) and adult lung repair after injury (24-27). Although the importance of Wnt/β-catenin signaling in regulating inflammation is emerging, only limited evidence is available for its implication in acute pulmonary inflammation (28-31). Wnt/β-catenin signaling inhibits the acute inflammatory response by suppressing proinflammatory cytokines (TNFα and IL-6) (31,32), chemokines (IL-8 and CCL2) (33,34), adhesion molecule (VCAM-1 and ICAM-1) (34,35), and other inflammatory mediators (NOS2, TC1, and COX-2) (34,36) through interacting with NFκB signaling and TLR-mediated signaling (33,36,37). In inflammatory lung diseases, suppression of Wnt/β-catenin signaling can be observed in COPD (38) and asthma patients (32,39), and contributes to the dysfunctional epithelial repair. Inhibition of Wnt/β-catenin signaling is also reported in mechanical ventilation (MV)-insulted and S. pneumoniae-infected lungs (40,41). Elevation of Wnt antagonist sFRP1 in experimental emphysema is recently discovered to be substantially responsible for the depression of Wnt/β-catenin signaling (42). Taken with the

reduced capacity of BAL from ARDS patients to activate Wnt/β-catenin signaling in fibroblasts (106), it is important to identify the potential deposition of Wnt antagonists in the alveolar space and explore the emerging roles of Wnt/β-catenin signaling in the pathogenesis of ALI/ARDS.

By regulating inflammatory response of endothelial cells and homeostasis of epithelial cells, Wnt antagonist Dkk1 contributes to several inflammatory diseases such as atherosclerosis, arthritis, and osteoporosis (19,28,43). In idiopathic pulmonary fibrosis (IPF) patients, Dkk1, potentially released from activated platelets, is found to accumulate in alveolar space and BAL (44).

In the current study, we utilized a clinically relevant two-hit acute lung inflammation model induced by low tidal volume MV and moderate dose of LPS (45), and identified platelet-derived Dkk1 as a major Wnt antagonist accompanied with suppression of Wnt/β-catenin signaling in AEC. The same phenomenon was further confirmed in murine models of bacterial or influenza viral pneumonia. The administration of Wnt3a or neutralization of Dkk1 significantly reduced ICAM-1/VCAM-1-mediated neutrophil trafficking during acute lung inflammation. By targeting their promoters, Wnt/β-catenin signaling negatively regulated ICAM-1 and VCAM-1 expression in AEC. Our results indicated a novel function of Wnt/β-catenin signaling in AEC and a distinctive communication between platelets and alveolar epithelium. We thus conclude that platelet-derived Wnt antagonist Dkk1 plays an important role in the control of Wnt/β-catenin signaling to regulate ICAM-1/VCAM-1-mediated acute inflammatory response, and the pharmacological interferences of platelet function, Dkk1 production, or Wnt/β-catenin signaling may constitute new therapeutic methods to restrict the pathogenesis of acute pulmonary inflammation.

3.3 Materials and methods

3.3.1 Animals

Male C57BL/6N mice were purchased from Jackson Laboratory (Bar Harbor, ME, USA). Male Sprague-Dawley rats were purchased from Charles River Breeding Laboratories (Wilmington, MA). All the animals were housed and cared for by OSU Laboratory Animal Resource Unit (LARU) operated by the Center for Veterinary Health Sciences (Stillwater, OK). All animal experimental procedures were reviewed and approved by the Institutional Animal Care Committee (IACUC) of Oklahoma State University.

3.3.2 Cell culture

The AEC I cell line, E10 cell was a generous gift from M. Williams (Pulmonary Center, Boston University School of Medicine, MA) and was cultured in CMRL-1066 medium (Invitrogen, CA) containing 10% heat-inactivated fetal bovine serum (FBS) (Atlantic Biological, Miami, FL) and 2.5 mM L glutamax® (Invitrogen, CA). Cells were maintained at 37 °C in a humidified atmosphere containing 5% CO_2.

3.3.3 Mouse AEC II and AEC isolation and culture

AEC II (>90%) or AEC I-enriched preparation (33% AEC I and 66% AEC II) from Male C57BL/6N mice (6-8 weeks of age) were isolated as described previously (46). Lungs were cleared of blood by perfusion with solution II (0.9% NaCl, 0.1% glucose, 10 mM HEPES, pH 7.4, 5 mM KCl, , 1.7 mM $CaCl_2$, 1.3 mM $MgSO_4$, 3 mM Na_2HPO_4, 3 mM NaH_2PO_4, 0.1 mg/ml streptomycin sulfate, and 0.06 mg/ml penicillin G). AEC II was released from the lungs by intratracheally instilled elastase three times (8 caseinolytic units/ml final concentration in 3 ml solution II, Worthington Biomedical, Freehold, NJ) for 20 min each at 37°C. Then the lungs were chopped and further incubated with DNase I (100 µg/ml, Sigma-Aldrich, St. Louis, MO) for 45 mins at 37°C with gentle agitation. The resulting cell suspension was filtered sequentially through 160-, 37- and 15-µm nylon filters and centrifuged for 10 mins at 250 x *g* at 4°C. The cell pellet was resuspended in DMEM (GIBCO, Grand Island, NY) and incubated in a 100-mm petri dish

coated with mouse IgG (75 μg/dish) for 1 hour. The nonadherent cells were centrifuged again and resuspended in DMEM containing 10% FBS. Cell viability was determined by trypan blue exclusion. AEC II was then seed in 12-well tissue culture plates (Corning) at 1 x 10^6 cells/well in DMEM supplemented with 10% FBS, penicillin, and streptomycin. AEC II was cultured for four to five days to allow them trans-differentiate into AEC I-like cells. For AEC I-enriched preparation, lungs were cleared of blood as described above and filled with an enzyme mix (3 ml) consisting of dispase (250 units/ml, BD Biosciences, Franklin Lakes, NJ) and elastase (4 units/ml), and incubated at 37°C for 15 mins for two runs. After being chopped, lung tissues were further digested with the addition of DNase I (100 μg/ml) for 45 mins at 37°C, with intermittent shaking. The digested lungs were filtered sequentially through 160-, 37- and 15-μm nylon filters and centrifuged for 10 mins at 250 x *g* at 4 °C. Cells were then resuspended in DMEM containing 10% FBS. Cytospins with either purified AECII or AECI cell-enriched preparations were subsequently carried out with 2 x10^5 cells/slide and the cells were subjected to immunofluorescence.

3.3.4 Rat AEC II isolation

Rat AEC II were isolated from male Sprague-Dawley rats (180-200 g) as previously described in our lab (47). The lungs were perfused using solution I (0.9% NaCl, 0.1% glucose, 30 mM HEPES, 6 mM KCl, 0.1 mg/ml streptomycin sulfate, 0.07 mg/ml penicillin G, 0.07 mg/ml EGTA, 3 mM Na2HPO4, and 3 mM NaH2PO4, at pH 7.4) to clear red blood cells. Then the lungs were lavaged with solution II (solution I plus 3 mM MgSO4 and 1.5 mM CaCl2), and digested with elastase (3 units/ml) for 3 *X* 12 mins at 37°C, and chopped with a Mcllwain tissue chopper. The cell suspension was further digested with 100 ng/ml DNase I and filtered through 160- and 37-μm nylon mesh once and 15-μm nylon mesh twice. Then cells were seeded on rat IgG-coated polystyrene bacteriological plates twice for 45 and 30 mins to remove macrophages. The unattached cells were collected by centrifugation. The isolated AEC II had a purity of 90%

and a viability of over 98%. The AEC II were seeded onto 12-well tissue culture plastic plates at a density of 1 x 10^6 cells/plate in DMEM with 10% FBS.

3.3.5 Preparation of conditional medium

Murine L-Wnt3a cell line (ATCC, Manassas, VA) producing soluble recombinant mouse Wnt3a and control murine L cell line (ATCC, Manassas, VA) were cultured in DMEM containing 10% FBS, 1% L-glutamine, and 0.4 mg/ml G418 (Invitrogen, Carlsbad, CA). To generate Wnt3a or control (Con)-conditional medium (CM), cells were cultured in G418-free growth medium for 4 days and changed into fresh G418-free medium for additional 3 days. The cultured media were mixed, sterile-filtered, aliquoted, and stored at -80°C until use. The activity of Wnt3a_CM was determined by TOPflash assay performed in E10 cells. Wnt3a_CM normally showed an approximately 6-fold increase of the reporter activity compared with Con_CM. To concentrate the soluble Wnt3a, 20 ml Wnt3a_CM or Con_CM were reduced into 2 ml 10X Wnt3a_CM or 10X Con_CM by an ultra-filtration kit (Millipore, Billerica, MA).

3.3.6 Murine acute pulmonary inflammation model induced by LPS and mechanical ventilation

A two-hit acute lung injury model with a moderate dose of LPS, followed by low tidal volume mechanical ventilation was adopted as described before (45). Male C57BL/6N mice (6-8 weeks of age) were divided into six groups (n=8/group): 1) spontaneous breathing non-ventilated control (Blank), 2) LPS in PBS with mechanical ventilation (LM), 3) LPS in Control conditional medium with mechanical ventilation (LM+Con_CM), 4) LPS in Wnt3a conditional medium with mechanical ventilation (LM+Wnt3a_CM), 5) LPS and mouse IgG2b in PBS with mechanical ventilation (LM+Control IgG), and 6) LPS and anti-Dkk1 antibody in PBS with mechanical ventilation (LM+Anti-Dkk1). Mice were anesthetized with ketamine (80 mg/kg) and xylazine (10 mg/kg) intraperitoneally, and half dose 2 hours later. Tracheotomy was performed to expose the trachea. Mice were intratracheally instilled with LPS (*Escherichia coli* serotype 0111:B4, Sigma-

Aldrich; 0.5 µg/g bodyweight, 1.5 µl/g) or 10X conditional medium (1µl/g). Sixty minutes later, mice were ventilated on a small animal ventilator (SAR-830/AP; CWE Inc) with following settings: respiratory rate = 125 breaths per minute; inspiratory and expiratory ratio = 1:2; tidal volume (Vt) = 12 ml/kg bodyweight; PEEP = 3 cm of H_2O and an inspired oxygen fraction of 0.21 for 150 mins. In Dkk1 neutralization experiments, LPS was co-administered intratracheally into the lungs with functional blocking mAb against mouse Dkk1 (86 µg/mouse, purified mouse anti-human Dkk1, MAB1096, R&D Systems. Inc, Minneapolis, MN) and isotype–matched control (purified mouse IgG1 isotype control, R&D Systems, Inc). Mechanical ventilation with the same settings was started after 60 mins and continued for additional 150 mins as described above. At the end of protocol, blood was collected by cardiac puncture.

3.3.7 Murine model of bacterial pneumonia

Male C57BL/6N mice (6-8 weeks) were anesthetized intraperitoneally with ketamine (80 mg/kg body weight) and xylazine (10 mg/kg body weight). After intranasal inoculation of *E.coli* (Strain 19138 from ATCC, 700,000 CFU/mouse), mice were housed for 24 hours and monitored every 8 hours**.** At the end of protocol, mice were sacrificed and blood collected by cardiac puncture.

3.3.8 Murine model of influenza viral pneumonia

Male C57BL/6N mice (6-8 weeks of age) were anesthetized with intraperitoneal injection of ketamine (80 mg/kg body weight) and xylazine (10 mg/kg body weight), and inoculated intranasally with H1N1 influenza virus A/Puerto Rico/8/1934 (250 pfu/mouse, ATCC). Mice were continually monitored for clinical signs such as ruffled fur and respiratory distress every 12 hours. Animals were sacrificed on days 0 - 7 post infection and blood collected by cardiac puncture.

3.3.9 Rat model of hyperoxia-induced acute lung injury

The hyperoxia model was used previously in our laboratory (47). Male Sprague-Dawley rats (180-220 g) were exposed to >95% oxygen in a sealed Plexiglas chamber for 48, 60 or 72 hours. The CO_2 in the chamber was removed by soda lime (Sigma-Aldrich). The control rats were exposed to room air. The oxygen concentration was continuously monitored using an oxygen sensor (OxyCheq, Marianna, Florida) and the flow rate was maintained at 8 L/min using a flow meter. Rats had free access to food and water. At the end of experiment, rats were sacrificed by abdominal arterial puncture.

3.3.10 Bronchoalveolar lavage analysis

The mouse lungs were lavaged with 1 ml of normal saline three times. Bronchoalveolar lavage (BAL) fluid was collected and centrifuged at 380 x *g* for 10 mins at 4°C. BAL cell pellets were resuspended in 200 µl of normal saline for subsequent analysis. Cell- free BAL fluid and lavaged lung tissue samples were frozen in liquid nitrogen and stored in a −80°C freezer. Total cell numbers were counted with a standard hemocytometer. Immune cell differential count was performed on the air dried cytospin slides visualized by Wright-Giemsa staining (Sigma-Aldrich). The total protein concentration in BAL was determined by BCA protein assay kit (Pierce, Rockford, IL).

3.3.11 Lung tissue myeloperoxidase (MPO) activity assay

Whole lung tissues were homogenized in 1 ml homogenization buffer (50 mM potassium phosphate, pH 6.0) by a dounce homogenizer and centrifuged at 14,000 *g* for 15 mins at 4°C. The pellet was resuspended in 1 ml homogenization buffer containing 50 mM hexadecyltrimethylammonium bromide (HTAB, Sigma-Aldrich). The samples were sonicated on ice for 20 seconds, freeze-thawed twice and centrifuged at 14,000 x *g* for 10 mins at 4°C. 2.9 ml of the homogenization buffer containing 0.167 mg/ml O-danisidine dihydrochloride (Sigma-Aldrich) and 0.0005% hydrogen peroxide (Sigma-Aldrich) was added to 100 µl of samples and

absorbance at 460 nm was measured for 20 mins at 2-min intervals. MPO activities were expressed as absorbance per min per milligrams of total protein.

3.3.12 ELISA

Dkk1, sVCAM-1, IL-6, and TNFα in BAL or plasma were determined by ELISA according to the manufacturers' instructions (Quantikine mouse sVCAM-1 and Dkk1 immunoassay; R&D Systems, Minneapolis, MN; and mouse IL-6, TNFα ELISA Ready-SET-Go; eBiosciences, San Diego, CA).

3.3.13 Platelet isolation and stimulation

Murine platelets were isolated from C57BL/6N mice (6-8 weeks of age) as described previously with some modifications (19). Blood was collected into 3.8% sodium citrate (pH 7.4) (2:1, volume) by cardiac puncture, and centrifuged at 250 x *g* for 10 mins to obtain the platelet-rich plasma (PRP). For platelet stimulation, PRP was treated by 100 μM thrombin receptor activating peptide (SFLLRN, Sigma-Aldrich) for indicated times and then centrifuged at 657 x *g* for 7 mins. The supernatant was collected as plasma and the platelet pellet was collected as well. For platelet releasate (PR) collection, PRP was centrifuged at 657 x *g* for 7 mins to pellet the platelets. Platelets were then resuspended in Tyrodes-HEPES buffer and stimulated by 0.1 U/ml thrombin (Sigma-Aldrich) for 90 mins. PR was collected by centrifugation at 2500 x *g* for 10 mins at 4°C.

3.3.14 Cell-based Dkk1 binding assay

The binding of Dkk1 to cultured mouse AEC was assayed using an ELISA protocol modified from a previous report (9). Freshly isolated mouse AEC II was cultured on fibronectin-coated 96-well plate until 100% confluence. Recombinant mouse Dkk1 (R&D Systems, Minneapolis, MN) was added into wells at different doses for 12 hours. Cells were fixed, washed

with PBS containing 0.05% Tween-20, and incubated with anti-mouse Dkk1 (1:200, Abcam, San Francisco, CA) mouse monoclonal antibody for 2 hours at room temperature. After being washed again, the cells were incubated with HRP-conjugated goat anti-mouse IgG for 1 hour. The cells were washed again and a TMB (Tetramethylbenzidine) substrate solution (Invitrogen, Carlsbad, CA) was added into the wells and color developed in 30 mins. The intensity of the color was then measured at 450 nm.

3.3.15 Western blot

The cells and whole lung tissues were homogenized and lysed in M-PER Mammalian Protein Extraction Reagent containing 1% Halt Protease/Phosphatase Inhibitor Cocktail (Pierce, Rockford, IL) at 4°C, followed by freeze/thaw cycles. The proteins were separated in 8-12% SDS-PAGE gels and transferred to nitrocellulose membranes. Then the membranes were blocked with 5% dried milk in Tris-buffered saline (10 mM Tris/HCl, 100 mM NaCl and 0.05% Tween; pH 7.5) (TBS-T) for 1 hour at room temperature and incubated overnight at 4°C with anti-Dkk1 (1:500, ab61275, Abcam, San Francisco, CA), anti-activated β-catenin (1:1000, Millipore, Billerica, MA), anti-β-catenin (1:2000, BD Transduction Laboratories, San Jose, CA), anti-VCAM-1 (1:1000, Santa Cruz Biotechnology, Santa Cruz, CA), anti-ICAM-1 (1:500, Abcam, San Francisco, CA), anti-CD41 (1:1000, BD Transduction Laboratories, San Jose, CA), anti-CD141 (1:1000, BD Transduction Laboratories, San Jose, CA), anti-T1α (1:200, 8.1.1, DHSB, Iowa City, IO), anti-p-P65 (ser536) (1:1000, Cell Signaling Technology, Danvers, MA), anti-P65 (1:1000, Cell Signaling Technology, Danvers, MA) and anti-β-actin (1:2000, BD Transduction Laboratories) antibodies. The blots were then rinsed in TBS-T, and incubated for 1 hour at room temperature with horseradish peroxidase (HRP) labled goat anti-rabbit, goat anti-mouse, or goat-anti-hamster secondary antibodies (1:2000, Jackson Immunoresearch, West Grove, PA). After wash, the blot was developed by SuperSignal West Pico Chemiluminescent Substrate (Pierce, Rockford, IL).

3.3.16 RNA isolation and Real-time PCR

Table III.1. Real time-PCR primer sequences

Gene	Species	Forward primers	Reverse primers
18S	Mouse	ATTGCTCAATCTCGGGTGGCTG	CGTTCTTAGTTGGTGGAGCGATTTG
Axin2	Mouse	TGACTCTCCTTCCAGATCCCA	TGCCCACACTAGGCTGACA
β-catenin	Mouse	GAAGCACAAGCGAACCGACTA	GTGGAGTGGAAGAGCGACT
Bmp4	Mouse	TTCCTGGTAACCGAATGCTGA	CCTGAATCTCGGCGACTTTTT
CCD1	Mouse	GCGTACCCTGACACCAATCTC	CTCCTCTTCGCACTTCTGCTC
Wnt1	Mouse	ATACGACCCCGTTTCTGCTG	TTCCACTCCCTCACCTTCAAAGC
Wnt3a	Mouse	TGGCTGAGGGTGTCAAAGC	CGTCTCACTGCGAAAGCTACT
Wnt7b	Mouse	TTTGGCGTCCTCTACGTGAAG	CCCCGATCACAATGATGGCA
Wnt11	Mouse	GCTGGCACTGTCCAAGACTC	CTCCCGTACCTCTCTCCA
Dkk1	Mouse	CTCATCAATTCCAACGCGATCA	GCCCTCATAGAGAACTCCCG
Dkk2	Mouse	CTGATGCGGGTCAAGGATTCA	CTCCCCTCCTAGAGAGGACTT
Dkk3	Mouse	CTCGGGGGTATTTTGCTGTGT	TCCTCCTGAGGGTAGTTGAGA
Dkk4	Mouse	GTACTGGTGACCTTGCTTGGA	CCGTTCATCGTGAAACGCTAAG
sFRP1	Mouse	TGGCCCGAGATGCTCAAATG	GGTTGTACCTTGGGGCTTAGA
KRM1	Mouse	ACAGCCAACGGTGCAGATTAC	TGTTGTACGGATGCTGGAAAG
KRM2	Mouse	GCTGCTTCGTGGACTCTGG	CCCTTCATGCGGCAGAATC
LPR5	Mouse	CTATCCGCAGGGCGTACCTA	CGAGTCACCTCAATTCTGTCAG
LPR6	Mouse	TTGTTGCTTTATGCAAACAGACG	GTTCGTTTAATGGCTTCTTCGC
ICAM-1	Mouse	GAGAGTGGACCCAACTGGAA	GCCACAGTTCTCAAAGCACA
VCAM-1	Mouse	CAATGGGGTGGTAAGGAA	GTCACAGCGCACAGGTAAGA
IL-6	Mouse	TAGTCCTTCCTACCCCAATTTCC	TTGGTCCTTAGCCACTCCTTC
IL-1β	Mouse	GTTTCTGCTTTCACCACTCCA	GAGTCCAATTTACTCCAGGTCAG
TNFα	Mouse	CCGGGAGAAGAGGGATAGCTT	TCGGACAGTCACTCACCAAGT
KC	Mouse	CTGGGATTCACCTCAAGAACATC	CAGGGTCAAGGCAAGCCTC
LIX	Mouse	TCCAGCTCGCCATTCATGC	TTGCGGCTATGACTGAGGAAG
MCP-1	Mouse	TTAAAAACCTGGATCGGAACCAA	GCATTAGCTTCAGATTTACGGGT
MIP-2	Mouse	CACTCTCAAGGGCGGTCAAA	TACGATCCAGGCTTCCCGGT
TGFβ	Mouse	CTCCCGTGGCTTCTAGTGC	GCCTTAGTTTGGACAGGATCTG
IL-10	Mouse	AGCAACCGTGGAGGACCA	CCATCAGCAGGACCCTATAATCA
Axin2	Rat	TGGTGCATACCTCTTCCGGACTTT	TTTCCTCCATCACCGCCTGAATCT
β-catenin	Rat	CAGTCCGAGATCAGCAGTCTCAT	GGACAAGCCACAGGACTACAAGA
Bmp4	Rat	CCCTGGTCAACTCCGTTAATTCT	CACCTTGTCGTACTCGTCCAGAT
CCD1	Rat	TGGGAAGTTGTGTTGGGTCGAG	TAATGCCATCACGGTCCCTACTTC
Wnt1	Rat	ATAGCCTCCTCCACGAACCT	GGAATTGCCACTTGCACTCT
Wnt3a	Rat	ACCTGGAGAAGGCTGGAAAT	ATGTGATCCAGGATGGTCGT
Wnt7b	Rat	AGCCAACCATCATCTGCAACA	GGCATTCATCGATACCCATC
Wnt11	Rat	TCACTCCGACCTGGTCTACTT	CTCAGTGATGCGGCATTCTTC
18S	Rat	TCCCAGTAAGTGCGGGTCATA	CGAGGGCCTCACTAAACCATC

Total RNA was extracted from cultured cells and whole lung tissues using TRI-Reagent (Molecular Research Center, Cincinnati, OH). Obtained RNA was digested with TURBO DNase (Ambion, Austin, TX, USA) to remove the genomic DNA contamination and quantified by Nanodrop (Wilmington, DE). 1 μg RNA were reverse-transcribed into cDNA using M-MLV reverse transcriptase (Invitrogen, Carlsbad, CA), random primers, and oligo dT (Promega, Madison, WI). Real-time PCRs were performed on 7900HT Fast Real-Time PCR System (Applied Biosystem, Foster City, CA) using SYBR Green I (Eurogentec, CA). The primers were

designed using Primer Express® (Applied Biosystems, Foster City, CA), and listed in Table III.1. PCRs were consisted of an initial denaturation step at 94°C for 5 min, followed by 40 cycles of amplification (94°C for 30 s, 60°C for 1min). A dissociation curve was generated after each PCR to view the specificity of the amplification. The data was normalized to mouse 18S rRNA.

3.3.17 Immunohistochemistry

Immunohistochemistry in lung tissue was performed as described as before (48). Briefly, 4 μm tissue sections were stained by the sequential use of a monoclonal mouse anti-Dkk1 antibody (1:50, Abcam, San Francisco, CA) and a biotin-conjugated goat anti-mouse IgG antibody (Jackson Immunoresearch, Newmarket, UK). The reaction was visualized using ABC reagent (Vector Labs, CA), followed by incubation with TSATM-plus horseradish peroxidase system (Vector Labs, CA). Tissue sections were counterstained with hematoxylin and viewed under a Nikon Eclipse E600 microscope. The pictures were captured by Photometrics CoolSnap CCD camera (Roper Scientific) and processed by Metavue software (Universal Imaging Co.).

3.3.18 Dual-luciferase assay

For promoter activity, E10 cells were seeded in 96-well plastic plates. After reaching ~85% confluence, the cells were transfected with 100 ng/well pGL3_phVCAM-1, pGL3_phICAM-1 (Switchgear Genomics, Menlo Park, CA) or pGL3 (Promega, Madison, WI) along with 2 ng/well phRL-TK (Promega, Madison, WI) with or without P65_pcDNA3.0 (Addgene, Cambridge, MA) for indicated time using lipofectamine 2000 (Invitrogen, Carlsbad, CA). For NFκB signaling activity, E10 cells were transfected with 100 ng/well pNFκB_luc (NFκB response element, Promega, Madison, WI) plasmid along with 2 ng/well phRL-TK (Promega, Madison, WI) with or without P65_pcDNA3.0 (Addgene, Cambridge, MA) for indicated times. For TOP/FOPFLASH assay, E10 cells were transfected with 100 ng/well TOPflash or FOPflash (Millipore, MA) along with 2 ng/well phRL-TK (Promega, Madison, WI)

for indicated times. At the end of experiment, cells were lysed in passive cell lysis buffer (Promega, Madison, WI). Dual-luciferase assay was performed using the Dual-Luciferase® Reporter Assay System (Promega, Madison, WI).

3.3.19 Flow Cytometry

Fluorescence activated cell sorter (FACS) analysis of freshly isolated platelets was performed to quantify the activity of platelets by detecting the surface expression of P-Selectin (CD62P) according to a previous report (49). Briefly, platelet-rich plasma was collected from mice, fixed in 1% paraformaldehyde for 10 mins, and suspended in FACS buffer (BD Biosciences). Then 1 x 10^8 cells were staining with PE-CD62P (eBioscience, San Diego, CA) and FITC-CD41 (platelet marker, eBioscience, San Diego, CA) antibodies or compatible IgGs (mouse IgG1κ for CD62P and rat IgG1κ for CD41) for 30 mins in room temperature. FACS analysis (Accuri™ C67; BD Biosciences) was performed to identify the percentage of PE-CD62P positive cells in FITC-CD41 positive populations.

3.3.20 Isolation rat neutrophils and alveolar macrophages

Neutrophils were isolated from Sprague-Dawley rats (200-250 g) by Histopaque 1119/1077 (Sigma-Aldrich , St. Louis, MO) gradients method as described before (50). Briefly, 5 ml of freshly collected rat blood (anticoagulated by sodium citrate, 4% w/v Solution) was put on the top of the gradient mixture (2.5 ml of Histopaque 1077 and 2.5 ml of Histopaque 1119). This mixture was centrifuged at 400 x *g* for 30 minutes. The second ring (from top to bottom) was collected and incubated with RBC Lysis Buffer (BD Biosciences, Franklin Lakes, NJ) to remove the erythrocytes. Finally, the cells were washed with HBSS (Hank's Balanced Salt Solution) at pH 7.2 at 270 x *g* for 8 min and resuspended in DMEM containing 10% FBS. Alveolar macrophages (AMϕ) were isolated from Sprague-Dawley rats (200-250 g) by bronchoalveolar lavage. Rats were lavaged with 7 ml sterile PBS containing 2 mM EDTA (pH 7.2) until a BAL

volume of 100 ml was recovered (approximately 18 times). AMϕ was washed twice in PBS and resuspended in DMEM containing 10% FBS.

3.3.21 Cell adhesion assay

E10 cells were plated into 12-well plate, grown to 90% confluence, treated as indicated in the results section and incubated with rat anti-mouse ICAM-1(10 μg/ml, clone YN1/1.7.4, R&D System) or rat anti-mouse VCAM-1 (10 μg/ml, M/K-2.7, R&D System). Freshly isolated rat AMϕ or neutrophils were added onto E10 cells monolayer and incubated for 30 mins. Nonadherent cells were removed by washing each well four times with culture medium very carefully. The remaining cells were fixed in 4% paraformaldehyde and visualized by Wright-Giemsa staining (Sigma-Aldrich, St. Louis, MO). The attached AMϕ and neutrophils were counted.

3.3.22 Immunofluorescence

Cells were fixed in 4% formaldehyde for 15 mins, followed by incubation in 0.3% Triton X-100 for 10 mins. After being blocked in 10% FBS for 30 mins, the cells were then incubated with anti-SP-C (1:200, Santa Cruz Biotechnology, Santa Cruz, CA), anti-T1α (1:50, 8.1.1, DHSB, Iowa City, IA), anti-β-catenin (1:200, BD Transduction Laboratories, San Jose, CA), or anti-P65 (1:200, Cell Signaling Technology, Danvers, MA) antibodies at 4 ℃ overnight. The cells were rinsed with PBS and then incubated with Alexa 488-conjugated anti-mouse or anti-hamster antibodies (1:250) for 1 h followed by DAPI nuclear staining. Finally, cells were washed and viewed by a Nikon Eclipse TE2000-U inverted fluorescence microscope.

3.3.23 Statistical analysis

All data were given as mean ± s.e.m. For analysis of statistical differences, one-way ANOVA with post hoc *Tukey's* test for multiple comparisons, two-tailed Wilcoxon ranked test

for non-parametric comparisons, or Student's *t*-test for two sets of data were applied. Significance was assumed when p values were < 0.05.

3.4 Results

3.4.1 Inhibition of Wnt/β-catenin signaling comes together with deposition of Dkk1 in the lungs during acute pulmonary inflammation.

Wnt/β-catenin signaling is involved in several different inflammatory lung diseases by regulating cell survival, repair and fibroproliferation (25,38,51). To determine whether Wnt/β-catenin signaling is modulated during acute lung inflammation, we quantified the mRNAs expression of the major components (downstream genes and Wnt ligands) of Wnt/β-catenin signaling in whole lung homogenates and freshly isolated AEC from the lungs challenged with LPS and mechanical ventilation (LM). As depicted in Fig. III. 1A, mRNA expression of downstream genes (Axin2, β-Catenin, Bmp4, and CCND1) was all significantly depressed in both injured lungs and AEC. The mRNA levels of canonical Wnt ligands (Wnt1, Wnt3a, Wnt7b, and Wnt11) were also remarkably reduced in LM-challenged lungs and AEC compared to control except that Wnt7b was slightly increased in injured lungs. The protein level of the central signaling transducer β-catenin and its activated form were both significantly decreased in LM-challenged lungs (Fig. III. 1B).

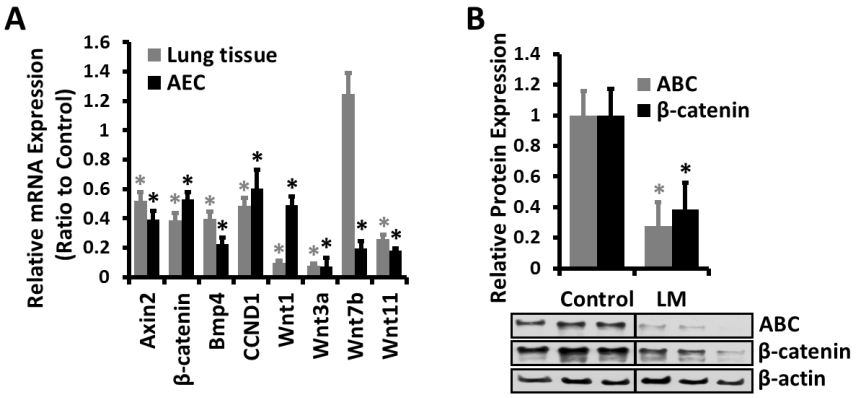

Fig. III. 1. Wnt/β-catenin signaling is inhibited during LPS and mechanical ventilation induced acute pulmonary inflammation. Mice were treated with LPS and mechanical ventilation (LM). Non-ventilated mice were used as a control. (A) The mRNA levels of Wnt signaling components in whole lungs and fresh isolated alveolar epithelia cells (AEC) of LM animals were analyzed by Real-time PCR and plotted as ratios over the control animals with 18S rRNA as a reference gene. (B) The protein levels of activated β-catenin and total β-catenin in whole lungs of Control and LM animals with β-actin as an internal control. Density of bands was quantified by ImageJ and normalized to control mice. Data are expressed as means ± s.e.m. (n=5 animals) and statistical significance determined by Student's *t*-test. *p < 0.05 v.s. Control.

In another murine model of influenza viral pneumonia, mRNAs of downstream genes (Axin2, β-Catenin, and Bmp4) and canonical Wnt ligand (Wnt3a) were also dramatically inhibited (Fig. III. 2A). Activated form of β-catenin (ABC) was reduced during acute viral infection (Fig. III. 2C). However, mRNA expression of other canonical Wnt ligands (Wnt1, Wnt7b, and Wnt11) (Fig. III. 2B) and protein expression of β-catenin (Fig. III. 2C) were not decreased in influenza viral pneumonia. Similarly, the down-regulation of Wnt target genes, Wnt ligands and β-catenin protein was also observed in hyperoxia-induced acute lung injury (Fig. III. 3).

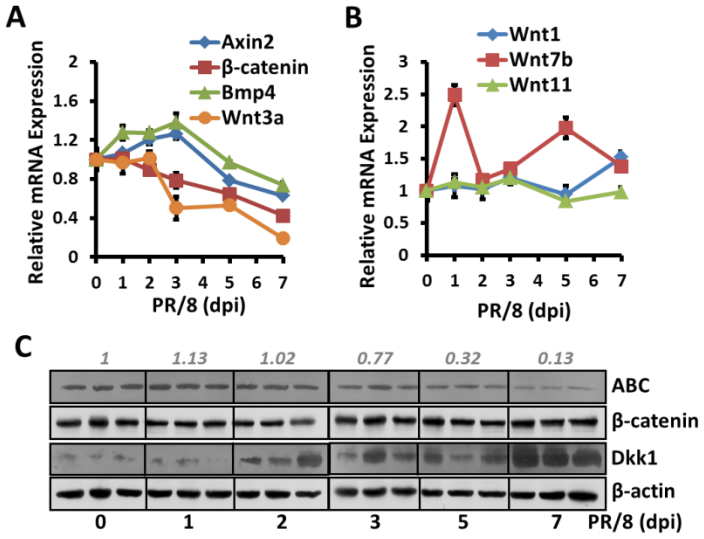

Fig. III. 2. Wnt/β-catenin signaling is depressed during H1N1 influenza virus-mediated acute pulmonary inflammation. Mice were intranasally inoculated with H1N1 influenza A/PR/8/34 virus (250 pfu) and housed for 1 to 7 days. (n=3/group). The mRNA levels of Wnt signaling components (A) and Wnt

ligands (B) in whole lung tissue were measured by Real-time PCR and normalized to control animals (without infection) using 18S rRNA as a reference gene. (C) The protein levels of activated β-catenin (ABC), total β-catenin, and Dkk1 in whole lung tissue of infected animals using β-actin as an internal control. Density of ABC bands was quantified by ImageJ, normalized to control mice, and labeled on the top. Data are shown as means ± s.e.m. (n=3 animals).

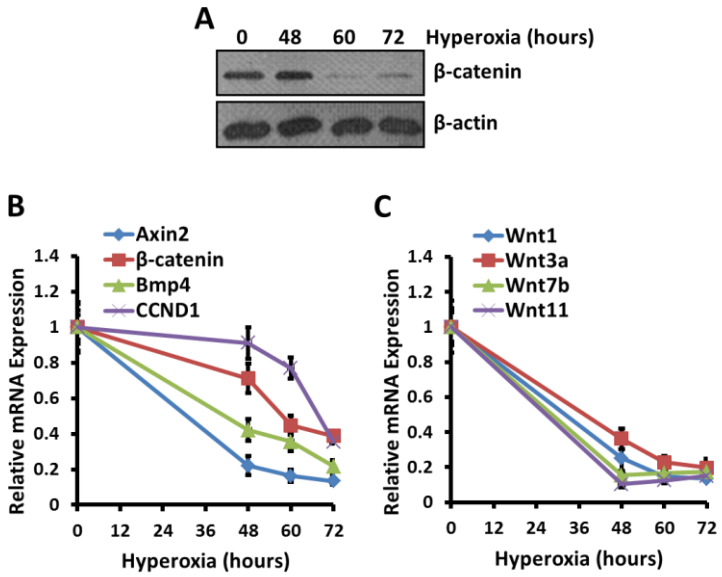

Fig. III. 3. Wnt/β-catenin signaling is down-regulated in hyperoxia-associated acute lung injury. The rats were exposed to 95% oxygen for 0, 48, 60 or 72 hours. (A) The protein level of β-catenin was determined by Western blot using β-actin as an internal control. The mRNA levels of Wnt target genes (B) and Wnt ligands (C) were analyzed by Real-time PCR using rat 18S rRNA as reference and normalized to control rat. The results are means ± s.e.m. (n = 4 rats).

To identify the Wnt antagonist that is potentially responsible for this down-regulation, we screened mRNA expression of several Wnt antagonists (sFRP1 and Dkk1-4) in LM-challenged lungs and found that only Dkk1 was increased (Fig. III. 4A). Dkk1 protein was also up-regulated by LM (Fig. III. 4B). Furthermore, mRNA and protein expression of Dkk1 were greatly induced in influenza virus-infected lungs (Fig. III. 4C and G). Interestingly, Dkk1, which was reported to accumulate in the lungs of IPF patients (44), was also significantly deposited in alveoli of both the LM-challenged and influenza virus-infected lungs (Fig. III. 4F). However, Dkk1 mRNA in freshly isolated AEC (data not shown) and Dkk1 protein in BAL of the LM-challenged and

influenza virus-infected lungs (Fig. III. 4D and E) were almost undetectable. Instead, Dkk1 in plasma from both injured animals were remarkably increased compared with control animals (Fig. III. 4D and E). Based on more detailed BAL analyses, profound infusion of Dkk1 into BAL during acute viral infection came after endothelial cells damage and disruption of alveolar-vascular barrier (Fig. III. 4E and G). This indicated that Dkk1 deposited in alveoli was originated from the circulating system. Our results also implied a potential paracrine regulatory mechanism of Dkk1 on Wnt/β-catenin signaling in AEC during acute pulmonary inflammation.

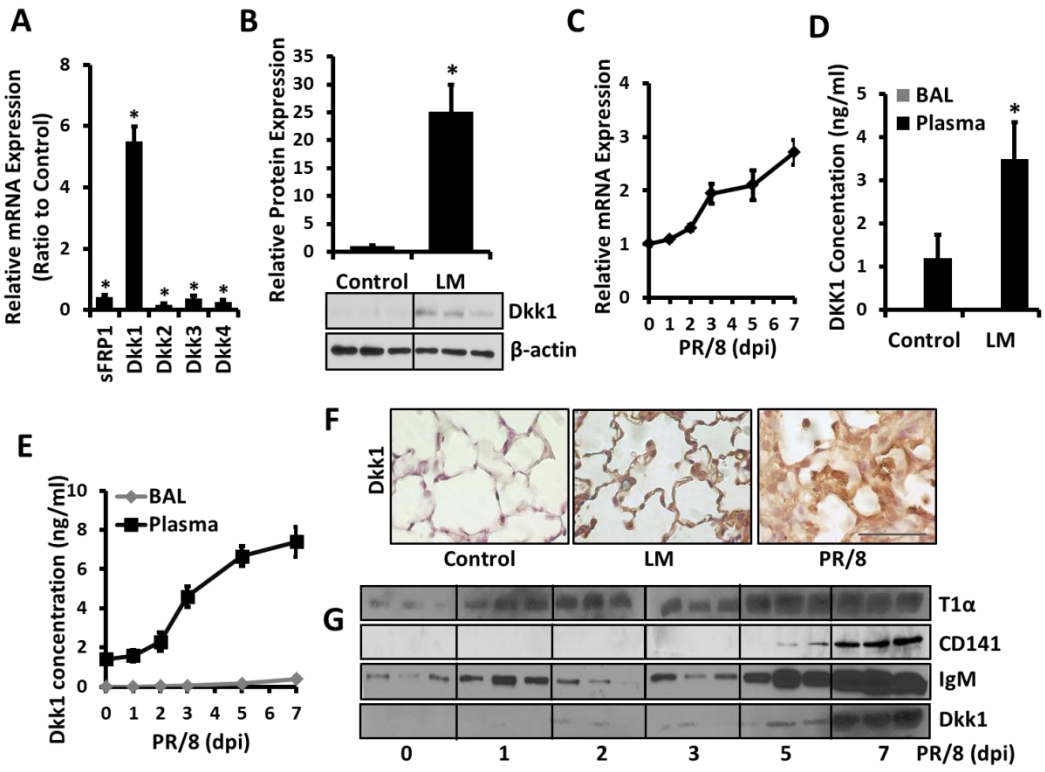

Fig. III. 4. Dkk1 is accumulated in the lung during acute pulmonary inflammation. (A) The mRNA expression of Wnt antagonists (sFRP1 and Dkk1-4) in whole lungs of LM-challenged and control mice was determined by Real-time PCR and plotted as ratios over control animals with 18S rRNA as a reference. (B) The protein level of Dkk1 in whole lung of control and LM-challenged animals was measured by Western blot using β-actin as a loading control. Density of bands was quantified by ImageJ and normalized to β-actin. Result was expressed as a ratio to control animal. (C) The mRNA level of Dkk1 in whole lung tissue of H1N1 influenza virus PR/8-infected mice for 0 to 7 days was analyzed by Real-time PCR and normalized to control mice with 18S rRNA as a reference. (D) Dkk1 concentrations in BAL and plasma of mice following LM challenge (D) and H1N1 influenza virus PR/8 infection (E) were measured by ELISA. (F) Immunostaining of Dkk1 in the lungs of Control, LM-challenged, and H1N1 influenza virus PR/8-infected (7 dpi) mice. Scale bar = 75 μm. (G) The protein levels of T1α (AEC I marker), CD141 (endothelial cells marker), IgM (epithelial-endothelial barrier damage marker), and Dkk1 in BAL of H1N1 influenza virus PR/8-infected mice (0-7 dpi) were determined by Western blot. Data are expressed as means ± s.e.m. (n=3-8 animals) and statistical significance determined by Student's *t*-test. *$p < 0.05$ v.s. Control.

3.4.2 Dkk1 is released from activated platelets and binds to AEC during acute pulmonary inflammation-associated thrombocytopenia

Platelets were recently identified as the major source of Dkk1 in the circulation system (19). Platelets were also activated in the development of acute pulmonary inflammation and other inflammatory diseases (13,18,52). Thus, we first measured the number of circulating platelets in LM-challenged, live bacteria-infected, and influenza virus-infected animals. As we expected, there was a rapid and transient reduction in the number of circulating platelets, which reflects the clinical condition of thrombocytopenia, in animal models of influenza pneumonia (Fig. III. 5A). In other two animal models of acute lung inflammation, the numbers of circulating platelets were also dramatically decreased (Fig. III. 5B). Although the number of platelets was the lowest at 2 dpi, platelet activity was increased at the same time point as shown by the increased surface expression of CD62P, the marker of platelet activation (18-20) (Fig. III. 5C). Surprisingly, Dkk1 protein expression was strongly elevated in the isolated platelets from all three animal models (Fig. III. 5D-F). Dkk1 was very fast released from activated platelets upon stimulation of thrombin receptor by SFLLRN (Fig. III. 6A and B). To determine potential paracrine regulation of Dkk1 from platelets on the Wnt/β-catenin signaling in AEC, we measured the binding affinity of Dkk1 to AEC and found that the affinity was significantly increased upon TNFα/IL-1β stimulation (Fig. III. 6C). This increase was likely due to specific Dkk1 receptor Kermen-1(KRM1) and co-receptor for Wnt ligands (LRP5 and LRP6) since these receptors were up-regulated by TNFα/IL-1β treatment as well (Fig. III. 6D). The binding of Dkk1 to AEC depressed Wnt/β-catenin signaling (Fig. III. 7) as we expected. Our results here showed that Dkk1 released from platelets can be utilized to manipulate Wnt/β-catenin signaling in AEC.

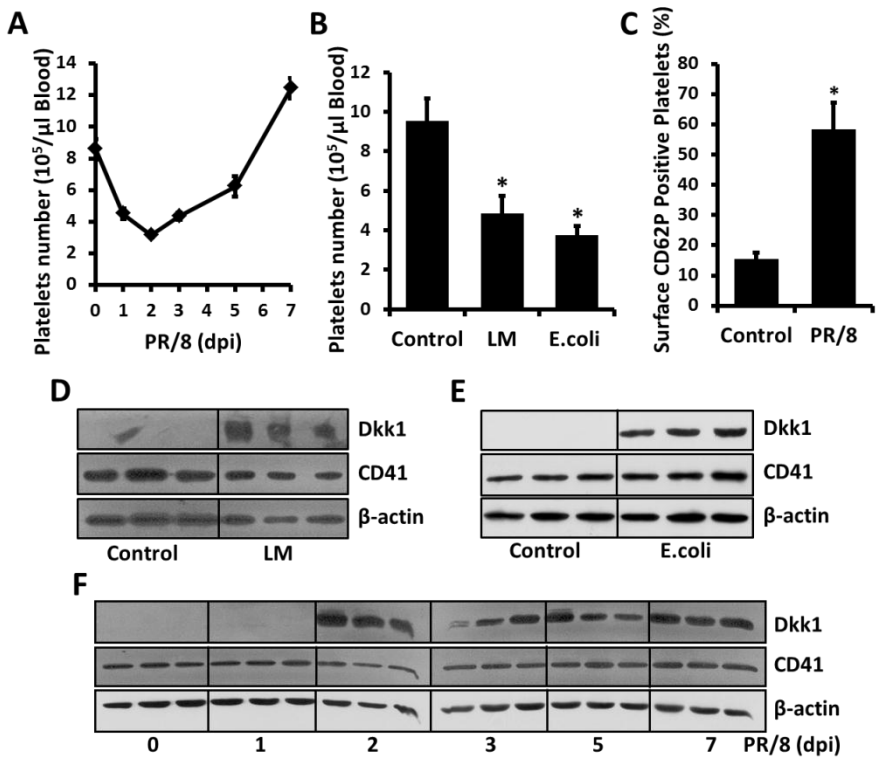

Fig. III. 5. Dkk1 protein is induced in activated platelets during acute pulmonary inflammation-associated thrombocytopenia. (A, B) Circulating platelets count in H1N1 influenza virus PR/8-infected, LM-challenged, and live bacteria *E.coli*-infected mice. (C) Platelets were isolated from the H1N1 influenza virus PR/8-infected mice (2 dpi) and labeled with PE-CD62P and FITC-CD41 (1 μg/ml of each). Surface expression of CD62P (activation marker) were detected by FACS. (D-F) Protein levels of Dkk1 and CD41 (platelets marker) in circulating platelets of LM-challenged, live bacteria *E.coli*-infected, and PR/8-infected mice were measured by Western blot with β-actin as a loading control. Data are expressed as means ± s.e.m. (n = 3-8 mice) and tested for statistical significance by Student's *t*-test. *$p < 0.01$ v.s. control mice.

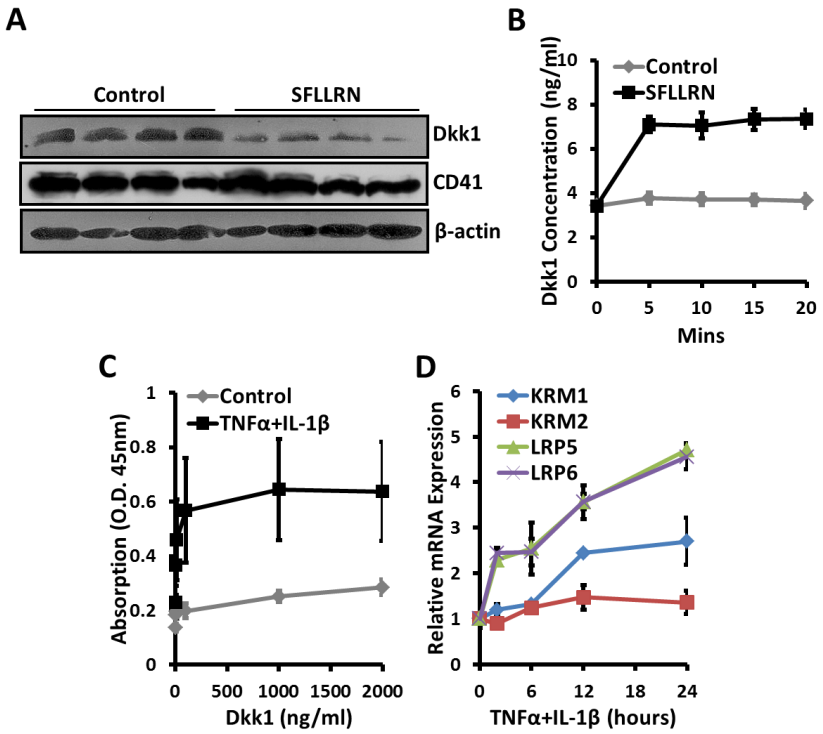

Fig. III. 6. Dkk1 is released from activated platelets and binds to AEC during acute pulmonary inflammation. Platelet-rich plasma (PRP) were isolated from LM-challenged mice and incubated with 100 μM SFLLRN for 20 mins (A) or 5-20 mins (B). The protein levels of Dkk1 and CD41 in platelets (A) and Dkk1 concentrations in plasma (B) were determined by Western blot and ELISA, respectively. (C) Primary mouse AEC II was cultured for 4 days and then stimulated with TNFα and IL-1β (20 ng/ml of each) for 24 hours. Recombinant mouse Dkk1 was added to the cells at indicated concentration for 2 hours. Cell-based ELISA was performed to quantify the binding of Dkk1 to the stimulated AEC. (D) mRNA levels of Dkk1 receptors (KRM1, KRM2, LRP5, and LRP6) were analyzed by Real-time PCR in the TNFα/IL-1β-stimulated AEC and normalized to control. Data are expressed as means ± s.e.m. from 3 independent preparations.

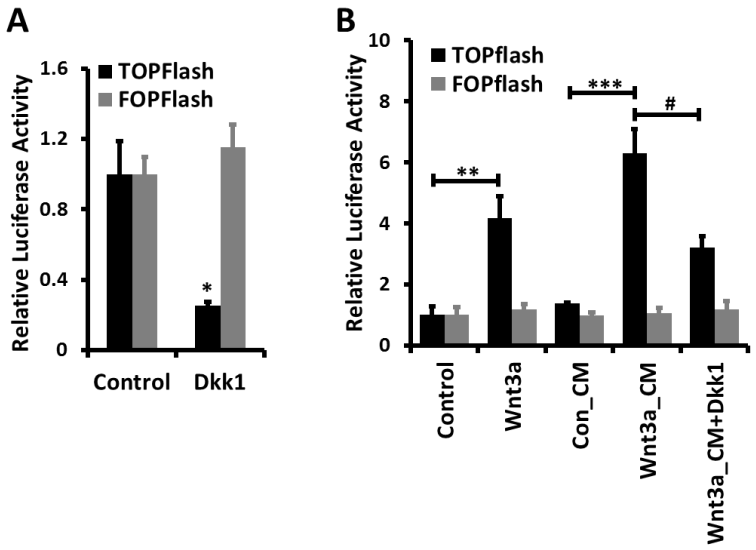

Fig. III. 7. Dkk1 inhibits Wnt/β-catenin signaling in AEC. E10 cells were transfected with TOPFlash or FOPFlash and pRL-TK plasmids for 24 hours and then treated with 200 μM Dkk1 for 24 hours (A) or incubated with 200 ng/ml recombinant human Wnt3a or 50% Con_CM or Wnt3a_CM together with 200 μM Dkk1 for 24 hours (B). Dual-luciferase assay was performed. TOPFlash or FOPflash *Firefly* luciferase activity was normalized to pRL-TK *Renilla* luciferase activity. The final results were normalized to untreated control. Data are expressed as means ± s.e.m. from 3 independent preparations and tested for statistical significance by Student's *t*-test or ANOVA analysis followed with posthoc *Tukey's* test. * $p < 0.05$ v.s. Control. **, ***, and #, were represented as $p < 0.05$.

3.4.3 Neutralization of Dkk1 attenuates neutrophil infiltration during acute pulmonary inflammation

Blocking of platelet-leukocyte interaction (53), platelet depletion (54), and anti-platelet therapy (55,56) are protective in the development of acute lung inflammation. Neutralization of Dkk1 was also reported to limit inflammatory bone loss (57). Here we investigated the effect of Dkk1 antibody neutralization in alveolar space on the development of acute lung inflammation. Neutrophils were the major recruited inflammatory cells into alveolar space in our two-hit acute lung inflammation model as revealed by differential immune cell count analysis of BAL (Fig. III. 8A). Neutralization of Dkk1 intratracheally inhibited neutrophil infiltration into alveoli remarkably (Fig. III. 8A). Whole lung myeloperoxidase (MPO) activity, which is considered as a marker of neutrophil sequestrations in the lung (58), was also reduced by anti-Dkk1 antibody

(Fig. III. 8B). Since Dkk1 is an inhibitor of Wnt/β-catenin signaling (57), our results imply a potential role of Wnt/β-catenin signaling in regulating acute lung inflammation.

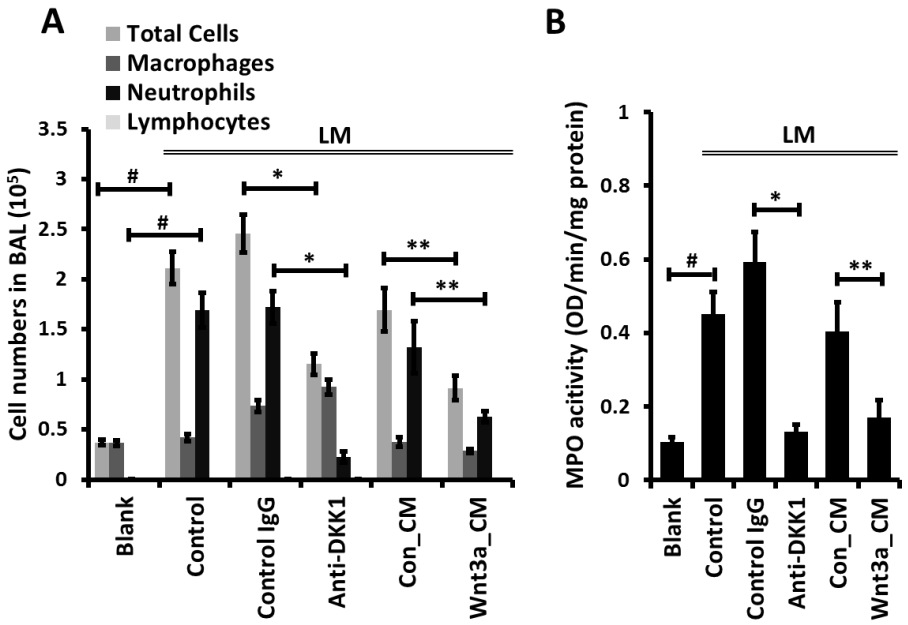

Fig. III. 8. Intratracheal neutralization of Dkk1 or administration of Wnt3a attenuates neutrophil infiltration during LM-induced acute pulmonary inflammation. Mice were intratracheally instilled with LPS together with isotype-matched control IgG or function-blocking mAb against Dkk1 (86 μg/mouse) and then mechanically ventilated (LM). Mice were also intratracheally co-administered with control (Con_CM) or Wnt3a conditional medium (Wnt3a_CM) along with LPS and ventilated. (A) Differential immune cell number in BAL was counted. (B) MPO activity in whole lung tissue was measured. Data are expressed as means ± s.e.m. (n=5-8 animals). Statistical significance was determined by one-way ANOVA analysis with posthoc *Tukey's* test. *, **, and # were represented as $p < 0.05$.

3.4.4 Administration of Wnt3a blocks ICAM-1/VCAM-1-mediated neutrophils infiltration during acute pulmonary inflammation

We activated Wnt/β-catenin signaling by administration of Wnt3a intratracheally and investigate its effect on the development of acute lung inflammation. Compared with control conditional medium group (LM+Con_CM), Wnt3a (LM+Wnt3a_CM) significantly reduced the recruitment of neutrophils into alveolar space, decreased the total cell number in BAL, and attenuated MPO activity in the whole lung tissue (Fig. III. 8A, B).

Activation and transmigration of neutrophils are mediated by a series of adhesion molecules and chemotactic signaling (1). We moved on to investigate the potential effect of Wnt/β-catenin signaling on this process. The mRNA expression of ICAM-1 and VCAM-1 was significantly inhibited by Wnt3a in the LM-insulted lungs (Fig. III. 9A and B). This impaired synthesis also led to remarkable reduction of sVCAM-1 concentration in BAL of injured lungs (Fig. III. 9C). However, the major chemokines (KC, LIX, MCP-1, and MIP-2) involved in neutrophils infiltration were not changed by Wnt3a (Fig. III. 9D).

Wnt/β-catenin signaling was also reported to limit inflammatory functions of macrophages by reducing release of TNFα and IL-6 (31,32). Here we observed that IL-6 in BAL was markedly reduced after administration of Wnt3a in LM-insulted lungs (Fig. III. 9E) and this reduction was also due to attenuated IL-6 mRNA synthesis by Wnt3a (Fig. III. 9F). However, mRNA expression and BAL level of TNFα showed no significant difference between Wnt3a-treated and control mice upon in the LPS+MV challenge (Fig. III. 9D and G). Our results revealed a potentially novel mechanism that Wnt/β-catenin signaling utilized to control neutrophil infiltration during acute inflammation.

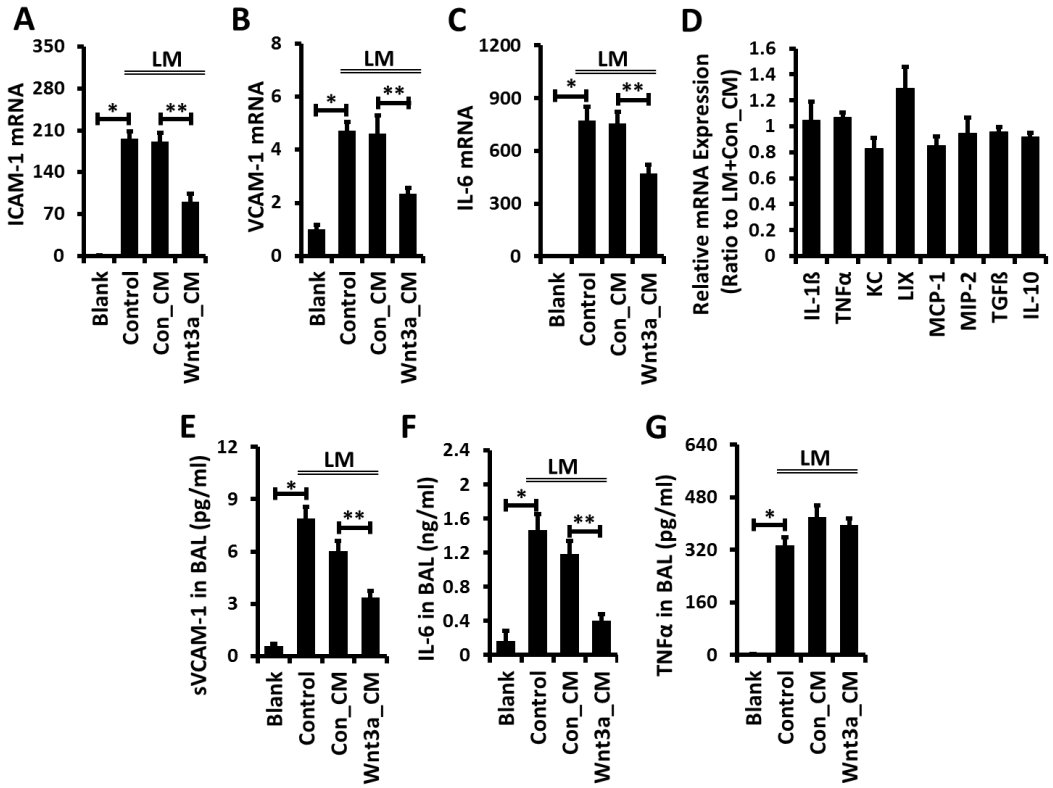

Fig. III. 9. Wnt3a reduces the expression of adhesion molecules ICAM-1/VCAM-1 during LM-induced acute pulmonary inflammation. Mice were intratracheally challenged by LPS together with control (Con_CM) or Wnt3a conditional medium (Wnt3a_CM) and then mechanically ventilated (LM). mRNA levels of ICAM-1 (A), VCAM-1 (B), and IL-6 (C) in whole lung tissue were measured by Real-time PCR and were normalized to blank control. (D) Real-time PCR was also performed to analyze mRNA levels of other cytokines (IL1β, TNFα, TGFβ, and IL-10) and chemokines (KC, LIX, MCP-1, and MIP-2) in LM+Wnt3a_CM mice. Result was normalized to LM+Con_CM mice. Concentrations of sVCAM-1 (E), IL-6 (F), and TNFα (G) in BAL were measured by ELISA. Data are expressed as means ± s.e.m. and tested for statistical significance by ANOVA analysis with posthoc *Tukey's* test. (n=5-8 animals). * and ** were represented as $p < 0.05$.

3.4.5 Activation of Wnt/β-catenin signaling inhibited TNFα-induced ICAM-1/VCAM-1 expression

Both ICAM-1 and VCAM-1 are expressed in AEC and mediate the infiltration of immune cells during acute lung inflammation (7-9). To further elucidate the mechanism of Wnt/β-catenin signaling-mediated inhibition of ICAM-1 and VCAM-1 expression in injured

lungs, we performed *in vitro* studies using E10 cells (a mouse type I cell line) and cultured primary mouse AEC II (AEC I-like cells). TNFα stimulated the expression of VCAM-1 and ICAM-1 in a dose- and time- dependent manner in E10 cells (Fig. III. 10A-D) and primary AEC I-like cells (Fig. III. 10E, F). Wnt3a strongly reduced both ICAM-1 and VCAM-1 expression stimulated by TNFα (Fig. III. 11 and III. 12A-C). On the other hand, Dkk1 displayed the opposite effect on the induction of ICAM-1 and VCAM-1 expression (Fig. III. 12A-C). More importantly, platelet releasate augmented the TNFα-stimulated ICAM-1 and VCAM-1 expression in primary mouse AEC and this augmentation was blocked by Dkk1 neutralization antibody (Fig. III. 12D, E). Our results further support the potential implication of platelet-derived Dkk1 in controlling ICAM-1 and VCAM-1 expression during acute lung inflammation.

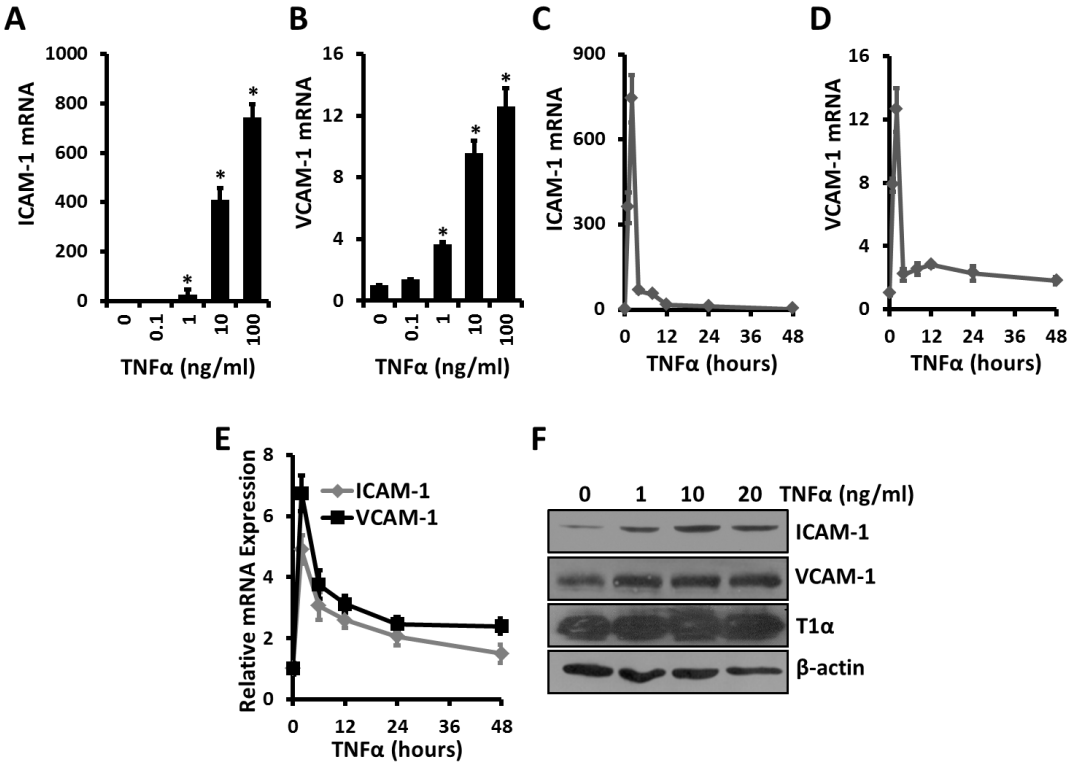

Fig. III. 10. ICAM-1 and VCAM-1 expressions were stimulated by cytokines in AEC. E10 cells were stimulated by different doses of TNFα for 2 hours (A, B), or treated by 100 ng/ml TNFα for indicated time points (C, D). Primary mouse AEC II were cultured for 4 days and then stimulated by 20 ng/ml TNFα for indicated time (E). mRNA expression of ICAM-1 (A, C, and E) and VCAM-1 (B, D, and E) was determined by Real-time PCR with 18S rRNA as a reference, and normalized to untreated cells. (F)

Primary mouse AEC II were cultured for 4 days and then stimulated with different doses of TNFα for 24 hours. Protein expression of ICAM-1, VCAM-1, and T1α (AEC I marker) was measured by Western blot using β-actin as a loading control. Data are expressed as mean ± s.e.m. (n=3). Statistical significance was determined by one-way ANOVA analysis with posthoc *Tukey's* test. * $p < 0.05$ v.s. Control.

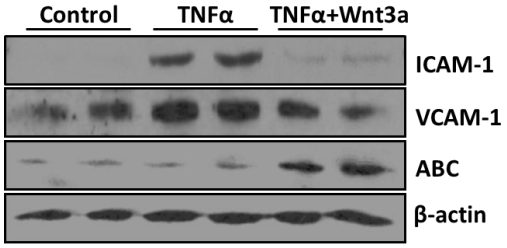

Fig. III. 11. Wnt/β-catenin signaling inhibits ICAM-1 and VCAM-1 protein expression in AEC. E10 cells were pretreated with recombinant human Wnt3a (200 ng/ml) for 24 hours and then stimulated by TNFα (20 ng/ml) for additional 24 hours. Protein levels of ICAM-1, VCAM-1, and activated β-catenin (ABC) were determined by Western blot using β-actin as an internal control.

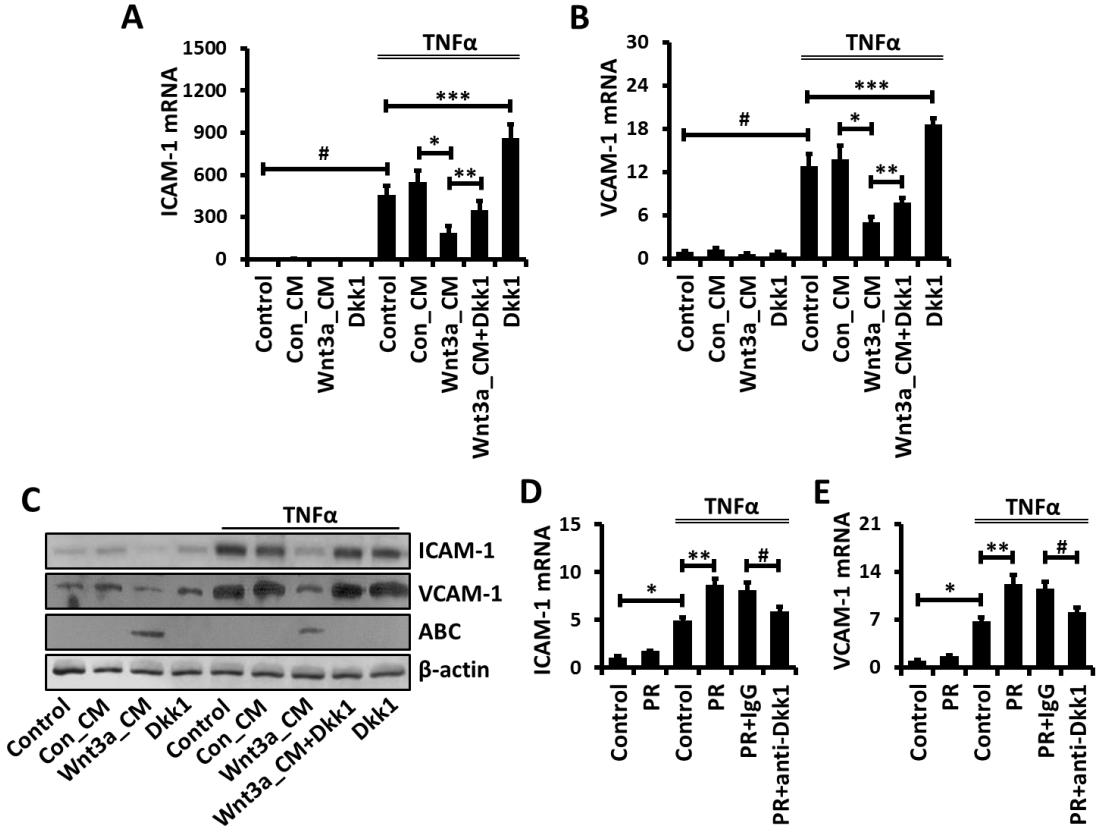

Fig. III. 12. Platelet-derived Wnt antagonist, Dkk1 is implicated in the stimulation of TNFα-mediated

ICAM-1/VCAM-1 expression in AEC. E10 cells were incubated with 50% Con_CM or Wnt3a_CM together with 200 μM Dkk1 for 12 hours and then stimulated with 20 ng/ml TNFα for 2 hours (A, B) or 24 hours (C). Platelets were isolated from LM-challenged mice, resuspended in Tyrodes-HEPES buffer, and treated by 0.1 U/ml thrombin for 90 mins. Platelet releasate (PR) was collected and added to cultured primary mouse AEC together with isotype-matched control IgG or function-blocking mAb against Dkk1 (10 μg/ml) for 24 hours. After that, mouse AEC was stimulated with TNFα (20 ng/ml) for 2 hours (D, E). The mRNA levels of ICAM-1 (A, D) and VCAM-1 (B, E) were measured by Real-time PCR using mouse 18S rRNA as reference and normalized to control untreated cells. (C) Protein levels of ICAM-1, VCAM-1, and activated β-catenin (ABC) were determined by Western blot with β-actin as an internal control. Data are expressed as means ± s.e.m. from three independent preparations and tested for statistical significance by ANOVA analysis followed with posthoc *Tukey's* test. *, **, *** and # were represented as $p < 0.05$.

Since Wnt/β-catenin signaling normally regulates the promoter regions of its target genes (59), we examined study the effect of Wnt3a on the promoter activities of ICAM-1 and VCAM-1. Wnt3a significantly depressed the TNFα-stimulated ICAM-1 and VCAM-1 promoter activities (Figure III. 13A, B). The promoters of ICAM-1 and VCAM-1 contain several NF-κB (P50/P65) binding sites, which are essential for their activation (12). We future explored whether Wnt3a can block NF-κB-mediated ICAM-1 and VCAM-1 expression. By overexpressing P65 in E10 cells, the promoter activities of both ICAM-1 and VCAM-1 were remarkably induced and this induction was inhibited by Wnt3a (Fig. III. 13C and D). Our results suggested both ICAM-1 and VCAM-1 were the target genes of Wnt/β-catenin signaling.

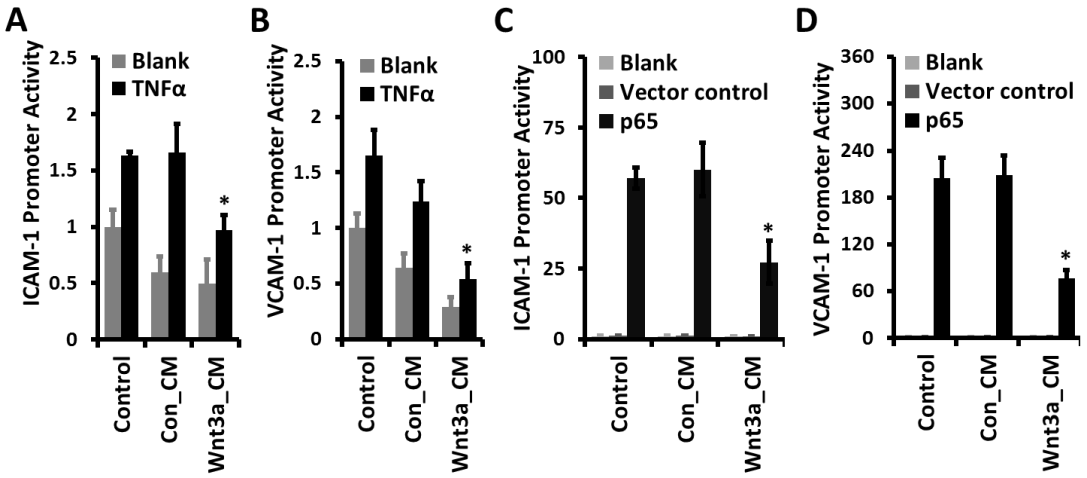

Fig. III. 13. Wnt/β-catenin signaling inhibits ICAM-1 and VCAM-1 promoter activities in AEC. (A, B) E10 cells were transfected with a luciferase expression plasmid containing ICAM-1 or VCAM-1 promoter along with pRL-TK plasmid for 12 hours, and incubated with 50% control or Wnt3a_CM for 12 hours, and finally stimulated by 20 ng/ml TNFα for 24 hours. (C, D) E10 cells were incubated with 50% control or Wnt3a_CM for 12 hours, and then transfected with pcDNA3.0-based control or p65 overexpression plasmid, luciferase expression plasmid containing ICAM-1 or VCAM-1 promoter along with pRL-TK plasmid. Dual-luciferase assay was performed. The results were expressed as the ratio of ICAM-1 (A, B) or VCAM-1 (C, D) promoter-associated Firefly luciferase activity to pRL-TK Renilla luciferase activity, and normalized to control. Data were expressed as means ± s.e.m. from three independent preparations and tested for statistical significance by ANOVA analysis followed with posthoc *Tukey's* test. * $P<0.05$ v.s. Con_CM.

Functional crosstalk between NF-κB signaling and Wnt/β-catenin signaling has been reported to regulate cell response to cytokines (33,36). The same inhibitory effect of Wnt3a on NF-κB signaling activity stimulated by TNFα or P65 overexpression was observed in E10 cells (Fig. III. 14). However, we cannot detect the physical interaction between β-catenin and P50/P65 as previously reported (33) (Fig. III. 15). Wnt3a did not have effects on the activation and nuclear translocation of P65 upon TNFα stimulation either (Fig. III. 16).

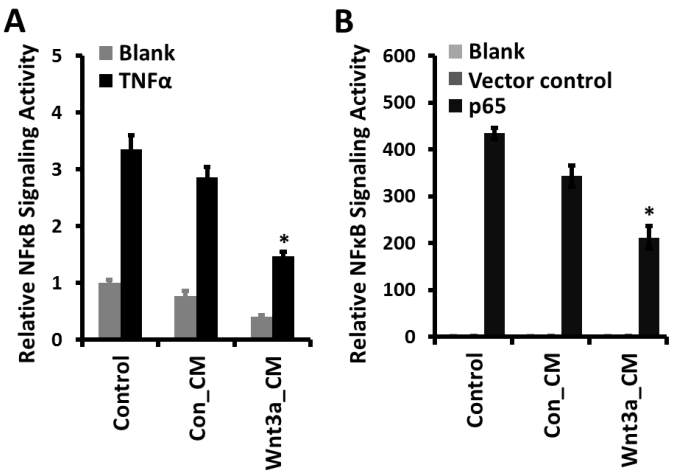

Fig. III. 14. Wnt3a suppresses NFκB signaling in AEC. (A) E10 cells were transfected with luciferase expression plasmid containing NFκB transcriptional response element along with pRL-TK plasmid for 12 hours, and incubated with 50% control or Wnt3a_CM for 12 hours, and finally stimulated by 20ng/ml TNFα for 24 hours. (B) E10 cells were incubated with 50% control or Wnt3a_CM for 12 hours, and then transfected with pcDNA3.0-based control or p65 overexpression plasmid, luciferase expression plasmid containing ICAM-1 or VCAM-1 promoter along with pRL-TK plasmid. Dual-luciferase assay was performed. The results were expressed as the ratio of NFκB transcriptional response element-associated Firefly luciferase activity (representing NFκB signaling activity) to pRL-TK Renilla luciferase activity, and normalized to control. Data were expressed as means ± s.e.m. from three independent preparations and tested for statistical significance by ANOVA analysis followed with posthoc *Tukey's* test.. * $P<0.05$ v.s. Con_CM.

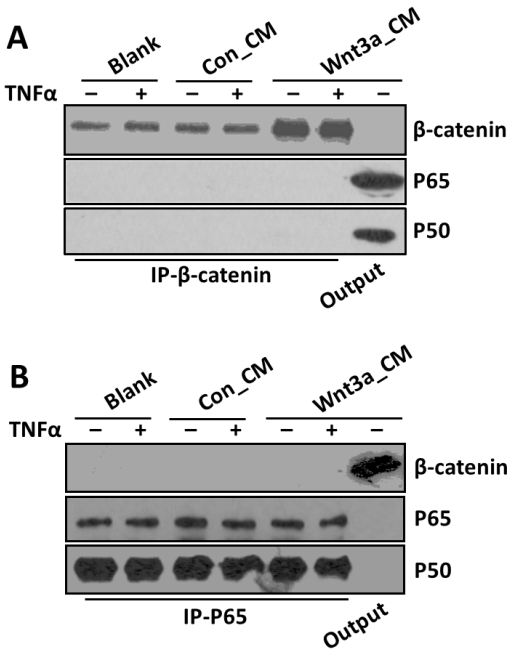

Fig. III. 15. No detectable interaction between β-catenin and P65/P50 in AEC. E10 cells were incubated with 50% Con_CM or Wnt3a_CM for 12 hours and then stimulated by 20 ng/ml TNFα for 24 hours. β-catenin (A) and P65 (B) were pulled down from lysed cells by immunoprecipitation and probed with indicated antibodies by Western blot. Output was used as positive control.

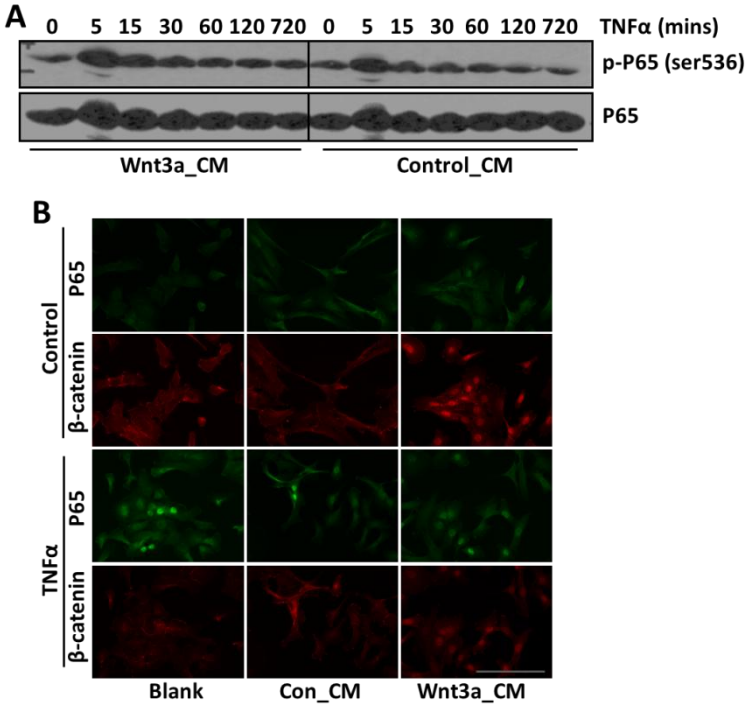

Fig. III. 16. Wnt3a does not affect activation and translocation of P65 upon TNFα stimulation of AEC. E10 cells were incubated with 50% Con_CM or Wnt3a_CM for 12 hours and then stimulated by 20

ng/ml TNFα for indicated time points (A) or 2 hours (B). (A) Protein levels of p-P65 (ser536) and P65 were measured by Western blot. (B) Immunofluorescence staining of P65 and β-catenin under indicated conditions. Scale bar = 40 μm.

3.4.6 Activation of Wnt/β-catenin signaling attenuates ICAM-1/VCAM-1-mediated adhesion of alveolar macrophages and neutrophils to AEC

We further explored the functional significance of Wnt/β-catenin signaling-mediated inhibition of ICAM-1 and VCAM-1 expression. Both adhesion molecules are essential for neutrophil and macrophage adhesiveness (8,9), and facilitate transepithelial migration of monocytes upon influenza virus infection (7). We used an *in vitro* cell culture model to examine the adhesion of primary rat alveolar macrophages (AMϕ) or neutrophils to E10 cells. TNFα significantly increased the percentage of attached AMϕ or neutrophils to E10 cells (Fig. III. 17A and B). These increases were totally eliminated by the immunoblockage with either anti-ICAM-1 or anti-VCAM-1 antibodies. Furthermore, Wnt3a dramatically reduced the adhesion of both types of immune cells to E10 cells. On the other hand, pretreatment by Dkk1 further increased attachment of AMϕ or neutrophils to E10 cells. Our results demonstrated a novel and complex cellular communication network in alveoli during progression of acute lung inflammation (Fig. III. 18). Modulating platelet-derived Wnt antagonist Dkk1 to control neutrophils infiltration could represent an intriguing new therapeutic avenue for patients with acute pulmonary inflammation.

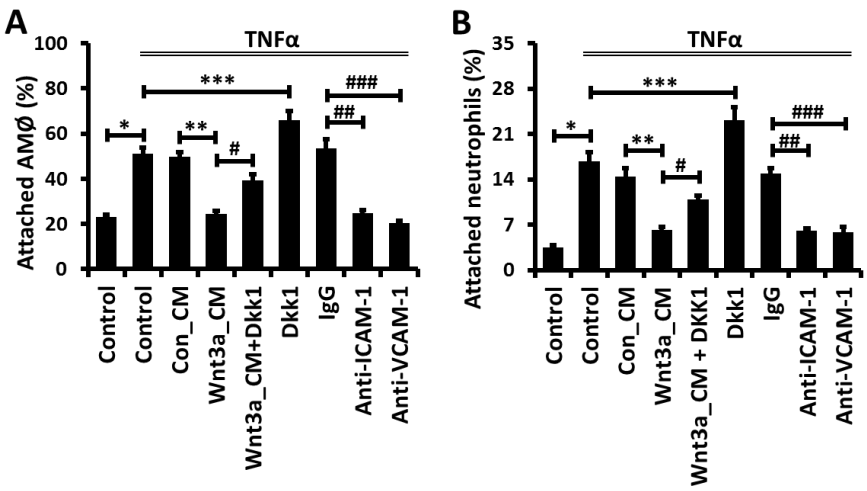

Fig. III. 17. Wnt/β-catenin signaling reduces ICAM-1/VCAM-1-mediated adhesion of alveolar macrophages and neutrophils to AEC. E10 cells were incubated with 50% Con_CM or Wnt3a_CM together with 200 μM Dkk1 for 12 hours and then stimulated by 20 ng/ml TNFα for 24 hours (A, B, the first 6 bars). E10 cells were incubated with control IgG or blocking mAbs against ICAM-1 or VCAM-1 for 30 mins, and then stimulated by 20 ng/ml TNFα for 24 hours (A, B, the last 3 bars). Then adhesion of freshly isolated alveolar macrophages (AMØ) or neutrophils to E10 cells were assayed. Values were presented as a percent of attached AMØ or neutrophils from three independent experiments and tested for statistical significance by ANOVA analysis followed with posthoc *Tukey's* test. Data were expressed as means ± s.e.m. *, **, ***, #, ##, and ### were represented as $p < 0.05$.

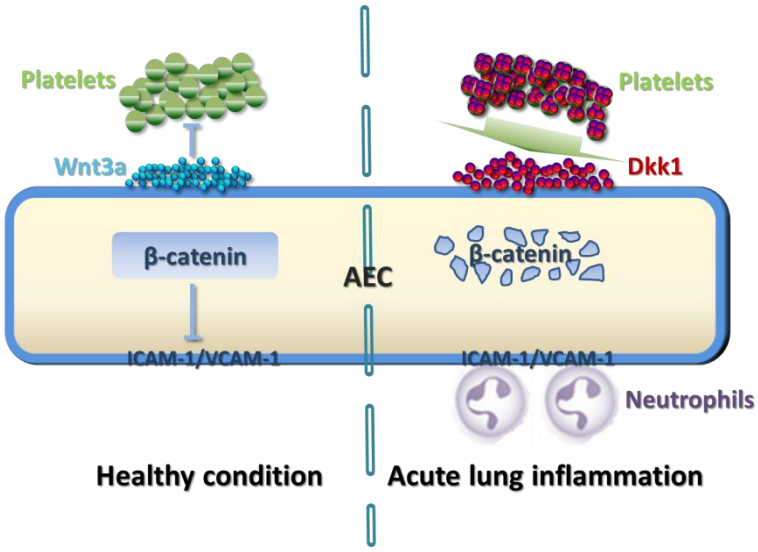

Fig. III. 18. Implication of platelet-derived Wnt antagonist Dkk1 in ICAM-1/VCAM-1-mediated neutrophilic acute pulmonary inflammation. During the initial stage of acute pulmonary inflammation, Dkk1 is induced and released from activated platelets. Released Dkk1 diffuses into alveoli, binds to alveolar epithelial cells (AEC) and inhibits Wnt/β-catenin signaling, which in turn gives rise to stimulation

of ICAM-1/VCAM-1 expression by pro-inflammatory cytokines and mediates the neutrophil infiltration into alveoli. Wnt3a can counterstrike with Dkk1 to activate Wnt/β-catenin signaling in AEC and inhibit platelet activity as well (88), which consequently limits the promotion of ICAM-1/VCAM-1 expression, impairs the neutrophil infiltration, and finally attenuates the development of acute pulmonary inflammation.

3.5 Discussion

Although great efforts have been spent to understand the mechanism of ALI/ARDS, morbidity and mortality of patients are still remain at high level, and formidable challenges persist (60,61). Neutrophil is an essential component of the innate immune system and vital to our lives. However, inflammatory damage delivered by activated neutrophils also contributes to progression of ALI/ARDS (1,5,62). Lung edema and endothelial and epithelial cell injuries accompanied by infiltration of neutrophils are broadly accepted as the classic paradigms of pulmonary acute inflammation (63). There are also evidences that activated platelets contribute to pathologic syndromes of pulmonary inflammation (14,17,18,52). In this study, using both *in vitro* and *in vivo* models, we demonstrated a novel regulation of neutrophil recruitment by alveolar epithelial cells, which were affetced by platelets in acute inflammatory phase of ALI. We identified platelet-derived Dkk1 as a key modulator of Wnt/β-catenin signaling in AEC during ALI. More importantly, Wnt3a strongly activated Wnt/β-catenin signaling in AEC, inhibited ICAM-1 and VCAM-1-mediated neutrophil adhesion, and finally reduced neutrophil infiltration into alveolar spaces in acute pulmonary inflammation.

In this study, we utilized a mouse model in which acute lung inflammation results from a combination of low dose intratracheal LPS instillation and noninjurious mechanical ventilation (MV) (45). The synergistic interaction between infectious insults and MV contributes to the pathogenesis of ALI/ARDS (64). Priming of the lungs with LPS or live bacteria makes the animals more susceptible to mechanical ventilation (65,66). In this “double hit” paradigm, acute lung injury develops and is characterized as synergistic increased cytokine release, activated

neutrophil transmigration into the lungs, damage of alveolar epithelia cells and loss of vascular integrity [51].

In the two-hit model of acute lung inflammation, depression of Wnt/β-catenin signaling in AEC was accompanied by accumulation of Wnt antagonist Dkk1 and reduction of Wnt agonists' synthesis (Fig. III. 1). The similar phenomenon was also noticed in influenza virus pneumonia, bacteria pneumonia and hyperoxic acute lung injury (Fig. III. 1, 3, and 4). Our observations are consistent with the previous reports of suppression of Wnt/β-catenin signaling in inflammatory lung diseases. In emphysema and COPD patients, dysfunctional repair is associated with decreased Wnt/β-catenin signaling (38,42). In asthma patients, several intracellular signaling molecules of the Wnt/β-catenin signaling were significantly reduced (32,39). In mechanical ventilation (MV)-insulted and *S. pneumoniae* -infected lungs, Wnt/β-catenin signaling is also inhibited (40,41). On the other hand, up-regulation of Wnt/β-catenin signaling has also been demonstrated in resolution stage of acute lung injury (51,67). Wnt/β-catenin signaling is activated in AEC II and essential for alveolar epithelium repair following acute injury (25). Interestingly, transepithelial migration of neutrophils also activates Wnt/β-catenin signaling in AEC II and accelerates the process of repair (24). Activation of Wnt/β-catenin in AEC is likely initialized by Wnt7b (68) (Fig. III. 2), which has been shown to activate Wnt/β-catenin signaling in airway ciliated epithelial cells following injury (26). All of these studies indicate a dynamic, complicated, and subtle response of Wnt/β-catenin signaling in inflammatory lung diseases. Considering a great number of Wnt/β-catenin signaling agonists and antagonists are in the pre-clinical development stage (69), characterizing the role of Wnt/β-catenin signaling will open a new window to explore our potential to control these diseases.

It is not very clear about the relative contribution of selectins (P, E, and L-selectins) and other adhesion molecules (VCAM-1, ICAM-1, and JAMs) to the whole infiltration process (capture, rolling, adhesion, and transmigration) of inflammatory cells during acute lung

inflammation (1,5). Based on ours and several other *in vitro* studies, VCAM-1 and ICAM-1 are able to mediate the adhesion of neutrophils and macrophages to alveolar epithelial cells (8,9). They also modulate monocyte transepithelial migration upon influenza virus infection (7). However, considering its exclusive expression on the apical surface of AEC (10,70), ICAM-1 is unlikely to mediate neutrophils transmigration across the alveolar epithelium from the basolateral side *in vivo* even though adherence of neutrophils to the apical surface of cultured AEC is ICAM-1 dependent (Fig. III. 17B). Similar complexity is also observed *in vivo* that inhibition of ICAM-1 is protective in ALI but ICAM-1 knockout mice display no protective effect (71). Thus, more attention is put on VCAM-1 (72,73). Recently, a new function of VCAM-1 was discovered, i.e. soluble VCAM-1 shed from AEC I surface behaves as a chemokine to attract neutrophils into alveolar space (unpublished results from our lab).

Wnt/β-catenin signaling has been demonstrated to regulate several inflammatory response processes *in vitro* (32,33,74). However, no information is available regarding its role in acute pulmonary inflammation.Wnt3a has anti-inflammatory functions in macrophages by reducing TNFα and IL-6 release (31,32). The same attenuated response of IL-6 but not TNFα was observed in our two-hit model of acute pulmonary inflammation. Besides, attenuated neutrophil infiltration was the major hallmark of activation of Wnt/β-catenin signaling during acute pulmonary inflammation (Fig. III. 8A). Previously, it has been found that Wnt/β-catenin signaling suppresses VCAM-1 expression by marrow stromal and hematopoietic cells (35). Wnt/β-catenin signaling also attenuates transendothelial migration of monocytes (74). Here we successfully discovered that both ICAM-1 and VCAM-1 were the potential target genes of Wnt/β-catenin signaling in modulating neutrophil infiltration. Using E10 cells and transdifferentiated cells from AEC II as *in vitro* models of AEC I, we confirmed that the transcriptional regulation of Wnt/β-catenin signaling on VCAM-1 and ICAM-1 expression was through their promoter activities. We also observed a functional crosstalk between NF-κB signaling and Wnt/β-catenin signaling that

regulates inflammatory response including ICAM-1 and VCAM-1 expression as reported (33,36). However, we cannot verify the physical interaction between β-catenin and NF-κB protein (P50/65) (33,37) (Fig. III. 15). The detailed mechanism how Wnt/β-catenin signaling regulates ICAM-1/VCAM-1 expression still needs further investigation in AEC.

By far, sFRP1 is the only Wnt antagonist reported to be augmented in inflammatory lung diseases including hyperoxic acute lung injury and emphysema (42). The BALs from ARDS patients have a reduced capacity to activate Wnt/β-catenin signaling in fibroblasts [109], indicating that there is potentially elevation of Wnt antagonists or reduction of Wnt agonists in ARDS BALs. From this standing point, elevation of Dkk1 in alveolar region identified in our study adds a new layer of information into this field. Recent evidence has already pointed to an important role of Dkk1 in development of inflammation diseases such as atherosclerosis, arthritis, and pulmonary fibrosis by controlling fracture repair and pulmonary epithelial homeostasis (19,28,44). However, it is unclear whether the increased level of Dkk1 actively modulates these inflammatory diseases or is a consequence of the inflammatory process (43). Our current study suggests a profound role of elevated Dkk1 and subsequent depression of Wnt/β-catenin signaling in the pathoprogression of acute lung inflammation by regulating ICAM-1/VCAM-1-mediated immune cell infiltration. As a potential therapeutic target, Dkk1 is developed as a serum biomaker of inflammatory diseases and cancer patients (75-77). Neutralization therapy targeting Dkk1 has also shed light on osteolytic disease patients (43,57). Here we discovered the elevation of Dkk1 in both BAL and plasma in animal models of acute lung inflammation (Fig. III. 4). If the same scenario can be confirmed in human patients, using Dkk1 neutralization therapy to limit acute pulmonary inflammation could reveal a safer way compared to that using Wnt3a to interfere with Wnt/β-catenin signaling activity in the lung, since it avoids the aberrant activation of Wnt/β-catenin signaling, which could lead to fibroproliferation of AEC (51) and eventually pulmonary fibrosis or carcinoma (78,79).

Acute lung inflammation is associated with increased platelet activation in the blood stream and sequestration in pulmonary vascular beds (13,17,18). The classic contribution of platelets to the progression of ALI/ARDS is their unique property of aggregation with neutrophils or monocytes, amplifying the inflammatory response and disrupting barrier function of endothelial cells (14,18,21). Blocking of platelet-leukocyte interaction (53), platelet depletion (54,80), and anti-platelets therapy (55,81) are protective in ALI/ARDS. As the major source of Dkk1 in the blood (19), platelets are likely the contributor to the Dkk1 in alveolar space considering the big difference in Dkk1 levels between BAL and plasma (Fig. III. 4C and E). In addition to Dkk1, other platelet products like RANTES and CD40L are found in the alveolar spaces (22,44,62). However, for the first time we reported a specific and functional communication between platelets and AEC in inflammatory lung diseases. Manipulation of platelet function and life cycle by anticoagulants (82,83) or platelet-stimulating agents (84) could potentially be utilized to modulate Wnt/β-catenin signaling activity in patients. Interestingly, Wnt3a can also negatively regulate platelet function such as adhesion, activation, defense granule secretion and aggregation (85). The dual function of Wnt3a in regulating inflammation needs to be interpreted carefully.

The role of platelets in the host response to pathogen invasion is increasingly appreciated (86,87). Clinical severe thrombocytopenia is also frequently observed in patients with pneumonia (88) and other acute lung inflammatory diseases (89). This was observed in our *in vivo* lung inflammation mouse models (Fig. III. 5A and B). However, how platelets are activated and recruited into pulmonary region during pneumonia is still not fully understood (13). With functional TLR-4 expression (90,91), platelets can respond to LPS treatment and bacterial infection (Fig. III. 5D and E). It is also reported that influenza virus can interact with platelets and consequentially induce their activation (92,93) (Fig. III. 5F). Besides, hyperoxia can also induce platelet activation and lung sequestration (94). Since T1α protein (podoplanin, AEC I marker)

possesses a platelet aggregation-stimulating domain (95,96), a hypothesis that T1α is implicated in platelet recruitment and activation following AEC I damage during lung injury was also recently proposed (97). Here we provided an additional piece of evidence in our *in viv*o model of influenza viral pneumonia to support this new hypothesis. From the scope of time frame, release of T1α into BAL and potentially plasma due to injury of AEC I at 1 dpi (Fig. III. 4G) might be able to trigger the sequestration and activation of platelets (Fig. III 5C and F), and subsequent deposition of Dkk1 in the lung start from 2 dpi (Fig. III. 1D).

Almost all the pharmacologic therapies evaluated in clinical trials have not proven effective. Stem cells therapy is emerged as a new hope for the ALI/ARDS patients (98). Both bone marrow-derived mesenchymal stem cells (MSC) and induced pluripotent stem (iPS) cells have been reported to attenuate ALI/ARDS though improving fluid clearance, reducing neutrophil accumulation and augmenting lung repair (99,100). By far, researchers identified Keratinocyte Growth Factor (KGF) (101), interleukin 1 receptor antagonist (IL1RN) (102), insulin-like growth factor 1(IGF-1) (103), and prostaglandin E(2) (104) as potential paracrine factors secreted from the stem cells, which mediate their protective effects. Since Wnt/β-catenin signaling is known to be essential to maintain the phenotype and proper function of stem cells (26,105), it is worth to explore the potential contribution of Wnt ligands or modulators from stem cells in their protective effects in ALI/ARDS.

In summary, our results demonstrated a novel function of Wnt/β-catenin signaling in the regulation of neutrophil infiltration during acute lung inflammation. Platelet-derived Dkk1 was identified as the major Wnt antagonist contributed to the depression of Wnt/β-catenin signaling, which led to up-regulation of ICAM-1 and VCAM-1 in AEC. Modulation of Wnt/β-catenin signaling by Wnt3a or Dkk1 neutralization successfully prevented neutrophil-mediated acute pulmonary inflammation. Our study on platelet-derived Wnt antagonist Dkk1 in ICAM-

1/VCAM-1-mediated neutrophil infiltration opens a new field in the ALI/ARDS research and provides insights for future drug development and new therapeutic strategies of exploration.

3.6 Acknowledgments

We thank Dr. Mary Williams (Boston University) for providing E10 cells with the permission of Dr. Al Malkinson (University of Colorado). Hamster anti-mouse T1α antibody developed by Dr. Andrew Farr (University of Washington) was obtained from the Developmental Studies Hybridoma Bank developed under the auspices of the NICHD and maintained by The University of Iowa. pcDNA3.0-based P65 overexpression plasmid was constructed by Dr. Stephen Smale (University of California, Los Angeles) and obtained from Addgene (Cambridge, MA).

3.7 Reference

1. Grommes, J. and Soehnlein, O. (2011) *Molecular Medicine* **17,** 293-307
2. Narasaraju, T., Yang, E., Samy, R. P., Ng, H. H., Poh, W. P., Liew, A. A., Phoon, M. C., van Rooijen, N., and Chow, V. T. (2011) *American Journal of Pathology* **179,** 199-210
3. Grommes, J., Vijayan, S., Drechsler, M., Hartwig, H., Morgelin, M., Dembinski, R., Jacobs, M., Koeppel, T. A., Binnebosel, M., Weber, C., and Soehnlein, O. (2012) *Plos One* **7,**
4. Tate, M. D., Deng, Y. M., Jones, J. E., Anderson, G. P., Brooks, A. G., and Reading, P. C. (2009) *Journal of Immunology* **183,** 7441-7450
5. Segel, G. B., Halterman, M. W., and Lichtman, M. A. (2011) *Journal of Leukocyte Biology* **89,** 359-372
6. Beck-Schimmer, B., Madjdpour, C., Kneller, S., Ziegler, U., Pasch, T., Wuthrich, R. P., Ward, P. A., and Schimmer, R. C. (2002) *European Respiratory Journal* **19,** 1142-1150
7. Herold, S., von Wulffen, W., Steinmueller, M., Pleschka, S., Kuziel, W. A., Mack, M., Srivastava, M., Seeger, W., Maus, U. A., and Lohmeyer, J. (2006) *Journal of Immunology* **177,** 1817-1824
8. Rosseau, S., Selhorst, J., Wiechmann, K., Leissner, K., Maus, U. R., Mayer, K., Grimminger, F., Seeger, W., and Lohmeyer, J. (2000) *Journal of Immunology* **164,** 427-435

9. Beck-Schimmer, B., Schimmer, R. C., Madjdpour, C., Bonvini, J. M., Pasch, T., and Ward, P. A. (2001) *American Journal of Respiratory Cell and Molecular Biology* **25,** 780-787

10. Mendez, M. P., Morris, S. B., Wilcoxen, S., Greeson, E., Moore, B., and Paine, R. (2006) *American Journal of Physiology-Lung Cellular and Molecular Physiology* **290,** L962-L970

11. Ward, P. A. (2003) *The European respiratory journal. Supplement* **44,** 22s-23s

12. Collins, T., Read, M. A., Neish, A. S., Whitley, M. Z., Thanos, D., and Maniatis, T. (1995) *Faseb Journal* **9,** 899-909

13. Weyrich, A. S. and Zimmerman, G. A. (2012) *Annu. Rev. Physiol.*

14. Caudrillier, A. and Looney, M. R. (2012) *Current Pharmaceutical Design* **18,** 3260-3266

15. Chi, X., Zhi, L., Gelderman, M. P., and Vostal, J. G. (2012) *Plos One* **7,**

16. Kornerup, K. N., Salmon, G. P., Pitchford, S. C., Liu, W. L., and Page, C. P. (2010) *Journal of Applied Physiology* **109,** 758-767

17. Zarbock, A. and Ley, K. (2009) *Frontiers in Bioscience* **14,** 150-158

18. Bozza, F. A., Shah, A. M., Weyrich, A. S., and Zimmerman, G. A. (2009) *American Journal of Respiratory Cell and Molecular Biology* **40,** 123-134

19. Ueland, T., Otterdal, K., Lekva, T., Halvorsen, B., Gabrielsen, A., Sandberg, W. J., Paulsson-Berne, G., Pedersen, T. M., Folkersen, L., Gullestad, L., Oie, E., Hansson, G. K., and Aukrust, P. (2009) *Arteriosclerosis Thrombosis and Vascular Biology* **29,** 1228-1234

20. Danese, S., Katz, J. A., Saibeni, S., Papa, A., Gasbarrini, A., Vecchi, M., and Fiocchi, C. (2003) *Gut* **52,** 1435-1441

21. Dixon, J. T., Gozal, E., and Roberts, A. M. (2012) *Archives of Physiology and Biochemistry* **118,** 72-82

22. Pittet, J. F., Mackersie, R. C., Martin, T. R., and Matthay, M. A. (1997) *American Journal of Respiratory and Critical Care Medicine* **155,** 1187-1205

23. Weng, T. T. and Liu, L. (2010) *Respiratory Research* **11,**

24. Zemans, R. L., Briones, N., Campbell, M., McClendon, J., Young, S. K., Suzuki, T., Yang, I. V., De Langhe, S., Reynolds, S. D., Mason, R. J., Kahn, M., Henson, P. M., Colgan, S. P., and Downey, G. P. (2011) *Proceedings of the National Academy of Sciences of the United States of America* **108,** 15990-15995

25. Flozak, A. S., Lam, A. P., Russell, S., Jain, M., Peled, O. N., Sheppard, K. A., Beri, R., Mutlu, G. M., Budinger, G. R. S., and Gottardi, C. J. (2010) *Journal of Biological Chemistry* **285,** 3157-3167

26. Volckaert, T., Dill, E., Campbell, A., Tiozzo, C., Majka, S., Bellusci, S., and Langhe, S. P. (2011) *Journal of Clinical Investigation* **121,** 4409-4419

27. Crosby, L. M. and Waters, C. M. (2010) *American Journal of Physiology-Lung Cellular and Molecular Physiology* **298,** L715-L731

28. Diarra, D., Stolina, M., Polzer, K., Zwerina, J., Ominsky, M. S., Dwyer, D., Korb, A., Smolen, J., Hoffmann, M., Scheinecker, C., van der Heide, D., Landewe, R., Lacey, D., Richards, W. G., and Schett, G. (2007) *Nature Medicine* **13,** 156-163

29. Manicassamy, S., Reizis, B., Ravindran, R., Nakaya, H., Salazar-Gonzalez, R. M., Wang, Y. C., and Pulendran, B. (2010) *Science* **329,** 849-853

30. Chong, Z. Z., Li, F. Q., and Maiese, K. (2007) *Cellular Signalling* **19,** 1150-1162

31. Neumann, J., Schaale, K., Farhat, K., Endermann, T., Ulmer, A. J., Ehlers, S., and Reiling, N. (2010) *Faseb Journal* **24,** 4599-4612

32. Lee, H., Bae, S., Choi, B. W., and Yoon, Y. (2012) *Immunopharmacology and Immunotoxicology* **34,** 56-65

33. Sun, J., Hobert, M. E., Duan, Y. L., Rao, A. S., He, T. C., Chang, E. B., and Madara, J. L. (2005) *American Journal of Physiology-Gastrointestinal and Liver Physiology* **289,** G129-G137

34. Kim, J., Kim, J., Kim, D. W., Ha, Y., Ihm, M. H., Kim, H., Song, K., and Lee, I. (2010) *Journal of Immunology* **185,** 1274-1282

35. Malhotra, S. and Kincade, P. W. (2009) *Experimental Hematology* **37,** 19-30

36. Du, Q., Zhang, X. L., Cardinal, J., Cao, Z. X., Guo, Z., Shao, L. F., and Geller, D. A. (2009) *Cancer Research* **69,** 3764-3771

37. Deng, J. O., Miller, S. A., Wang, H. Y., Xia, W. Y., Wen, Y., Zhou, B. H. P., Li, Y., Lin, S. Y., and Hung, M. C. (2002) *Cancer Cell* **2,** 323-334

38. Wang, R., Ahmed, J., Wang, G. Q., Hassan, I., Strulovici-Barel, Y., Hackett, N. R., and Crystal, R. G. (2011) *Plos One* **6,**

39. Sharma, S., Tantisira, K., Carey, V., Murphy, A. J., Lasky-Su, J., Celedon, J. C., Lazarus, R., Klanderman, B., Rogers, A., Soto-Quiros, M., Avila, L., Mariani, T., Gaedigk, R., Leeders, S., Torday, J., Warburton, D., Raby, B., and Weiss, S. T. (2010) *American Journal of Respiratory and Critical Care Medicine* **181,** 328-336

40. Villar, J., Cabrera, N. E., Casula, M., Valladares, F., Flores, C., Lopez-Aguilar, J., Blanch, L., Zhang, H. B., Kacmarek, R. M., and Slutsky, A. S. (2011) *Intensive Care Medicine* **37,** 1201-1209

41. Hoogendijk, A. J., Diks, S. H., van der Poll, T., Peppelenbosch, M. P., and Wieland, C. W. (2011) *Plos One* **6,**

42. Foronjy, R., Imai, K., Shiomi, T., Mercer, B., Sklepkiewicz, P., Thankachen, J., Bodine, P., and D'Armiento, J. (2010) *American Journal of Pathology* **177,** 598-607

43. Ke, H. Z., Richards, W. G., Li, X. D., and Ominsky, M. S. (2012) *Endocrine Reviews* **33,** 747-783

44. Pfaff, E. M., Becker, S., Gunther, A., and Konigshoff, M. (2011) *European Respiratory Journal* **37,** 79-87

45. Altemeier, W. A., Matute-Bello, G., Gharib, S. A., Glenny, R. W., Martin, T. R., and Liles, W. C. (2005) *Journal of Immunology* **175,** 3369-3376

46. Mishra, A., Chintagari, N. R., Guo, Y., Weng, T., Su, L., and Liu, L. (2011) *Journal of Cell Science* **124,** 657-668

47. Chen, Z. M., Chintagari, N. R., Guo, Y. J., Bhaskaran, M., Chen, J. W., Gao, L., Jin, N. L., Weng, T. T., and Liu, L. (2007) *Free Radical Biology and Medicine* **43,** 628-642

48. Weng, T. T., Gao, L., Bhaskaran, M., Guo, Y. J., Gou, D. M., Narayanaperumal, J., Chintagari, N. R., Zhang, K. X., and Liu, L. (2009) *Journal of Biological Chemistry* **284,** 28021-28032

49. Skripchenko, A., Kurtz, J., Moroff, G., and Wagner, S. J. (2008) *Transfusion* **48,** 1469-1477

50. Sethi, S., Singh, M. P., and Dikshit, M. (1999) *Blood* **93,** 333-340

51. Douglas, I. S., del Valle, F. D., Winn, R. A., and Voelkel, N. F. (2006) *American Journal of Respiratory Cell and Molecular Biology* **34,** 274-285

52. Gawaz, M., Langer, H., and May, A. E. (2005) *Journal of Clinical Investigation* **115,** 3378-3384

53. Zarbock, A., Singbartl, K., and Ley, K. (2006) *Journal of Clinical Investigation* **116,** 3211-3219

54. Looney, M. R., Nguyen, J. X., Hu, Y. M., Van Ziffle, J. A., Lowell, C. A., and Matthay, M. A. (2009) *Journal of Clinical Investigation* **119,** 3450-3461

55. Erlich, J. M., Talmor, D. S., Cartin-Ceba, R., Gajic, O., and Kor, D. J. (2011) *Chest* **139,** 289-295

56. Caudrillier, A., Kessenbrock, K., Gilliss, B. M., Nguyen, J. X., Marques, M. B., Monestier, M., Toy, P., Werb, Z., and Looney, M. R. (2012) *Journal of Clinical Investigation* **122,** 2661-2671

57. Heiland, G. R., Zwerina, K., Baum, W., Kireva, T., Distler, J. H., Grisanti, M., Asuncion, F., Li, X. D., Ominsky, M., Richards, W., Schett, G., and Zwerina, J. (2010) *Annals of the Rheumatic Diseases* **69,** 2152-2159

58. Bradley, P. P., Priebat, D. A., Christensen, R. D., and Rothstein, G. (1982) *Journal of Investigative Dermatology* **78,** 206-209

59. Angers, S. and Moon, R. T. (2009) *Nature Reviews Molecular Cell Biology* **10,** 468-477

60. Matthay, M. A., Ware, L. B., and Zimmerman, G. A. (2012) *Journal of Clinical Investigation* **122,** 2731-2740

61. Vincent, J. L. (2011) *Acute Kidney Injury, Acute Lung Injury and Septic Shock: How Does Mortality Compare?*, KARGER, BASEL

62. Bhargava, M. and Wendt, C. H. (2012) *Translational Research* **159,** 205-217

63. Matthay, M. A. and Zimmerman, G. A. (2005) *American Journal of Respiratory Cell and Molecular Biology* **33,** 319-327

64. Altemeier, W. A., Matute-Bello, G., Frevert, C. W., Kawata, Y., Kajikawa, O., Martin, T. R., and Glenny, R. W. (2004) *American Journal of Physiology-Lung Cellular and Molecular Physiology* **287,** L533-L542

65. O'Mahony, D. S., Liles, W. C., Altemeier, W. A., Dhanireddy, S., Frevert, C. W., Liggitt, D., Martin, T. R., and Matute-Bello, G. (2006) *Critical Care* **10,**

66. Matute-Bello, G., Frevert, C. W., and Martin, T. R. (2008) *American Journal of Physiology-Lung Cellular and Molecular Physiology* **295,** L379-L399

67. Villar, J., Cabrera, N. E., Valladares, F., Casula, M., Flores, C., Blanch, L., Quilez, M. E., Santana-Rodriguez, N., Kacmarek, R. M., and Slutsky, A. S. (2011) *Plos One* **6,**

68. Apparao, K. B. C., Newman, D. R., Zhang, H. Y., Khosla, J., Randell, S. H., and Sannes, P. L. (2010) *Anatomical Record-Advances in Integrative Anatomy and Evolutionary Biology* **293,** 938-946

69. Rey, J. P. and Ellies, D. L. (2010) *Developmental Dynamics* **239,** 102-114

70. Madjdpour, C., Oertli, B., Ziegler, U., Bonvini, J. M., Pasch, T., and Beck-Schimmer, B. (2000) *American Journal of Physiology-Lung Cellular and Molecular Physiology* **278,** L572-L579

71. Doerschuk, C. M., Quinlan, W. M., Doyle, N. A., Bullard, D. C., Vestweber, D., Jones, M. L., Takei, F., Ward, P. A., and Beaudet, A. L. (1996) *Journal of Immunology* **157,** 4609-4614

72. Callicutt, C. S., Sabek, O., Fukatsu, K., Lundberg, A. H., Gaber, L., Wilcox, H., Kotb, M., and Gaber, A. O. (2003) *Surgery* **133,** 186-196

73. Tumurkhuu, G., Koide, N., Dagvadorj, J., Morikawa, A., Hassan, F., Islam, S., Naiki, Y., Mori, I., Yoshida, T., and Yokochi, T. (2008) *Clinical and Experimental Immunology* **152,** 182-191

74. Tickenbrock, L., Schwable, J., Strey, A., Sargin, B., Hehn, S., Baas, M., Choudhary, C., Gerke, V., Berdel, W. E., Muller-Tidow, C., and Serve, H. (2006) *Journal of Leukocyte Biology* **79,** 1306-1313

75. Shen, Q. J., Fan, J., Yang, X. R., Tan, Y. X., Zhao, W. F., Xu, Y., Wang, N., Niu, Y. D., Wu, Z., Zhou, J., Qiu, S. J., Shi, Y. H., Yu, B., Tang, N., Chu, W., Wang, M., Wu, J. H., Zhang, Z. G., Yang, S. L., Gu, J. R., Wang, H. Y., and Qin, W. X. (2012) *Lancet Oncology* **13,** 817-826

76. Kim, K. I., Park, K. U., Chun, E. J., Choi, S. I., Cho, Y. S., Youn, T. J., Cho, G. Y., Chae, I. H., Song, J., Choi, D. J., and Kim, C. H. (2011) *Journal of Korean Medical Science* **26,** 1178-1184

77. Seifert-Held, T., Pekar, T., Gattringer, T., Simmet, N. E., Scharnagl, H., Stojakovic, T., Fazekas, F., and Storch, M. K. (2011) *Atherosclerosis* **218,** 233-237

78. Chilosi, M., Poletti, V., Zamo, A., Lestani, M., Montagna, L., Piccoli, P., Pedron, S., Bertaso, M., Scarpa, A., Murer, B., Cancellieri, A., Maestro, R., Semenzato, G., and Doglioni, C. (2003) *American Journal of Pathology* **162,** 1495-1502

79. Mazieres, J., He, B., You, L., Xu, Z., and Jablons, D. M. (2005) *Cancer Letters* **222,** 1-10

80. Grommes, J., Alard, J. E., Drechsler, M., Wantha, S., Morgelin, M., Kuebler, W. M., Jacobs, M., von Hundelshausen, P., Markart, P., Wygrecka, M., Preissner, K. T., Hackeng, T. M., Koenen, R. R., Weber, C., and Soehnlein, O. (2012) *American Journal of Respiratory and Critical Care Medicine* **185,** 628-636

81. Torii, Y., Shimizu, T., Yokoi, T., Sugimoto, H., Katashiba, Y., Ozasa, R., Fujita, S., Adachi, Y., Maki, M., and Nomura, S. (2011) *International journal of general medicine* **4,** 677-680

82. Gustafsson, D., Bylund, R., Antonsson, T., Nilsson, I., Nystrom, J. E., Eriksson, U., Bredberg, U., and Teger-Nilsson, A. C. (2004) *Nature Reviews Drug Discovery* **3,** 649-659

83. Jackson, S. P. and Schoenwaelder, S. M. (2003) *Nature Reviews Drug Discovery* **2,** 775-789

84. Nurden, A. T., Viallard, J. F., and Nurden, P. (2009) *Lancet* **373,** 1562-1569

85. Steele, B. M., Harper, M. T., Macaulay, I. C., Morrell, C. N., Perez-Tamayo, A., Foy, M., Habas, R., Poole, A. W., Fitzgerald, D. J., and Maguire, P. B. (2009) *Proceedings of the National Academy of Sciences of the United States of America* **106,** 19836-19841

86. Yeaman, M. R. (2010) *Cellular and Molecular Life Sciences* **67,** 525-544

87. Flaujac, C., Boukour, S., and Cramer-Borde, E. (2010) *Cellular and Molecular Life Sciences* **67,** 545-556

88. Mirsaeidi, M., Peyrani, P., Aliberti, S., Filardo, G., Bordon, J., Blasi, F., and Ramirez, J. A. (2010) *Chest* **137,** 416-420

89. Bhadade, R. R., de Souza, R. A., Harde, M. J., and Khot, A. (2011) *Journal of Postgraduate Medicine* **57,** 286-290

90. Andonegui, G., Kerfoot, S. M., McNagny, K., Ebbert, K. V. J., Patel, K. D., and Kubes, P. (2005) *Blood* **106,** 2417-2423

91. Aslam, R., Speck, E. R., Kim, M., Crow, A. R., Bang, K. W. A., Nestel, F. P., Ni, H. Y., Lazarus, A. H., Freedman, J., and Semple, J. W. (2006) *Blood* **107,** 637-641

92. Rondina, M. T., Brewster, B., Grissom, C. K., Zimmerman, G. A., Kastendieck, D. H., Harris, E. S., and Weyrich, A. S. (2012) *Chest* **141,** 1490-1495

93. Terada, H., Baldini, M., Ebbe, S., and Madoff, M. A. (1966) *Blood-the Journal of Hematology* **28,** 213-&

94. Barazzone, C., TacchiniCottier, F., Vesin, C., Rochat, A. F., and Piguet, P. F. (1996) *American Journal of Respiratory Cell and Molecular Biology* **15,** 107-114

95. Kunita, A., Kashima, T. G., Morishita, Y., Fukayama, M., Kato, Y., Tsuruo, T., and Fujita, N. (2007) *American Journal of Pathology* **170,** 1337-1347

96. Uhrin, P., Zaujec, J., Breuss, J. M., Olcaydu, D., Chrenek, P., Stockinger, H., Fuertbauer, E., Moser, M., Haiko, P., Fassler, R., Alitalo, K., Binder, B. R., and Kerjaschki, D. (2010) *Blood* **115,** 3997-4005

97. Tyrrell, C., McKechnie, S. R., Beers, M. F., Mitchell, T. J., and McElroy, M. C. (2012) *Experimental Lung Research* **38,** 266-276

98. Matthay, M. A., Goolaerts, A., Howard, J. P., and Lee, J. W. (2010) *Critical Care Medicine* **38,** S569-S573

99. Hayes, M., Curley, G., and Laffey, J. G. (2012) *F1000 medicine reports* **4,** 2

100. Yang, K. Y., Shih, H. C., How, C. K., Chen, C. Y., Hsu, H. S., Yang, C. W., Lee, Y. C., Perng, R. P., Peng, C. H., Li, H. Y., Chang, C. M., Mou, C. Y., and Chiou, S. H. (2011) *Chest* **140,** 1243-1253

101. Lee, J. W., Fang, X. H., Gupta, N., Serikov, V., and Matthay, M. A. (2009) *Proceedings of the National Academy of Sciences of the United States of America* **106,** 16357-16362

102. Ortiz, L. A., DuTreil, M., Fattman, C., Pandey, A. C., Torres, G., Go, K., and Phinney, D. G. (2007) *Proceedings of the National Academy of Sciences of the United States of America* **104,** 11002-11007

103. Ionescu, L., Byrne, R. N., van Haaften, T., Vadivel, A., Alphonse, R. S., Rey-Parra, G. J., Weissmann, G., Hall, A., Eaton, F., and Thebaud, B. (2012) *American journal of physiology. Lung cellular and molecular physiology* **303,** L967-L977

104. Nemeth, K., Leelahavanichkul, A., Yuen, P. S. T., Mayer, B., Parmelee, A., Doi, K., Robey, P. G., Leelahavanichkul, K., Koller, B. H., Brown, J. M., Hu, X. Z., Jelinek, I., Star, R. A., and Mezey, E. (2009) *Nature Medicine* **15,** 42-49

105. Zhao, C., Blum, J., Chen, A., Kwon, H. Y., Jung, S. H., Cook, J. M., Lagoo, A., and Reyal, T. (2007) *Cancer Cell* **12,** 528-541

106. SR Russell, A Lam, A Flozak, and CJ Gottardi: Role for b-Catenin/TCF Signaling in Lung Repair after Injury. A108. THE AIRWAY EPITHELIUM: THE ENVIRONMENT, INJURY, AND REPAIR. American Thoracic Society International Conference. April 1, 2009, A2384

CHAPTER V

AXIN1: A NOVEL SCAFFOLD PROTEIN JOINS THE ANTIVIRAL NETWORK OF INTERFERON

4.1 Abstract

Acute respiratory infection by influenza virus is a persistent and pervasive public health problem. Antiviral innate immunity initiated by type I interferon (IFN) is the first responder to pathogen invasion and provides the first line of defense. We discovered that Axin1, a scaffold protein, was degraded during influenza virus infection of mice. We found that Axin1 boosted type I IFN response to influenza virus infection through the stimulation of JNK/c-Jun and Smad3 signaling. Axin1 also interacted with interferon-induced protein with tetratricopeptide repeats 1/2/3 (IFIT1/2/3), a viral RNA sensor complex. In addition, Axin1 specifically promoted the degradation of hnRNP M, a nucleoprotein required for efficient activity of influenza virus polymerases, and sequentially EZH2. Axin1 and its chemical stabilizer, XAV939, successfully reduced influenza virus replication and protected the mice from influenza virus infection. Thus, our study provides new mechanistic insights into the regulation of type I IFN response and presents a new potential therapeutics of targeting Axin1 against influenza virus infection.

Key words: Axin1, influenza virus, interferon, JNK/c-Jun, and Smad3

4.2 Introduction

The influenza virus belongs to the *Orthomyxoviridae* family and is classified into three types: A, B and C based on their internal protein sequences (1). With the global pandemic potential and up to 500,000 annual deaths worldwide during seasonal epidemics, influenza A virus is a major public health concern and causes enormous economic burden (2). Prevention relying on vaccination has several limitations, including the lag time for vaccine manufacture and the low coverage rate. Considering the increasing level of viral resistance to current anti-influenza drugs targeting neuraminidase (NA) or M2 channel (3), it is particularly important to develop novel antiviral medicine.

Discovered in 1957, Interferon (IFN) is a category of cytokines that can "interfere" with viral replication within host cells (4). IFN is now considered as the most potent vertebrate-derived agent for mobilizing antimicrobial effector that functions against invasive pathogens (5). Three types of IFN has been identified and classified according to the specification of their receptor complex (6). Type I interferons (IFNβ, 14 IFNαs, IFNδ, IFNε, IFNκ, IFNo and IFNτ), well known for their antiviral properties, mediate the initiation of both innate immune response and subsequent adaptive immunity to viruses. Type II interferon (IFNγ) stimulates broad immune responses to various pathogens other than viruses. Type III interferons (3 IFNλs) are also known to regulate antiviral response and proposed as ancestral type I IFN. It is widely accepted that viral attachment and viral dsRNA intermediates accumulating during virus life cycle are the primary mediators triggering IFN production, which ultimately results in expression of thousands of IFN-stimulated genes (ISGs) (OAS1, MX1, and etc.) and limits virus replication (7).

In the early phase of infection, Toll-like receptors (TLR), cytosolic RIG-1-like receptors (RIG-1 and MDA5), NOD-like receptors, and C-type lectin receptors are major viral sensors which can recognize influenza virus (8). Recently, the novel IFN-regulated viral RNA sensor, interferon-induced protein with tetratricopeptide repeats 1 (IFIT1) was discovered with a substantial antiviral activity (9). Activation of type I IFN expression by these pattern recognition

receptors (PRRs) is controlled by multiple transcription factors (TFs) including c-*Jun*/ATF2 (AP1), interferon regulatory factor 3/7 (IRF3/7), and p50/p65 (NF-κB) (10). Smad3, as a transcription factor, also enhances type I IFN expression by specifically cooperating with IRF7 (11). In the later phase of infection, secreted type I IFN stimulates type I IFN receptor (IFNAR1/2) in an autocrine and paracrine fashion, which leads to the activation of Janus kinase (JAK) – signal transducer and activator of transcription (STAT) pathway, and finally turns on cellular antiviral status (12).

Axin was discovered as a negative regulator of Axis formation in the development of mouse embryos (13). Axin proteins, present in two different isoforms (Axin1 and Axin2), act as an architectural platform for the degradation of the oncogenic protein β-catenin (14,15). Unlike Axin2, Axin1 has, in fact, emerged as a multifunction scaffolding protein for many other signaling pathways, including c-*Jun*-NH_2-kinase (JNK) mitogen-activated protein kinase (MAPK) signaling, p53 signaling, and transforming growth factor β (TGF-β) signaling (16). Axin1 forms a complex with MEKK1/4 and mediates JNK/c-*Jun* activation through MKK4/7 (17). Axin1 also promotes Smad3 phosphorylation in response to TGF-β (18), and downregulates the negative factor, Smad7, in TGF-β signaling (19). By forming a ternary complex, Axin1 stimulates p53 via activation of homeodomain-interacting protein kinase-2 (HIPK2) kinase (20). These intriguing β-catenin-independent roles of Axin1 suggest its involvement in multiple physiological and pathological processes. In the infectious diseases, Axin1 shows an inhibitory effect on bacterial *Salmonella* invasiveness and regulates inflammatory response during the infection (21). In addition, silencing of Axin1 up-regulates human immunodeficiency virus type I (HIV-1) gene expression and viral replication (22). Recently, XAV939 was discovered to specifically inhibit poly(ADP-ribose) polymerase tankyrase1/2 (TNK1/2), which induces poly(ADP-ribosyl)ation (PARylation) of Axin1 and in turn promotes its proteasome-mediated degradation (23).

In this study, we searched for novel host factors essential for influenza virus replication and IFN response during viral infection, and explored new antivirals based on the identified targets. We first discovered that Axin1 was degraded in a mouse model of influenza virus-associated pneumonia. We then demonstrated that Axin1 boosted IFN response and inhibited influenza virus replication through the activation of JNK/c-*Jun* pathway and Smad3 signaling. We also found the physical interaction between Axin1 and the viral RNA sensor, IFIT1. In addition, we found Axin1 specifically associated with two other host proteins, hnRNP M and EZH2, which are required for virus replication, and promoted their degradation. XAV939, an Axin stabilizer, attenuated influenza viral pneumonia and protected animals from lethal influenza virus challenge. Our studies, for the first time, recruited Axin1, the 16-years old scaffold protein, into the antiviral network of interferon.

4.3 Materials and Methods

4.3.1 Animals

All male C57BL/6N mice (6 – 8 weeks old) were obtained from Jackson Laboratory (Bar Harbor, ME), housed and cared for by the Laboratory Animal Resource Unit operated by the Center for Veterinary Health Sciences, Oklahoma State University. Experimental protocols were reviewed and approved by the Institutional Animal Care and Use Committee of Oklahoma State University.

4.3.2 Influenza virus

Influenza virus H1N1 strain A/Puerto Rico/8/1934 was obtained from American Type Culture Collection (ATCC, Manassas, VA), amplified in day-9 to day-10 embryonnated SPF eggs, and stored at -80^{o}C.

4.3.3 Mouse model of influenza viral pneumonia

Male C57BL/6N mice (6-8 weeks of age) were anesthetized with intraperitoneal injection of ketamine (80 mg/kg body weight) and xylazine (10 mg/kg body weight), and inoculated with influenza virus A/Puerto Rico/8/1934 H1N1 (250 pfu/mouse) intranasally. Mice were weighed daily for the evaluation of loss of body weights and clinical signs such as ruffled fur and respiratory distress. Animals were sacrificed on days 0 - 7 post infections. Unlavaged lungs were homogenized in liquid nitrogen by mortar and pestle, aliquoted and stored at -80^{o}C for further use.

4.3.4 BAL analysis

Lungs were lavaged with 1 ml of normal saline three times. Bronchoalveolar lavages (BAL) were centrifuged at 380 g for 10 min at 4^{o}C and the supernatants were stored at -80^{o}C for further analysis. Protein concentrations in BAL were measured by a Bio-Rad protein assay (Bio-Rad Laboratories, Hercules, CA). Lactate dehydrogenase (LDH) activity in BAL was determined by a Cytotoxicity Detection kit (Roche Applied Sciences, Indianapolis, IN) with type III L-lactic dehydrogenase (SIGMA, St. Louis, MO) as standards. BAL cells were resuspended in normal saline and total cells were counted using a hemocytometer. For differential cell counts, cytospinned cells on the glass slides were stained with Wright-Giemsa.

4.3.5 Histopathology

Unlavaged lungs were instilled with 4% paraformaldehyde in PBS at 20 cm H_2O pressure and fixed for 72 hours, embedded in paraffin and sectioned at 4 μm thickness. The sections were stained with hematoxylin and eosin and were examined under a light microscope.

4.3.6 Survival study of lethal dose influenza virus infection

Male C57BL/6N mice (6-8 week old) were challenged intranasally with a lethal dose (1,000 pfu) of influenza virus A/PR/8/34 H1N1 under anesthesia. XAV939 (SIGMA, St. Louis,

MO) was dissolved in dimethyl sulfoxide (DMSO) and given to the mice orally using metal oral gavage in a dose of 50 mg/kg mixed with 1% methylcellulose (50 µl/mouse) every day, beginning with a day before infection (-1 dpi) and continued until 2 or 4 days post infection. Control animals were given vehicle alone in the same formulation. All animals were observed daily for body weight loss and clinical signs such as ruffled fur, inactivity and difficulty in breathing.

4.3.7 Cell culture

Human embryonic kidney 293 (HEK293), human lung epithelial A549, and Madin-Darby canine kidney (MDCK) cells (ATCC, Manassas, VA) were maintained in Earle's Minimal Essential Medium (EMEM) complemented with 10% fetal bovine serum (FBS). Human epithelial type 2 (HEp2) cells (ATCC, Manassas, VA) were maintained in EMEM complemented with 10% FBS, Glutamine, and Non-Essential Amino Acids. E10 cells, a gift from Dr. Mary Williams (Boston University, MA), were cultured in CMRL1066 supplemented with 10% FBS and Glutamine. Cells were grown at 37°C in a humidified atmosphere containing 5% CO_2.

4.3.8 Primary mouse alveolar epithelial type II cells (AEC II) isolation

Murine AEC II were isolated from Male C57BL/6N mice (6-8 weeks of age) as described previously (24) . Lung was perfused with solution II (0.9% NaCl, 0.1% glucose, 10 mM HEPES, 1.3 mM $MgSO_4$, 5 mM KCl, , 1.7 mM $CaCl_2$, 0.1 mg/ml streptomycin sulfate, 0.06 mg/ml penicillin G, 3 mM $Na2HPO_4$ and 3 mM $NaH2PO_4$, pH 7.4) to clear the blood. AEC II was released from the lung by digestion with dispase (250 caseinolytic units/ml, BD Biosciences, Franklin Lakes, NJ). Then, the lung was chopped with a Mcllwain tissue chopper, and the lung slices were further digested with DNase I (100 µg/ml) for 45 min at 37^{o}C with intermittent shaking. The digested lung slices were then filtered through 160-, 37- and 15-µm nylon mesh sequentially. The filtrate was centrifuged at 250 g for 10 min at 4^{o}C. The cell pellet was resuspended in Dulbecco's Modifed Eagle's Medium (DMEM) supplemented with 10% FBS and

incubated in a 100 mm petridish coated with mouse IgG (75 μg/dish) for 1 hour. The unattached cells were spun down at 250 g for 10 min at 4^{o}C and resuspended in DMEM containing 10% FBS. The isolated AEC II had a purity of 90% as determined by SP-C staining and a viability of over 98% as assessed by trypan blue exclusion. AEC II were cultured in 12-well tissue culture plates at 1x10^{6} cells/well in DMEM containing 10% FBS, penicillin and streptomycin for 5 days before the use.

4.3.9 Plasmids and transfection

pCS2-based OE-GFP (15681), OE-Axin1 (21287) and OE-Axin2 (21279) plasmids were obtained from Addgene (Cambridge, MA). All three plasmids have myc-tag. pLKO.1 lentiviral vectors carrying shRNA control, shRNA_hnRNP M (1) and shRNA_hnRNP M (2) were purchased from Thermo Fisher Scientific (Waltham, MA). TOPFlash and FOPflash reporter plasmids were purchased from EMD Millipore (Billerica, MA). Smad3 signaling and ISRE-luc reporter plasmids were purchased from QIAGEN (Valencia, CA). pRL-TK *Renilla* luciferase plasmid was obtained from Progema (Madison, WI). HEK293 cells were cultured on 96-well tissue culture plates (dual luciferase assay) and 12-well tissue culture plates (all other experiments) until 90% confluence and then transfected with proper plasmids using Lipofectamine 2000 (Invitrogen, Carlsbad, CA).

4.3.10 *In vitro* influenza virus infection

HEK293, A549 and primary mouse AEC II were washed with serum-free complete DMEM and infected with influenza virus at a multiplicity of infection (MOI) of 2 in serum-free complete DMEM supplemented with 1 μg/ml L-1-tosylamide-2-phenylethyl chloromethyl ketone (TPCK)-treated trypsin (SIGMA, St. Louis, MO) for 1 hour. Then cells were changed into fresh serum-free complete medium and continually cultured for 2 to 48 hours.

4.3.11 *In vitro* respiratory syncytial virus (RSV) infection

HEK293 and Hep2 cells were infected with GFP-labeled RSV-A3 at a MOI of 0.1 or 1 in complete DMEM for 1 hour as described previously (25). Then cells were changed into fresh complete medium and continually cultured for 12 to 48 hours.

4.3.12 Quantitative real-time PCR

Total RNA was extracted from cells or lung tissues using TRI-Reagent (Molecular Research Center, Cincinnati, OH) and digested with TURBO DNase (Ambion, Austin, TX, USA) to remove the genomic DNA contamination. One μg of RNA was reverse-transcribed into cDNA using Moloney murine leukemia virus (M-MLV) reverse transcriptase (Invitrogen, Carlsbad, CA), random primers, and oligo dT (Promega, Madison, WI). Real-time PCR was carried out on 7900HT Fast Real-Time PCR System using SYBR Green I detection Master Mix (Eurogentec, CA) as described previously (26). The primers were designed using Primer Express® software (Applied Biosystems, Foster City, CA), and listed in Table IV. 1.

Table IV.1. Real-time PCR primer sequences

Gene	Species	Forward primers	Reverse primers
18S	Mouse	ATTGCTCAATCTCGGGTGGCTG	CGTTCTTAGTTGGTGGAGCGATTTG
Axin1	Mouse	CTCCAAGCAGAGGACAAAATCA	GGATGGGTTCCCCACAGAAATA
IFNβ1	Mouse	CAGCTCCAAGAAAGGACGAAC	GGCAGTGTAACTCTTCTGCAT
IFNα1	Mouse	TCTGATGCAGCAGGTGGG	AGGGCTCTCCAGACTTCTGCTCTG
IFNα7	Mouse	TGATGAGCTACTACTGGTCAGC	GATCTCTTAGCACAAGGATGGC
IFNλ1	Mouse	ATGAACGCTACACACTGCATC	CCATCCTTTTGCCAGTTCCTC
OAS1	Mouse	CTTTGATGTCCTGGGTCATGT	GCTCCGTGAAGCAGGTAGAG
MX1	Mouse	GAAGGCAAGGTCTTGGATG	GCTGACCTCTGCACTTGACT
IP10	Mouse	CCAAGTGCTGCCGTCATTTTC	GGCTCGCAGGGATGATTTCAA
18S	Human	GTAACCCGTTGAACCCCATT	CCATCCAATCGGTAGTAGCG
β-actin	Human	CATGTACGTTGCTATCCAGGC	CTCCTTAATGTCACGCACGAT
IFNβ1	Human	ATGACCAACAAGTGTCTCCTCC	GGAATCCAAGCAAGTTGTAGCTC
IFNα1	Human	GCCTCGCCCTTTGCTTTACT	CTGTGGGTCTCAGGGAGATCA
IFNα7	Human	AGGGCCTTGATACTCCTGG	TCCTCCTCCGGGAATCTGAAT
IFNλ1	Human	TCGGTAACTGACTTGAATGTCCA	TCGCTTCCCTGTTTTAGCTGC
OAS1	Human	TGTCCAAGGTGGTAAAGGGTG	CCGGCGATTTAACTGATCCTG
MX1	Human	GTTTCCGAAGTGGACATCGCA	CTGCACAGGTTGTTCTCAGC
IP10	Human	GTGGCATTCAAGGAGTACCTC	TGATGGCCTTCGATTCTGGATT
HA	H1N1 influenza	GGCCCAACCACAACACAAAC	AGCCCTCCTTCTCCGTCAGC
NP	H1N1 influenza	TGTGTATGGACCTGCCGTAGC	CCATCCACACCAGTTGACTCTTG
MP	H1N1 influenza	CTTCTAACCGAGGTCGAAACGTA	GGTGACAGGATTGGTCTTGTCTTTA

4.3.13 Western blot

The cells and homogenized lung tissue were lyzed in M-PER Mammalian Protein Extraction Reagent containing 1% Halt Protease and Phosphatase Inhibitor Cocktail (Pierce, Rockford, IL) by Dounce homogenizer followed by sonication and freeze/thaw cycles. The proteins were separated in 10% SDS-PAGE and transferred to nitrocellulose membranes. The blots were blocked for 1 hour at room temperature with 5% dried milk in Tris-buffered saline (10 mM Tris/HCl, 100 mM NaCl and 0.05% Tween; pH 7.5) (TBS-T) and incubated overnight at 4°C with anti-Axin1 (1:1000, Cell Signaling Technology, Danvers, MA), anti-Axin2 (1:1000, Cell Signaling Technology, Danvers, MA), anti-p-JNK1 (1:1000, Cell Signaling Technology, Danvers, MA), anti-JNK1 (1:1000, Cell Signaling Technology, Danvers, MA), anti-p-STAT1 (Tyr 701) (1:1000, Cell Signaling Technology, Danvers, MA), anti-STAT1 (1:1000, Cell Signaling Technology, Danvers, MA), anti-p-GSK-3β (*S9*) (1:1000, Cell Signaling Technology, Danvers, MA), anti-GSK-3β (1:2000, BD Transduction Laboratories, San Jose, CA), anti-p-c-Jun (1:1000, Cell Signaling Technology, Danvers, MA), anti-c-Jun (1:1000, Cell Signaling Technology, Danvers, MA), anti-p-ATF2 (1:1000, Cell Signaling Technology, Danvers, MA), anti-ATF2 (1:1000, Cell Signaling Technology, Danvers, MA), anti-nonO/p54(nrb) (1:1000, SIGMA, St. Louis, MO), anti-SFPQ (1:200, Santa Cruz Biotechnology, Santa Cruz, CA), anti-hnRNP M (1:200, Santa Cruz Biotechnology, Santa Cruz, CA), anti-EZH2 (1:1000, Cell Signaling Technology, Danvers, MA), anti-c-myc (1:2000, DHSB, Iowa City, IO), anti-RSV-M protein serum (1:50, Genscript, Piscataway, NJ), anti-RSV-G protein (1:200, Edward Walsh, University of Rochester School of Medicine, Rochester, NY) and anti-β-actin (1:2000, SIGMA, St. Louis, MO) antibodies. The blots were then rinsed in TBS-T, and incubated for 1 hour at room temperature with goat anti-rabbit, or goat anti-mouse secondary antibodies, coupled to horseradish peroxidase (1:2000, Jackson Immunoresearch, West Grove, PA). After being washed, the blots were developed by SuperSignal West Pico Chemiluminescent Substrate (Pierce, Rockford, IL). The densities of bands were quantified by ImageJ software (National Institutes of Health, Bethesda, Maryland [http://rsb.info.nih.gov/ij/]).

4.3.14 $TCID_{50}$ assay

MDCK cells in 96-well plates were infected with serial dilutions (10^{-1} to 10^{-7}) of virus samples in serum-free complete EMEM containing 1 μg/ml TPCK-treated trypsin for 1 hour. The cells were re-fed with the same medium for 4 days. $TCID_{50}$ values (median tissue culture infective dose) were calculated by the method of Reed and Muench (27).

4.3.15 Immunofluorescence

A549 cells were cultured on 24-well tissue culture plates. At the end of the experiment, the cells were briefly washed with ice-cold phosphate buffered saline (PBS) and fixed with 4% paraformaldehyde for 15 min in room temperature. After being washed with PBS again, the cells were permeabilized with 0.3% Triton X-100 for 10 min and blocked with 10% FBS for 1 hour at room temperature. After being rinsed, the cells were incubated overnight with primary antibodies against Axin1 (1:200), nonO/p54(nrb) (1:200), SFPQ (1:50), hnRNP M (1:50), and EZH2 (1:200). Subsequently, cells were washed with PBS and incubated with Alexa 568-conjugated goat anti-mouse and Alexa 488-conjugated goat anti-rabbit IgG (Invitrogen, Carlsbad, CA) for 1 hour. The nuclei were counterstained with 4',6-diamidino-2-phenylindole (DAPI, 1:1000, Invitrogen, Carlsbad, CA) for 2 min. Images were acquired using a Nikon Eclipse TE-2000 inverted fluorescence microscope.

4.3.16 Immunoprecipitation

Cells were lysed in the M-PER mammalian protein extraction reagent (supplemented with 1% Halt phosphatase and proteases inhibitor mixtures). The cell lysate (400 μg of protein) was incubated with anti-Axin1 antibody (2 μg) or control rabbit IgG (2 μg, Cell Signaling Technology, Danvers, MA) at 4°C for 1 h. Then 5 μl of protein A and 10 μl of protein G-agarose beads were added to the mixtures and incubated overnight at 4°C by gentle end-to-end mixing. The agarose beads were washed three times with ice-cold PBS. The proteins were eluted by

boiling in 1X SDS sample buffer for western blot analysis.

4.3.17 Statistics analysis

The results were analyzed by one-way ANOVA followed with posthoc *Tukey's* test for multiple comparisons of control and treatment groups, or Student's *t*-test using GraphPad Prism (version 6). Survival rate between groups was analyzed by Mantel-Cox χ^2 test on Kaplan-Meier probability estimates using GraphPad Prism. All results were reported as mean ± s.e.m. (n=3-8 for each condition).

4.4 Results

4.4.1 Axin1 is degraded during influenza viral pneumonia

We used a mouse model of viral pneumonia caused by a sub-lethal dose of H1N1 influenza virus infection (28). Weight loss was noticed on day 1 and markedly increased after day 5 (Fig. IV. 1A). The same trend was observed in protein concentration (Fig. IV. 1B) and LDH activity (Fig. IV. 1C) of BAL, indicating vascular leakage and loss of epithelial-endothelial barrier. This observation was also confirmed in histological section (Fig. IV. 1D), in which massive immune cell infiltration can be identified. The number of neutrophils in BAL significantly increased at Day 3 and persisted until day 7 (Fig. IV. 1E). While macrophage numbers were increased from day 5, infiltration of lymphocyte started from day 6 and this may represent the transition from innate immunity to adaptive immunity.

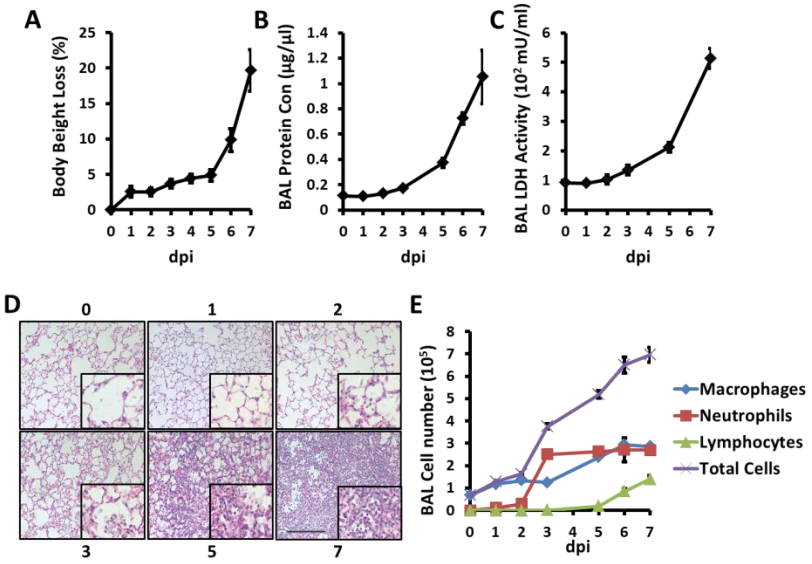

Fig. IV. 1. Acute lung inflammation and injury in influenza virus-infected mouse lungs. Mice were intranasally inoculated with H1N1 influenza A/PR/8/34 virus (250 pfu/mouse). The lung tissue and BALs were collected at 1 to 7 days post infection (dpi). (A) Body weight. (B) BAL protein concentration and (C) BAL LDH activity. (D) H&E staining of paraffin sections of lungs. Scale bar=100 μm. (E) Numbers of immune cells in BAL. Values were shown as means ± s.e.m., n=3

To assess the viral replication, we further measured viral gene expression including hemagglutinin (HA), nucleoprotein (NP) and matrix protein (MP). The expression of all three viral genes reached a plateau at day 3 (Fig. IV. 2A), suggesting that the viral load reached maximum at day 3. IFN response was initiated at day 1 as indicated by increases in mRNA expression of type I and type III IFNs as well as ISGs (Fig. IV. 2B). As a potential antiviral host factor, the expression of Axin1 protein, but not mRNA in the whole lung tissue was significantly reduced at day 1 (Fig. IV. 3A, B), suggesting that Axin1 is degraded in the lung at an early stage of influenza viral pneumonia.

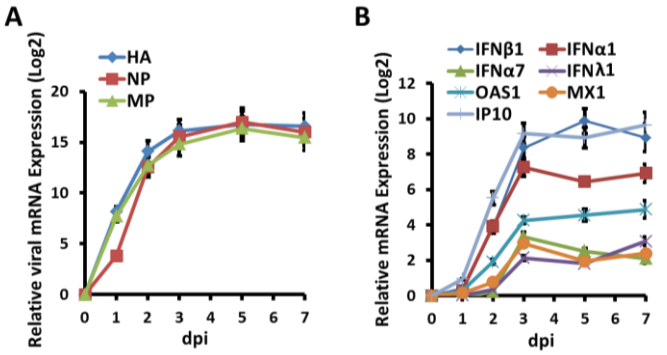

Fig. IV. 2. Virus replication and IFN response in influenza virus infected mouse lungs. Mice were challenged with H1N1 influenza A/PR/8/34 virus (250 pfu/mouse) intranasally and the lungs were collected at 1 to 7 dpi. Relative mRNA expressions of (A) viral genes (HA, NP, and MP), (B) type I IFN (IFNβ1, IFNα1, and IFNα7), type III IFN (IFNλ1), and ISGs (OAS1, MX1, and IP10) in whole lung tissues were measured by Real-time PCR and normalized to 18S rRNA. Results were expressed as Log2 (Value) and represented as means ± s.e.m., n=3

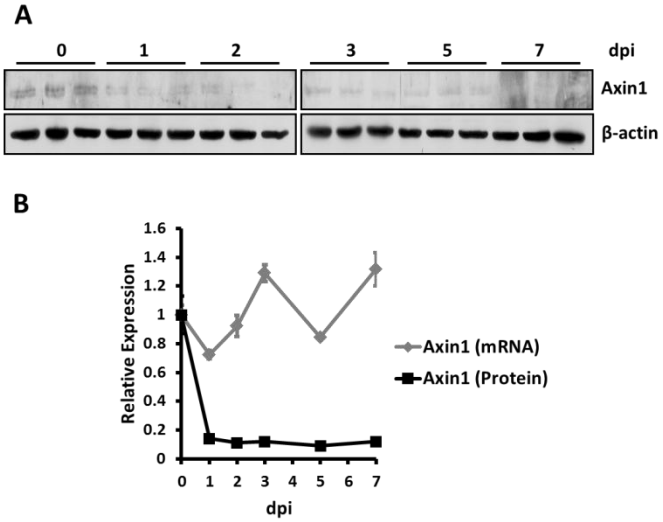

Fig. IV. 3. Axin1 is degraded during influenza pneumonia. Mice were intranasally infected with H1N1 influenza A/PR/8/34 virus (250 pfu/mouse) and the lungs were isolated at 1 to 7 dpi. (A) Axin1 protein levels in harvested lung tissues were measured by Western blot using β-actin as an internal control. (B) Relative band intensity of Axin1 was quantified and normalized to β-actin. mRNA expression of Axin1 in the same lung tissues were measured by Real-time PCR and normalized to 18S rRNA. Both results (protein and mRNA) were expressed as a ratio to control (0 dpi). Data shown are means ± s.e.m., n=3

4.4.2 Axin1 inhibits influenza virus replication through boosting IFN response

To evaluate the potential role of Axin1 in regulating influenza virus replication, we overexpressed Axin1 or Axin2 in HEK293 cells prior to influenza virus infection. Axin1 but not Axin2 inhibited mRNA expression of viral genes (Fig. IV. 4A, B and C) and virus replication (Fig. IV. 4D).

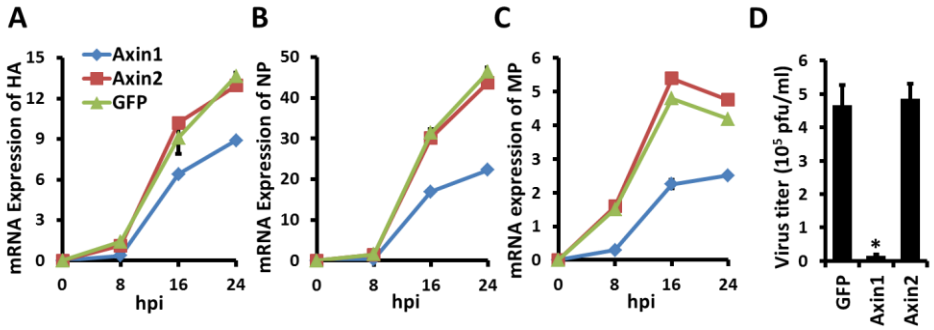

Fig. IV. 4. Axin1 inhibits influenza virus replication. HEK293 cells were transfected with OE-GFP, OE-Axin1, or OE-Axin2 plasmids for 24 hours and then infected with H1N1 influenza A/PR/8/34 virus (MOI=2). The cells were collected at 8 to 24 hours post infection (hpi). (A-C) mRNA expression of viral genes (HA, NP, and MP) was analyzed by Real-time PCR and normalized to β-actin. (D) Virus titer in the culture media (24 hpi) was measured by $TCID_{50}$ assay in MDCK cells. Values represent means ± s.e.m. of three independent experiments and statistical significance determined by one-way ANOVA analysis with posthoc *Tukey's* test. *P<0.001 v.s. OE-GFP.

Axin1 successfully boosted type I IFN mRNA expression including IFNβ1 (Fig. IV. 5A), IFNα1 (Fig. IV. 5B), and IFNα7 (Fig. IV. 5C). Accordingly, Axin1 also significantly augmented the expression of type I IFN-stimulated genes, including OAS1 (Fig. IV. 5D) and MX1 (Fig. IV. 5E). Axin1 also elevated type III IFN (IFNλ1) synthesis and response (Fig. IV. 6A and B). STAT1, the transcription factor essential for turning on ISG expression (29), was activated by Axin1 (Fig. IV. 5F). The activity of interferon-sensitive responsive element (ISRE), primarily responsible for the constitutive expression of ISGs (30), was notably increased as well (Fig. IV. 5G). Similarly, Axin1 drastically reduced RSV viral propagation (Fig. IV. 7A) and viral protein

synthesis (Fig. IV. 7B) through magnifying IFN response in HEK293 cells (Fig. IV. 7C). These results indicated that the cellular anti-viral machinery was turned on by Axin1.

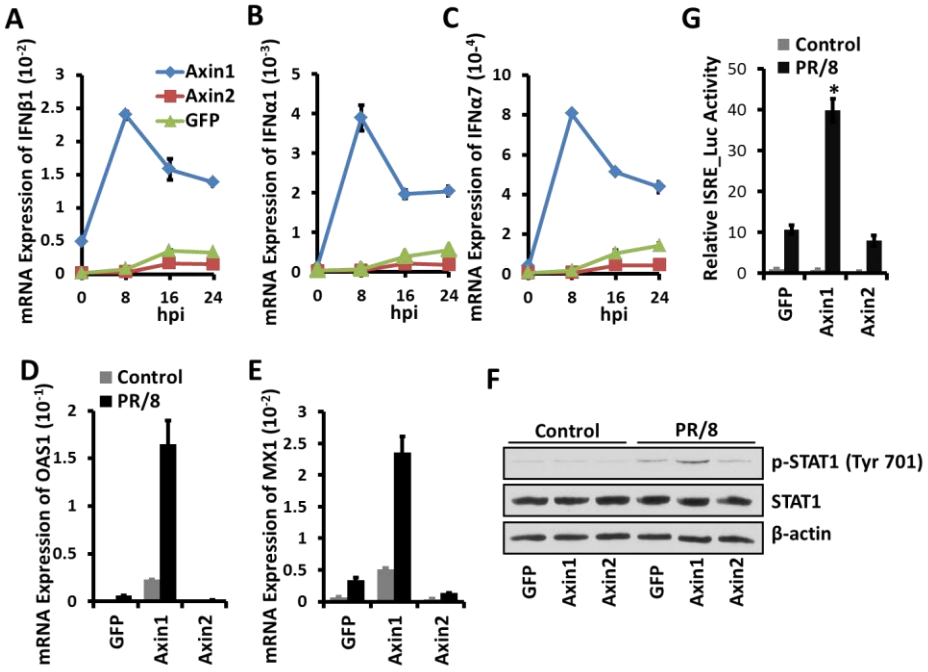

Fig. IV. 5. Axin1 stimulates type I IFN response during influenza virus infection. HEK293 cells were transfected with OE-GFP, OE-Axin1, or OE-Axin2 plasmids for 24 hours and then infected with H1N1 influenza A/PR/8/34 virus (MOI=2) for indicated times. mRNA expressions of (A-C) type I IFN (IFNβ1, IFNα1, and IFNα7) and (D-E) type I IFN-stimulated genes (OAS1 and MX1) (8 hpi) were measured by Real-time PCR and normalized to β-actin. (F) Western blot was carried out to determine the protein expression of p-STAT1 (Tyr 701) and total STAT1 with and without virus infection (2 hpi). The expression of β-actin was used as an internal control. (G) ISRE_Luc and pRL-TK plasmids were transfected into HEK293 cells together with OE-GFP, OE-Axin1, or OE-Axin2 plasmids for 24 hours. Cells were then infected with H1N1 influenza A/PR/8/34 virus (MOI=2) for 8 hours. Dual-luciferase assay was performed and the results were expressed as the ratio of ISRE_Luc *Firefly* luciferase activity to pRL-TK *Renilla* luciferase activity. Data shown are means ± s.e.m. of three independent experiments and tested for statistical significance by ANOVA analysis with posthoc *Tukey's* test. *P<0.01 v.s. OE-GFP.

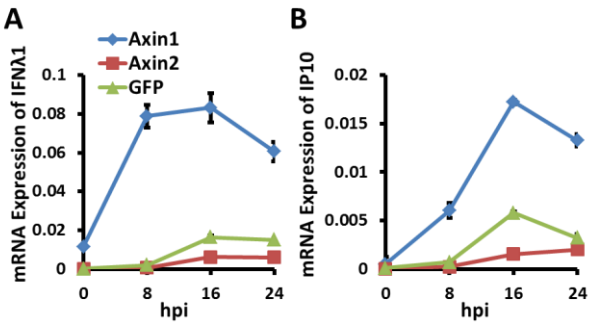

Fig. IV. 6. Axin1 elevates type III IFN response during influenza virus infection. OE-GFP, OE-Axin1, or OE-Axin2 plasmids were transfected into HEK293 cells. One day after transfection, cells were infected with H1N1 influenza A/PR/8/34 virus (MOI=2) for indicated times. mRNA expression of (A) type III IFN (IFNλ1) and (B) type III IFN-stimulated gene (IP10) was measured by Real-time PCR and normalized to β-actin. Values represent as means ± s.e.ms of three independent experiments.

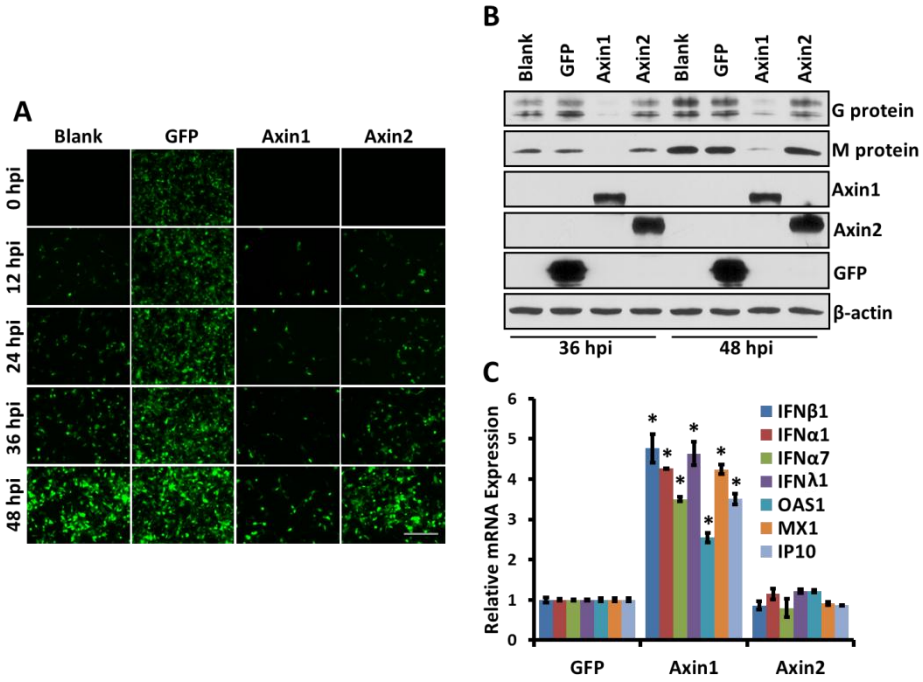

Fig. IV. 7. Axin1 inhibits RSV replication and boosts IFN response. HEK293 cells were transfected with OE-GFP, OE-Axin1, or OE-Axin2 plasmids for 24 hours and then infected with GFP-labeled RSV-A3 (MOI=1) for indicated times. (A) Green fluoresce image of infected cells. Scale bar=100 μm. (B) Viral proteins (G protein and M protein) levels were measured by Western blot in lysed cells with β-actin as a loading control. Myc-tagged Axin1, Axin2, and GFP protein levels were also determined using anti-myc antibody. (C) mRNA expression of type I IFN (IFNβ1, IFNα1, and IFNα7), type III IFN (IFNλ1), and ISGs (OAS1, MX1, and IP10) (12 hpi) was measured by Real-time PCR with β-actin as a reference gene.

Data shown are means ± s.e.m. and tested for statistical significance by ANOVA analysis with posthoc *Tukey's* test. *P<0.05 v.s. OE-GFP.

4.4.3 JNK/c-*Jun* and Smad3 mediate Axin1-stimulated IFN response

We further investigated the mechanism of Axin1-mediated stimulation of IFN response. Both Axin1 and Axin2 inhibited canonical Wnt/β-catenin signaling assessed by TOPflash assay (Fig. IV. 8A). This is consistent with their known function in the β-catenin degradation complex. However, since Axin1, but Axin2 induced IFN response, we further examined other cell signaling pathways only affected by Axin1, including TGF-β/Smad, JNK/c-*Jun*, and p53 signaling (16).

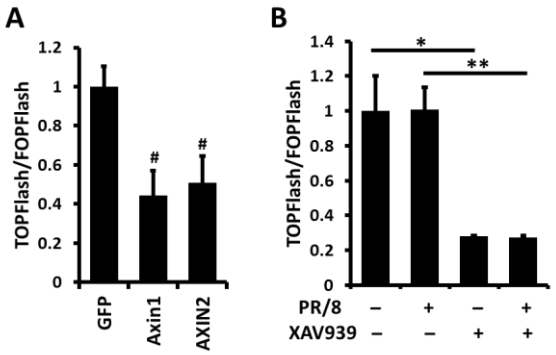

Fig. IV. 8. Axin and its stabilizer XAV939 inhibit Wnt/β-catenin signaling. (A) TOPFlash\FOPFlash and pRL-TK plasmids were transfected together with OE-GFP, OE-Axin1, or OE-Axin2 plasmids into HEK293 cells for 24 hours. (B) A549 cells were transfected with TOPFlash\FOPFlash and pRL-TK plasmids for 12 hours and then treated with XAV939 for 24 hours. After that, both HEK293 and A549 cells were infected with H1N1 influenza A/PR/8/34 virus (MOI=2) for 12 hours. Dual-luciferase assay was performed. TOPFlash or FOPlash *Firefly* luciferase activity was normalized to pRL-TK *Renilla* luciferase activity. The results were expressed as the ratio of normalized TOPFlash to FOPlash activity. Data shown are means ± s.e.m. of three independent experiments and tested for statistical significance by one –way ANOVA analysis with posthoc *Tukey's* test. # P<0.05 v.s. OE-GFP. * and ** represent P<0.05.

Axin1 activated JNK/c-Jun pathway by increasing the phosphorylation of both JNK1 and c-Jun. However, Axin2 had no effects on these processes. Both Axin1 and Axin2 did not ATF2 phosphorylation (Fig. IV. 9A and B). Axin1, but not Axin2, also triggered the activation of Smad3 signaling (Fig. IV. 9C).

SP600125, a specific JNK inhibitor (31), successfully blocked Axin1-stimulated IFN mRNA expression (Fig. IV. 10A-C and 11A), ISG expression (Fig. IV. 10D, 10E, and 11B) and ISRE activity (Fig. IV. 10F). SIS3, a specific Smad3 inhibitor (32), exhibits the same inhibitory effect on Axin1-elevated anti-viral machinery except IFNβ1 synthesis (Fig. IV. 10A) and MX1 expression (Fig. IV. 10E). However, only SIS3, but not SP600125 relived Axin1-mediated attenuation of influenza virus replication (Fig. IV. 12A-C). This result showed that both JNK/c-Jun pathway and Smad3 signaling participated in Axin1-stimulated IFN response through different mechanisms.

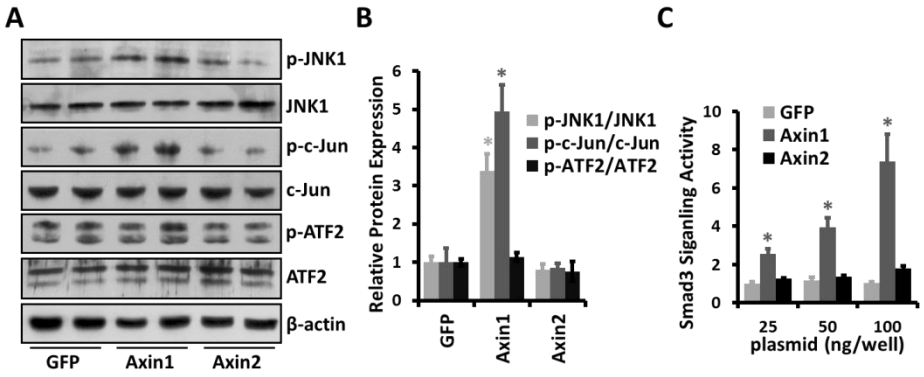

Fig. IV. 9. Axin1 activates JNK/c-Jun pathway and Smad3 signaling. (A) HEK293 cells were transfected with OE-GFP, OE-Axin1, or OE-Axin2 plasmids for 24 hours. The protein levels of phosphorylated JNK1 (p-JNK), total JNK (JNK), phosphorylated c-Jun (p-c-Jun), total c-Jun (Jun), phosphorylated ATF2 (p-ATF2), and total ATF2 (ATF2), were determined by Western blot. (B) Relative band intensities of phosphorylated proteins were quantified and normalized to respective total proteins. (C) Smad3 signaling reporter and pRL-TK plasmids were transfected together with different doses of OE-GFP, OE-Axin1, or OE-Axin2 plasmids into HEK293 cells for 24 hours. Dual-luciferase assay was performed. The results were expressed as a ratio of Smad3 signaling reporter Firefly luciferase activity to pRL-TK Renilla luciferase activity. Data shown are means ± s.e.m. of three independent experiments, and statistical significance determined by one-way ANOVA analysis with posthoc *Tukey's* test. *P<0.01 v.s. OE-GFP.

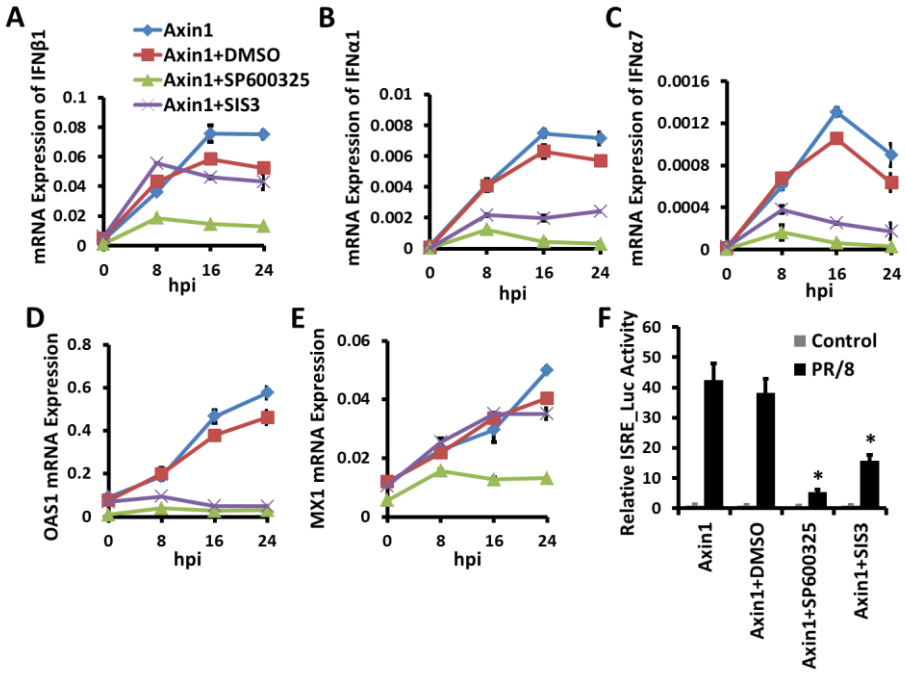

Fig. IV. 10. Inhibition of JNK/c-Jun and Smad3 signaling reduces Axin1-stimulated type I IFN response. HEK293 cells were pretreated with 10 μM SP600125 (JNK inhibitor), 10 μM SIS3 (Smad3 inhibitor), or 0.05% DMSO for 6 hours. The cells were then transfected with OE-Axin1 plasmid for 24 hours and then infected with H1N1 influenza A/PR/8/34 virus (MOI=2) for indicated times. The mRNA expression of (A-C) type I IFN (IFNβ1, IFNα1, and IFNα7) and (D-E) type I IFN-stimulated genes (OAS1 and MX1) was measured by Real-time PCR and normalized to β-actin. (F) HEK293 cells were pretreated with indicated inhibitors and transfected with ISRE_Luc and pRL-TK plasmids together with OE-Axin1 plasmid for 24 hours. Cells were then infected with H1N1 influenza A/PR/8/34 virus (MOI=2) for 8 hours. Dual-luciferase assay was carried out and the ISRE_Luc Firefly luciferase activity was normalized to pRL-TK Renilla luciferase activity. Data shown are means ± s.e.m. and tested for statistical significance by ANOVA analysis with posthoc *Tukey's* test. *P<0.05 v.s. OE-Axin1+DMSO.

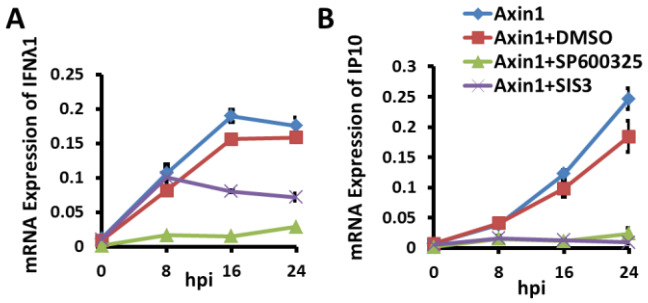

Fig. IV. 11. Blockage of JNK/c-Jun and Smad3 pathways attenuates Axin1-elevated type III IFN response. HEK293 cells were pretreated with 10 μM SP600125 (JNK inhibitor), 10 μM SIS3 (Smad3 inhibitor), or 0.05% DMSO. 6 hours later, the cells were transfected with OE-Axin1 plasmid for 24 hours

and then infected with H1N1 influenza A/PR/8/34 virus (MOI=2) for indicated times. mRNA expression of (A) type III IFN (IFNλ1) and (B) type III IFN-induced gene (IP10) was measured by Real-time PCR and normalized to β-actin. Values represent as means ± s.e.m of three independent experiments.

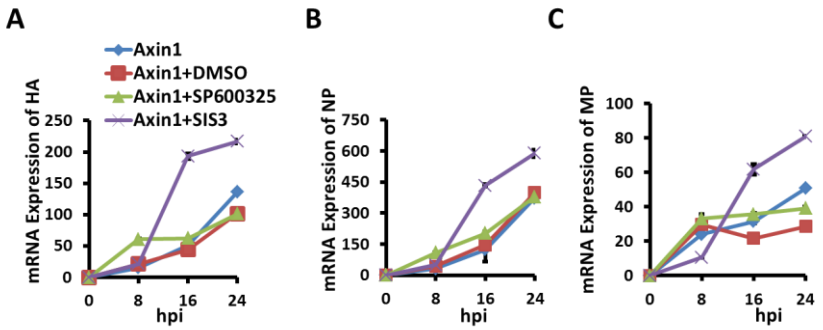

Fig. IV 12. Inhibition of Smad3 signaling relives Axin1-mediated attenuation of influenza virus replication. HEK293 cells were pretreated with 10 μM SP600125 (JNK inhibitor), 10 μM SIS3 (Smad3 inhibitor), or 0.05% DMSO for 6 hours. The cells were transfected with OE-Axin1 plasmid for 24 hours and then infected with H1N1 influenza A/PR/8/34 virus (MOI=2) for indicated times. mRNA expression of viral genes (HA, NP, and MP) were analyzed by Real-time PCR with β-actin as a reference. Values represent as means ± s.e.m of three independent experiments.

4.4.4 Axin1 interacts with a novel viral RNA sensor

To continually explore the details on Axin1-mediated activation of IFN response, we analyzed the potential physical interactions between Axin1 and classic viral RNA sensors that function in the RIG-1-like pathway (8,33,34). Unfortunately, Axin1 didn't interact with both RIG-1 and MDA5 (Fig. IV. 13). Surprisingly, Axin1 was identified to interact with IFIT1/2/3, a novel IFN-induced viral RNA sensor complex (9), during influenza virus infection by mass spectrometry (Table IV. 2). Our results brought Axin1 into the antiviral network of interferon as a scaffold protein.

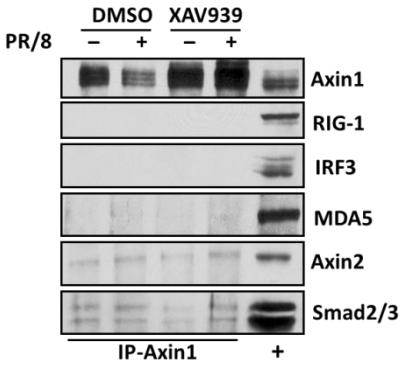

Fig. IV. 13. Axin1 does not interact with viral senors in the RIG-1 pathway. A549 cells were pretreated with 20 μM XAV939 or 0.05% DMSO for 24 hours. Cells were then infected with H1N1 influenza A/PR/8/34 virus (MOI=2) for 24 hours. Axin1 was pulled down from lysed cells by immunoprecipitation and probed with indicated antibodies by Western blot using Axin2 and Smad2/3 as positive controls (16).

	Bait					
	GFP			Axin1		
PR/8 (dpi)	0	8	24	0	8	24
IFIT1	0	0	0	0	8.7±1.4	6.3 ±1.3
IFIT2	0	0	0	0	7.3 ±1.3	7.7 ±0.7
IFIT3	0	0	0	0	4.7 ±0.3	12+1.5
IFIT5	0	0	0	0	0	0

Table IV. 2. Physical interaction between Axin1 and IFIT1/2/3 during influenza virus infection. HEK293 cells were transfected with OE-GFP or OE-Axin1 plasmids for 24 hours and then infected with H1N1 influenza A/PR/8/34 virus PR/8 (MOI=2) for 8 or 24 hours. Liquid chromatography and tandem mass spectrometry of protein complexes isolated by immunoprecipitation. Results are represented as number of peptides identified. Data are from three experiments and shown are means ± s.e.m.

4.4.5 XAV939 stabilizes Axin1 and attenuates influenza virus replication *in vitro*

To further validate the role of Axin1 against virus replication, XAV939, a tankyrase inhibitor (35), was utilized to stabilize Axin in A549 cells (Fig. IV. 14A and B). Axin1 was not degraded in A549 cells during influenza virus infection when XAV939 was present (Fig. IV. 14B). XAV939 significantly attenuated influenza viral gene expression (Fig. IV. 14C-E) and virus replication (Fig. IV. 14F) in A549 cells. XAV939 also notably inhibited influenza viral gene expression (Fig. IV. 15A-C) and virus replication (Fig. IV. 15D) in primary mouse alveolar

epithelial cells. Accordingly, XAV939 increased IFNα1 (Fig. IV. 15E) and MX1 (Fig. IV. 15F) expression during virus infection in primary mouse alveolar epithelial cells. Similarly, XAV939 dramatically reduced RSV viral protein synthesis (Fig. IV. 16A) and virus replication in HEp2 cells as well (Fig. IV. 16B).

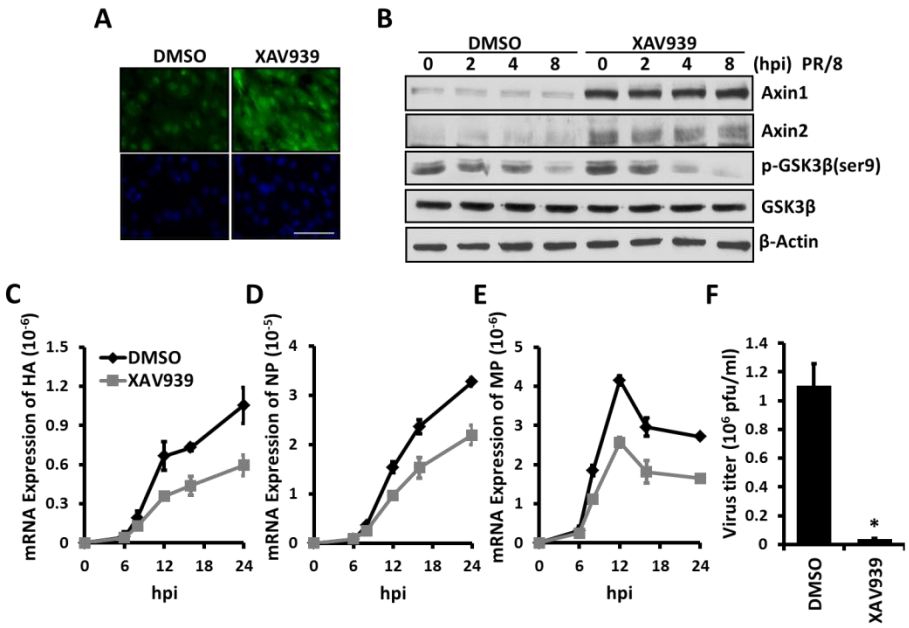

Fig. IV. 14. XAV939 stabilizes Axin and inhibits influenza virus replication in A549 cells. A549 cells were pretreated with 20 μM XAV939 or 0.05% DMSO for 24 hours. Cells were then infected with H1N1 influenza A/PR/8/34 virus (MOI=2) for indicated times. (A) Immunostaining of Axin1 (Green) with DAPI nuclear staining (Blue) after XAV939 treatment. (Scale bar=50 μm). (B) Western blot analysis of the indicated protein expression. (C-E) mRNA expression of viral genes (HA, NP, and MP) was analyzed by Real-time PCR and normalized to 18S rRNA. (F) Virus titers in the culture media (24 hpi) were measured by TCID50 assay in MDCK cells. Values represent means ± s.e.m. of three independent experiments and statistical significance determined by Student's *t*-test. *P<0.001 v.s. DMSO.

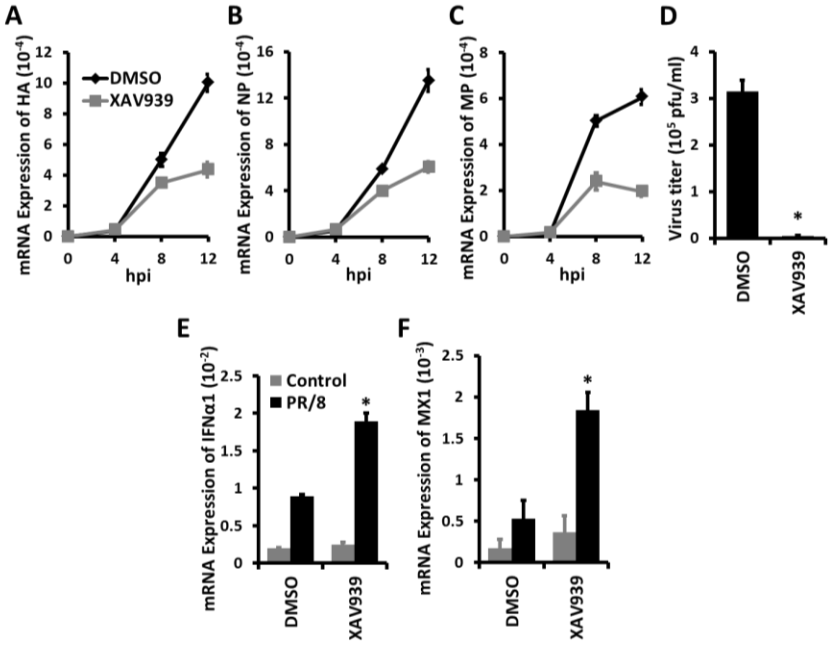

Fig. IV. 15. XAV939 reduces influenza virus replication and augments type I IFN response in primary mouse alveolar epithelial cells. Primary mouse alveolar epithelial cells were pretreated with 20 μM XAV939 or 0.05% DMSO for 24 hours. Cells were then infected with H1N1 influenza A/PR/8/34 virus PR/8 (MOI=2) for indicated times. (A-C) mRNA expression of viral genes (HA, NP, and MP) were analyzed by Real-time PCR and normalized to 18S rRNA. (D) Virus titer in the culture media (24 hpi) was measured by TCID50 assay in MDCK cells. mRNA expression of IFNα1 (E) and MX1 (F) (12 hpi) were measured by Real-time PCR and normalized to β-actin. Data shown are means ± s.e.m. of three independent experiments and tested for statistical significance by one–way ANOVA analysis with posthoc *Tukey's* test or Student's *t*-test . *P<0.05 v.s. DMSO.

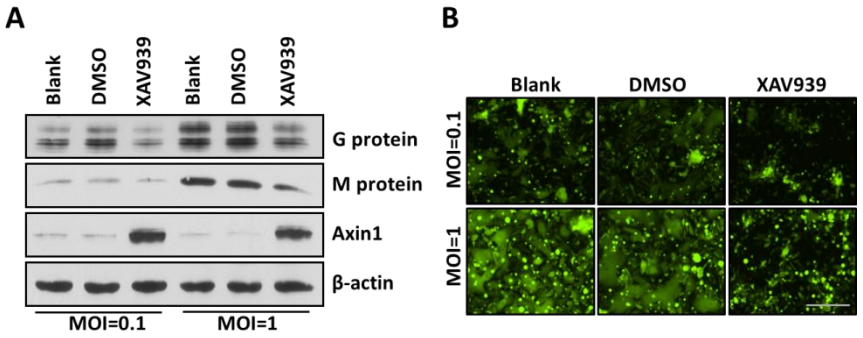

Fig. IV. 16. XAV939 reduces RSV replication. Hep2 cells were pretreated with 20 μM XAV939 or 0.05% DMSO for 24 hours. Cells were then infected with GFP-labeled RSV-A3 (MOI=0.1 or 1) for 48

hours. (A) Viral proteins (G protein and M protein) expression was measured by Western blot in lysed cells with β-actin as a loading control. (B) Green fluorescence image of infected cells. Scale bar=100 μm.

4.4.6 XAV939 protects mice from lethal influenza virus challenge

To evaluate the therapeutic application of Axin1 as a novel target to limit virus infection, XAV939 was further tested as a potential antiviral agent *in vivo* (Fig. IV. 17A). Oral administration of XAV939 for 24 hours successfully stabilized Axin1 in the mouse lung as previously reported (36) (Fig. IV. 17B). XAV939 also significantly attenuated influenza virus replication *in vivo* (Fig. IV. 17C) and dramatically improved the survival rate of animals challenged with a lethal dose of H1N1 influenza A/PR/8/34 virus at 1,000 pfu/mouse with two different strategies of XAV939 administration (-1 to 2 dpi or -1 to 4 dpi) (Fig. IV. 17D).

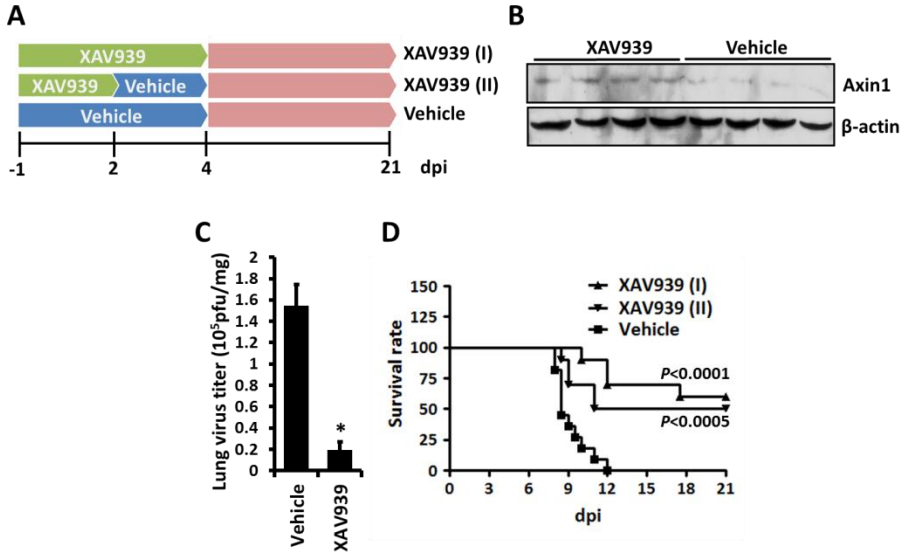

Fig. IV. 17. XAV939 stabilizes Axin1 and protects mice from lethal influenza virus challenge. Mice were challenged intranasally with a lethal dose (1,000 pfu) of H1N1 influenza A/PR/8/34 virus. XAV939 treatment was given orally and daily, beginning with one day before infection (-1 dpi) and continued until 2 (XAV939 (I)) or 4 (XAV939 (II)) days post infection. Control animals received vehicle alone. (A) The illumination of experimental design. (B) Axin1 protein expression in the lungs after a 24-hour treatment of XAV939. (C) Virus titer in the homogenized infected lungs at 2 dpi was measured by TCID50 assay in MDCK cells and normalized to total protein amount (n=5). Data shown are means ± s.e.m. and tested for

statistical significance by Student's *t*-test. (D) Survival rate (10-11 mice/group). Mantel-Cox χ^2 test on Kaplan-Meier survival data was used to compare the survival rate between groups.

4.4.7 Axin1 interacts with the host factors involved in antiviral response

As a scaffold protein, Axin1 could potentially interact with other host factors and incorporated into other cellular antiviral machinery against influenza virus replication. Besides regulating IFN response, Axin1 was also found to co-localized and interacted with four other host factors (nonO/p54(nrb), SFPQ, hnRNP M, and EZH2) that are involved in antiviral response (37-39) (Fig. IV. 18A, B). More interestingly, all of these identified interactions are lost during 24-hour influenza virus infection (Fig. IV. 18B).

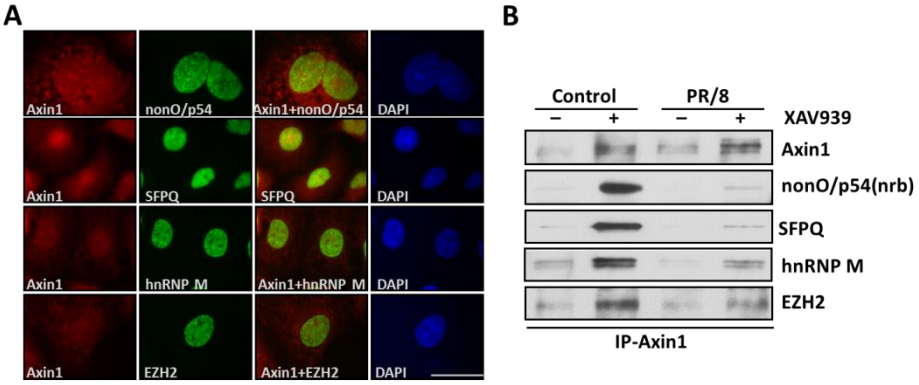

Fig. IV. 18. Interactions between Axin1 and NonO/p54, SFPQ, hnRNP M and EZH2 are lost during influenza virus infection. (A) Double immunostaining of Axin1 (Red) and NonO/p54, SFPQ, hnRNP M and EZH2 (Green) with DAPI nuclear staining (Blue) in A549 cells. Scale bar=10 μm. (B) A549 cells were pretreated with 20 μM XAV939 or 0.05% DMSO for 24 hours. Cells were then infected with H1N1 influenza A/PR/8/34 virus (MOI=2) for 24 hours. Axin1 was pulled down from lysed cells by immunoprecipitation and probed with indicated antibodies by Western blot.

XAV939 stimulated the degradation of all four proteins (Fig. IV. 19A). Axin1 and Axin2 both facilitated the degradation of nonO/p54(nrb) and SFPQ during influenza virus infection (Fig. IV. 19B). However, Axin1 specifically promoted the degradation of hnRNP M and EZH2 during viral infection (Fig. IV. 19B). Interestingly, knock down of hnRNP M led to loss of EZH2 (Fig. IV. 20). This result together with a previous report implied that hnRNP M and EZH2 could be

essential for influenza virus replication (40). More detailed studies need to be carried out to explore the mechanism of both proteins in regulating influenza virus life cycle.

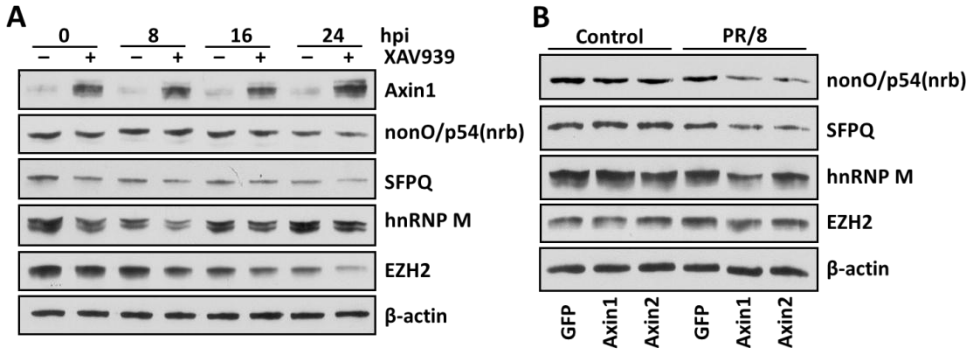

Fig. IV. 19. Axin1 specifically facilitates degradation of hnRNP M and EZH2 during influenza virus replication. (A) A549 cells were pretreated with 20 μM XAV939 or 0.05% DMSO for 24 hours. Cells were then infected with H1N1 influenza A/PR/8/34 virus (MOI=2) for indicated times. (B) HEK293 cells were transfected with OE-GFP, OE-Axin1, or OE-Axin2 plasmids for 24 hours and then infected with H1N1 influenza A/PR/8/34 virus (MOI=2) for 2 hours. Western blot was carried out to check the indicated protein expression using β-actin as an internal control.

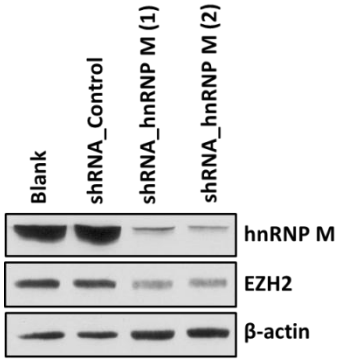

Fig. IV. 20. Loss of hnRNP M leads to degradation of EZH2. HEK293 cells were transfected with plasmids carrying two different shRNAs against hnRNP M or control shRNA for 72 hours. Western blot was performed to measure the protein expression of both hnRNP M and EZH2 in the lysed cells with β-actin as a loading control.

4.5 Discussion

The mortality rate of pneumonia and influenza virus infection continually declined through the 20th century because of the improvement of anteceded medical strategies for the

prevention of lung infections (2,41). However, acute pulmonary infection remains a substantial concern as acute lower respiratory infections still cause the most deaths and are the largest economic burden among all infectious diseases worldwide (2,42). Unlike respiratory syncytial virus (RSV), which is the major cause of respiratory illness (bronchiolitis or pneumonia) in young children (43), influenza virus has the ability to span on patients of all ages even adults (44). In our study, we discovered the protective effect of Axin1 and its stabilizer XAV939 on influenza virus and RSV infections. By interacting with IFIT1/2/3, a novel RNA virus sensor complex, Axin1 boosted antiviral type I IFN response through augmenting JNK/c-Jun and Smad3 signaling. Axin1 also interacted and promoted the degradation of hnRNP M and EZH2, two essential host factors for influenza virus replication, sequentially (Fig. IV. 21). Targeting Axin1 to regulate IFN response could potentially developed as broad-spectrum antivirals.

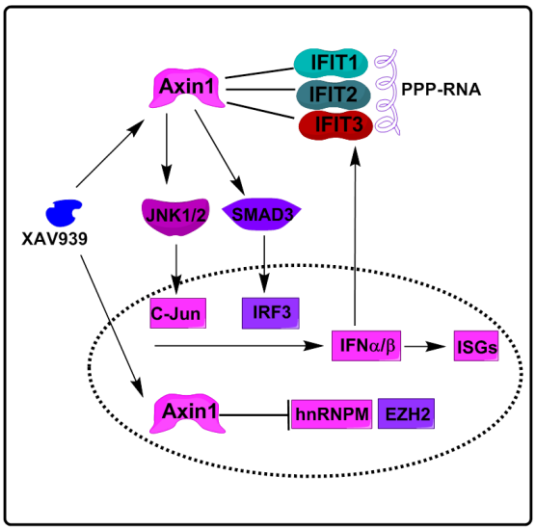

Fig. IV. 21. Axin1 joins the antiviral network of interferon. Axin1 interacts with the viral RNA sensor IFIT1/2/3 to initiates the type I IFN response against influenza virus replication through JNK/c-*Jun* and Smad3/IRF3 signaling. Axin1 also specifically promotes the sequential degradation of hnRNP M and EZH2, two essential host factors supporting influenza virus replication. As such, XAV939, Axin stabilizer, could be used as a potential broad-spectrum inhibitor against virus infection.

A unique feature in signaling transduction is that several different pathways depend on a group of crucial regulators referred to as scaffolds, which bind simultaneously several components in the same or different signaling routes and augment specificity` and efficacy during signal transduction (19). By serving as a multidomain scaffold, Axin1 coordinates several different protein complexes involved in regulating TGF-β/Smad, JNK/c-*Jun*, and p53 signaling (16). In this study, we found that both transcription factors, c-*Jun* and Smad3, were activated by Axin1 to facilitate IFN response. Instead of classic viral RNA sensors, RIG-1 and MAD5 (33,34), Axin1 was detected through a newly identified viral 5' triphosphate double stranded RNA (5'ppp-dsRNA) sensor complex IFIT1/2/3, which initiates IFN-mediated antiviral response (9). This positive-regulated signaling cycle mediated by Axin1 and IFIT1/2/3 (ISGs) remains to be determined (45).

Both IRF3 and IRF7 are well known to be essential for the cytosolic pathway-mediated type I IFN induction (46,47). Because Smad3 can only interact and cooperate with IRF7 (11), we have this special opportunity to explore the relative contribution of IRF3 and IRF7 to the activation of type I IFN synthesis and ISGs expression. In the recently established "two-step" model (10), IRF3 is primarily responsible for the initiation of IFNβ1 expression. IRF7 is then induced by IFNβ1 and comes into play in the later phase for IFNαs induction. Our results support this hypothesis because SIS3 (Smad3 inhibitor) only inhibited Axin1-induced expression of IFNα but not IFNβ1. In the same experiment setting, we also discovered an obvious difference between IRF3 and IRF7 in regulating OAS1 and MX1 expression (Fig. IV. 10D and E) as previously reported (48). As we expected, SIS3 successfully inhibited Axin1-mediated attenuation of virus replication. This result also partially confirmed that the effect of Axin1 on virus replication is through regulating type I IFN response.

In the promoter region of type I IFN genes, the assembly of ATF2 and c-*Jun* (AP1) is required for their substantial expression (49). In this study, we found that Axin1 only activated

JNK/*c-Jun* pathway without affecting p38/ATF2 activity. Unlike SIS3, SP600125 (JNK/*c-Jun* pathway inhibitor) failed to reverse Axin1-inhibited virus propagation even though it inhibited the Axin1-agumented type I IFN responses. This mismatch is probably because JNK/*c-Jun* pathway inhibitor itself can suppress influenza viral RNA and protein synthesis, and override the effect of attenuated type I IFN responses on virus replication (50).

Type I and Type III IFN activate the same STAT heterodimer (STAT1/2) to induce ISGs from IFN-stimulated response elements (ISREs) (5,51). Axin1 significantly stimulated STAT1 and subsequent ISREs activity. Our results reveal the same mechanism of Axin1 on regulating both Type I and Type III IFN synthesis because SIS3 and SP600125 exhibit the same inhibitory effect in both scenarios.

Axin2 did not amplify the type I IFN response and affect virus replication. The similar effect was also observed in bacterial *Salmonella* infection (21). Considering that both Axin1 and Axin2 inhibited Wnt/catenin signaling (14) (Fig. IV. 8A), the activation of type I IFN synthesis by Axin1 is obviously not through the manipulation of Wnt/catenin signaling. Influenza virus infection also had no effect on Wnt/catenin signaling (Fig. IV. 8B). However, the activation of Wnt/catenin signaling by Wnt3a dramatically promotes virus replication through an unknown mechanism *in vitro* and *in vivo* (Fig. IV. 22). On the other hand, Wnt3a has been reported to amplify IFN response (52) potentially through interaction between β-Catenin and LRRFIP1 (53), another cytosolic viral RNA sensor. However, this cannot explain the remarkable effect of Wnt/catenin signaling on virus amplification. Instead, it implicates the induction of type I IFN synthesis by Axin1 through JNK/*c-Jun* and Smad3 signaling is intensive enough to override the potential negative effect of suppressed Wnt/catenin signaling on ISREs response. Considering the side effect of type I IFN on sensitizing host to secondary bacterial pneumonia post influenza infection (54) and promoting cell death (55) as Axin1 normally involved (56), more detailed studies need to be carried out *in vivo*.

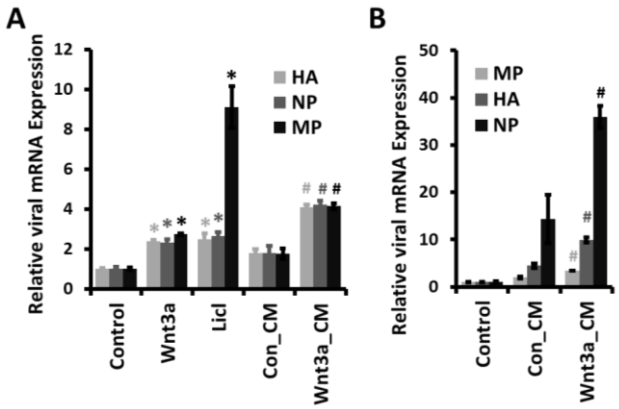

Fig. IV. 22. Activation of Wnt/β-catenin signaling amplify influenza virus replication. (A) E10 cells were pretreated with 250 ng/ml rhWnt3a, 25 mM LiCl, 50% Con_CM, or 50% Wnt3a_CM for 24 hours. Cells were then infected with H1N1 influenza A/PR/8/34 virus PR/8 (MOI=2) for 18 hours. (B) Mice were inoculated with influenza virus A/Puerto Rico/8/1934 H1N1 (250 pfu) intranasally. 50µl 10X Wnt3a_CM or Con_CM was given to the mice 4 hours before infection and 2 days post infection intranasally. Lungs were isolated on day 5 post infections. (n=4/group). mRNA expression of viral genes (HA, NP, and MP) were analyzed by Real-time PCR with 18S rRNA as a reference. The results were normalized to control and represent as means ± s.e.m. Statistical significance was tested by one –way ANOVA analysis followed by posthoc Tukey's test. *P<0.01 v.s. Control. #P<0.05 v.s. Con_CM.

Axin1 has been reported to be the rate limiting factor for the β-catenin destruction complex assembly due to its extremely low basal expression (57). This unique feature and its antiviral property make it a perfect host factor to be stabilized against virus infection. In this study, we utilized XAV939 to stabilize Axin1 and evaluated its potential antiviral activity against influenza virus *in vitro* and *in vivo*. XAV939 has previously been reported to inhibit herpes simplex virus replication (58). Oral administration of XAV939 successfully stabilizes Axin1 in the lung as previously reported (59). More importantly, XAV939 successfully reduces influenza virus replication *in vitro* and *in vivo*, and protects the mice from lethal influenza virus infection.

IFN exerts significant protection on limiting respiratory virus infection including highly pathogenic H5N1 influenza A virus infection in animals (60,61). However, viruses can block nearly all aspects of IFN regulatory pathway through intimate interplay to avoid the compromise of virus replication (62). In our study, we found that Axin1, as an antiviral mediator, was

degraded in influenza viral pneumonia *in vitro* but not *in vitro*. This could be due to complicated systemic response to virus infection, sophisticated paracrine signaling, and an adequate set of protein degradation machinery *in vivo*. Several other components of ubiquitin-proteasome pathway (USP34 and RNF146) and small ubiquitin-related modifier (SUMO) are also involved in regulating homeostasis of Axin1 (63-65). Targeting these molecules to stabilize Axin1 could also be potentially utilized against virus replication.

Functional genomics and proteomics have been given a great appreciation to provide a broad view of virus-host interactions (66,67). Recently, a quantitative proteomics study reveals reduced levels in paraspeckle proteins splicing factor proline-glutamine rich (SFPQ) and Non-POU domain-containing octamer-binding protein (nonO/p54(nrb)) in influenza A virus-infected cells (68). These proteins are frequently associated with heterogeneous nuclear ribonucleoprotein M (hnRNP M) in defined nuclear structure to influence splicing patterns of specific pre-mRNAs (69). A recent study further demonstrates that SFPQ, but not nonO/p54(nrb), is a host factor specifically required for influenza virus multiplication by increasing the efficiency of viral mRNA polyadenylation and transcription of viral RNPs (70). hnRNP M also interacts with influenza virus polymerase complex (71) and is essential to maintain the efficient activity of both H1N1 and H5N1 influenza virus polymerases (40). Since Axin1 and Axin2 both promoted degradation of SPFQ and nonO/p54(nrb), these two proteins less likely contribute to Axin1-specific antiviral property. More importantly, Axin1 specifically induced degradation of hnRNP M and EZH2, histone-lysine N-methyltransferase, sequentially. Recent data demonstrated that Axin1 is a central coordinator of c-Myc degradation through coupling to GSK3β signaling (72). Activation of GSK3β during influenza virus infection shown in our results (Fig. IV. 14B) could also be implicated in Axin1- mediated degradation of these host factors.

Taking advantage of host cellular signaling to support viral replication by influenza virus is very effective. However, this dependency might also be utilized to develop novel antiviral

approaches. Our work here is an example of translating this information into potential therapeutics. We discovered a novel function of Axin1 in limiting virus infection and incorporated this scaffold protein into the antiviral network of interferon.

4.6 Acknowledgements

We thank Dr. Mary Williams (Boston University) for providing E10 cells with the permission of Dr. Al Malkinson (University of Colorado). OE-GFP plasmid constructed by Dr. Frank Costantini (Columbia University) and OE-Axin1/2 plasmids generated by Dr. Michael Klymkowsky (University of Colorado) were obtained from Addgene. We also appreciate Dr. Kevin Tan and Dr. Harold A. Chapman (UCSF) for providing detailed protocol of XAV939 formulation used in animal study.

4.7 Reference

1. Medina, R. A. and Garcia-Sastre, A. (2011) *Nature Reviews Microbiology* **9,** 590-603
2. Mizgerd, J. P. (2012) *American Journal of Respiratory and Critical Care Medicine* **186,** 824-829
3. Muller, K. H., Kakkola, L., Nagaraj, A. S., Cheltsov, A. V., Anastasina, M., and Kainov, D. E. (2012) *Trends in Pharmacological Sciences* **33,** 89-99
4. Isaacs, A. and Lindenmann, J. (1957) *Proceedings of the Royal Society B-Biological Sciences* **147,** 258-267
5. Borden, E. C., Sen, G. C., Uze, G., Silverman, R. H., Ransohoff, R. M., Foster, G. R., and Stark, G. R. (2007) *Nature Reviews Drug Discovery* **6,** 975-990
6. Sadler, A. J. and Williams, B. R. G. (2008) *Nature Reviews Immunology* **8,** 559-568
7. Bowie, A. G. and Unterholzner, L. (2008) *Nature Reviews Immunology* **8,** 911-922
8. Barbalat, R., Ewald, S. E., Mouchess, M. L., and Barton, G. M. (2011) *Nucleic Acid Recognition by the Innate Immune System*, ANNUAL REVIEWS, PALO ALTO
9. Pichlmair, A., Lassnig, C., Eberle, C. A., Gorna, M. W., Baumann, C. L., Burkard, T. R., Burckstummer, T., Stefanovic, A., Krieger, S., Bennett, K. L., Rulicke, T., Weber, F., Colinge, J., Muller, M., and Superti-Furga, G. (2011) *Nature Immunology* **12,** 624-U177
10. Honda, K., Takaoka, A., and Taniguchi, T. (2006) *Immunity* **25,** 349-360

11. Qing, J., Liu, C., Choy, L., Wu, R. Y., Pagano, J. S., and Derynck, R. (2004) *Molecular and Cellular Biology* **24,** 1411-1425

12. Kawai, T. and Akira, S. (2006) *Nature Immunology* **7,** 131-137

13. Zeng, L., Fagotto, F., Zhang, T., Hsu, W., Vasicek, T. J., Perry, W. L., Lee, J. J., Tilghman, S. M., Gumbiner, B. M., and Costantini, F. (1997) *Cell* **90,** 181-192

14. Jho, E. H., Zhang, T., Domon, C., Joo, C. K., Freund, J. N., and Costantini, F. (2002) *Molecular and Cellular Biology* **22,** 1172-1183

15. Li, V. S. W., Ng, S. S., Boersema, P. J., Low, T. Y., Karthaus, W. R., Gerlach, J. P., Mohammed, S., Heck, A. J. R., Maurice, M. M., Mahmoudi, T., and Clevers, H. (2012) *Cell* **149,** 1245-1256

16. Cortese, M. S., Uversky, V. N., and Dunker, A. K. (2008) *Progress in Biophysics & Molecular Biology* **98,** 85-106

17. Zhang, Y., Neo, S. Y., Wang, X. H., Han, J. H., and Lin, S. C. (1999) *Journal of Biological Chemistry* **274,** 35247-35254

18. Furuhashi, M., Yagi, K., Yamamoto, H., Furukawa, Y., Shimada, S., Nakamura, Y., Kikuchi, A., Miyazono, K., and Kato, M. (2001) *Molecular and Cellular Biology* **21,** 5132-5141

19. Liu, W., Rui, H. L., Wang, J. F., Lin, S. Y., He, Y., Chen, M. L., Li, Q. X., Ye, Z. Y., Zhang, S. P., Chan, S. C., Chen, Y. G., Han, J. H., and Lin, S. C. (2006) *Embo Journal* **25,** 1646-1658

20. Rui, Y. N., Xu, Z., Lin, S. Y., Li, Q. X., Rui, H. L., Luo, W., Zhou, H. M., Cheung, P. Y., Wu, Z. G., Ye, Z. Y., Li, P., Han, J. H., and Lin, S. C. (2004) *Embo Journal* **23,** 4583-4594

21. Zhang, Y. G., Wu, S. P., Xia, Y. L., Chen, D., Petrof, E. O., Claud, E. C., Hsu, W., and Sun, J. (2012) *Plos One* **7,**

22. Kameoka, M., Kameoka, Y., Utachee, P., Kurosu, T., Sawanpanyalert, P., Ikuta, K., and Auwanit, W. (2009) *Aids Research and Human Retroviruses* **25,** 1005-1011

23. Huang, S. M. A., Mishina, Y. M., Liu, S. M., Cheung, A., Stegmeier, F., Michaud, G. A., Charlat, O., Wiellette, E., Zhang, Y., Wiessner, S., Hild, M., Shi, X. Y., Wilson, C. J., Mickanin, C., Myer, V., Fazal, A., Tomlinson, R., Serluca, F., Shao, W. L., Cheng, H., Shultz, M., Rau, C., Schirle, M., Schlegl, J., Ghidelli, S., Fawell, S., Lu, C., Curtis, D., Kirschner, M. W., Lengauer, C., Finan, P. M., Tallarico, J. A., Bouwmeester, T., Porter, J. A., Bauer, A., and Cong, F. (2009) *Nature* **461,** 614-620

24. Mishra, A., Chintagari, N. R., Guo, Y., Weng, T., Su, L., and Liu, L. (2011) *Journal of Cell Science* **124,** 657-668

25. Mitra, R., Baviskar, P., Duncan-Decocq, R. R., Patel, D., and Oomens, A. G. P. (2012) *Journal of Virology* **86,** 4432-4443

26. Weng, T. T., Gao, L., Bhaskaran, M., Guo, Y. J., Gou, D. M., Narayanaperumal, J., Chintagari, N. R., Zhang, K. X., and Liu, L. (2009) *Journal of Biological Chemistry* **284,** 28021-28032

27. Reed, L. and Muench, H. (1938) *American Journal of Hygiene* **27,** 493-497

28. Teijaro, J. R., Walsh, K. B., Cahalan, S., Fremgen, D. M., Roberts, E., Scott, F., Martinborough, E., Peach, R., Oldstone, M. B. A., and Rosen, H. (2011) *Cell* **146,** 979-990

29. Levy, D. E. and Darnell, J. E. (2002) *Nature Reviews Molecular Cell Biology* **3,** 651-662

30. Reid, L. E., Brasnett, A. H., Gilbert, C. S., Porter, A. C. G., Gewert, D. R., Stark, G. R., and Kerr, I. M. (1989) *Proceedings of the National Academy of Sciences of the United States of America* **86,** 840-844

31. Bennett, B. L., Sasaki, D. T., Murray, B. W., O'Leary, E. C., Sakata, S. T., Xu, W. M., Leisten, J. C., Motiwala, A., Pierce, S., Satoh, Y., Bhagwat, S. S., Manning, A. M., and Anderson, D. W. (2001) *Proceedings of the National Academy of Sciences of the United States of America* **98,** 13681-13686

32. Jinnin, M., Ihn, H., and Tamaki, K. (2006) *Molecular Pharmacology* **69,** 597-607

33. Yoneyama, M., Kikuchi, M., Natsukawa, T., Shinobu, N., Imaizumi, T., Miyagishi, M., Taira, K., Akira, S., and Fujita, T. (2004) *Nature Immunology* **5,** 730-737

34. Kato, H., Takeuchi, O., Sato, S., Yoneyama, M., Yamamoto, M., Matsui, K., Uematsu, S., Jung, A., Kawai, T., Ishii, K. J., Yamaguchi, O., Otsu, K., Tsujimura, T., Koh, C. S., Sousa, C. R. E., Matsuura, Y., Fujita, T., and Akira, S. (2006) *Nature* **441,** 101-105

35. Huang, S. M. A., Mishina, Y. M., Liu, S. M., Cheung, A., Stegmeier, F., Michaud, G. A., Charlat, O., Wiellette, E., Zhang, Y., Wiessner, S., Hild, M., Shi, X. Y., Wilson, C. J., Mickanin, C., Myer, V., Fazal, A., Tomlinson, R., Serluca, F., Shao, W. L., Cheng, H., Shultz, M., Rau, C., Schirle, M., Schlegl, J., Ghidelli, S., Fawell, S., Lu, C., Curtis, D., Kirschner, M. W., Lengauer, C., Finan, P. M., Tallarico, J. A., Bouwmeester, T., Porter, J. A., Bauer, A., and Cong, F. (2009) *Nature* **461,** 614-620

36. Ulsamer, A., Wei, Y., Kim, K. K., Tan, K., Wheeler, S., Xi, Y., Thies, R. S., and Chapman, H. A. (2012) *Journal of Biological Chemistry* **287,** 5164-5172

37. Landeras-Bueno, S., Jorba, N., Perez-Cidoncha, M., and Ortin, J. (2011) *Plos Pathogens* **7,**

38. Yao, L. Y., Yan, X. B., Dong, H. J., Nelson, D. R., Liu, C., and Li, X. Y. (2011) *Virology Journal* **8,**

39. Rato, S., Maia, S., Brito, P. M., Resende, L., Pereira, C. F., Moita, C., Freitas, R. P., Moniz-Pereira, J., Hacohen, N., Moita, L. F., and Goncalves, J. (2010) *Plos One* **5,**

40. Bortz, E., Westera, L., Maamary, J., Steel, J., Albrecht, R. A., Manicassamy, B., Chase, G., Martinez-Sobrido, L., Schwemmle, M., and Garcia-Sastre, A. (2011) *Mbio* **2,**

41. Fauci, A. S. and Morens, D. M. (2012) *New England Journal of Medicine* **366,** 454-461

42. Mizgerd, J. P. (2008) *New England Journal of Medicine* **358,** 716-727

43. Thompson, W. W., Shay, D. K., Weintraub, E., Brammer, L., Cox, N., Anderson, L. J., and Fukuda, K. (2003) *Jama-Journal of the American Medical Association* **289,** 179-186

44. Webster, R. G., Bean, W. J., Gorman, O. T., Chambers, T. M., and Kawaoka, Y. (1992) *Microbiological Reviews* **56,** 152-179

45. McDermott, J. E., Vartanian, K. B., Mitchell, H., Stevens, S. L., Sanfilippo, A., and Stenzel-Poore, M. P. (2012) *Plos One* **7,**

46. Honda, K., Yanai, H., Negishi, H., Asagiri, M., Sato, M., Mizutani, T., Shimada, N., Ohba, Y., Takaoka, A., Yoshida, N., and Taniguchi, T. (2005) *Nature* **434,** 772-777

47. Taniguchi, T., Ogasawara, K., Takaoka, A., and Tanaka, N. (2001) *Annual Review of Immunology* **19,** 623-655

48. Der, S. D., Zhou, A. M., Williams, B. R. G., and Silverman, R. H. (1998) *Proceedings of the National Academy of Sciences of the United States of America* **95,** 15623-15628

49. Honda, K., Yanai, H., Takaoka, A., and Taniguchi, T. (2005) *International Immunology* **17,** 1367-1378

50. Nacken, W., Ehrhardt, C., and Ludwig, S. (2012) *Biological Chemistry* **393,** 525-534

51. Pestka, S. (2007) *Journal of Biological Chemistry* **282,** 20047-20051

52. Shapira, S. D., Gat-Viks, I., Shum, B. O. V., Dricot, A., de Grace, M. M., Wu, L. G., Gupta, P. B., Hao, T., Silver, S. J., Root, D. E., Hill, D. E., Regev, A., and Hacohen, N. (2009) *Cell* **139,** 1255-1267

53. Yang, P. Y., An, H. Z., Liu, X. G., Wen, M. Y., Zheng, Y. Y., Rui, Y. C., and Cao, X. T. (2010) *Nature Immunology* **11,** 487-U50

54. Shahangian, A., Chow, E. K., Tian, X. L., Kang, J. R., Ghaffari, A., Liu, S. Y., Belperio, J. A., Cheng, G. H., and Deng, J. C. (2009) *Journal of Clinical Investigation* **119,** 1910-1920

55. Kayagaki, N., Yamaguchi, N., Nakayama, M., Eto, H., Okumura, K., and Yagita, H. (1999) *Journal of Experimental Medicine* **189,** 1451-1460

56. Li, Q. X., Wang, X., Wu, X. L., Rui, Y. N., Liu, W., Wang, J. F., Wang, X. H., Lion, Y. C., Ye, Z. Y., and Lin, S. C. (2007) *Cancer Research* **67,** 66-74

57. Lee, E., Salic, A., Kruger, R., Heinrich, R., and Kirschner, M. W. (2003) *Plos Biology* **1,** 116-132

58. Li, Z., Yamauchi, Y., Kamakura, M., Murayama, T., Goshima, F., Kimura, H., and Nishiyama, Y. (2012) *Journal of Virology* **86,** 492-503

59. Ulsamer, A., Wei, Y., Kim, K. K., Tan, K., Wheeler, S., Xi, Y., Thies, R. S., and Chapman, H. A. (2012) *Journal of Biological Chemistry* **287,** 5164-5172

60. Garcia-Sastre, A., Durbin, R. K., Zheng, H. Y., Palese, P., Gertner, R., Levy, D. E., and Durbin, J. E. (1998) *Journal of Virology* **72,** 8550-8558

61. Price, G. E., Gaszewska-Mastarlarz, A., and Moskophidis, D. (2000) *Journal of Virology* **74,** 3996-4003

62. Katze, M. G., He, Y. P., and Gale, M. (2002) *Nature Reviews Immunology* **2,** 675-687

63. Lui, T. T. H., Lacroix, C., Ahmed, S. M., Goldenberg, S. J., Leach, C. A., Daulat, A. M., and Angers, S. (2011) *Molecular and Cellular Biology* **31,** 2053-2065

64. Zhang, Y., Liu, S., Mickanin, C., Feng, Y., Charlat, O., Michaud, G. A., Schirle, M., Shi, X., Hild, M., Bauer, A., Myer, V. E., Finan, P. M., Porter, J. A., Huang, S. M., and Cong, F. (2011) *Nature Cell Biology* **13,** 623-U292

65. Kim, M. J., Chia, I. V., and Costantini, F. (2008) *Faseb Journal* **22,** 3785-3794

66. Katze, M. G., Fornek, J. L., Palermo, R. E., Walters, K. A., and Korth, M. J. (2008) *Nature Reviews Immunology* **8,** 644-654

67. Shapira, S. D., Gat-Viks, I., Shum, B. O. V., Dricot, A., de Grace, M. M., Wu, L. G., Gupta, P. B., Hao, T., Silver, S. J., Root, D. E., Hill, D. E., Regev, A., and Hacohen, N. (2009) *Cell* **139,** 1255-1267

68. Emmott, E., Wise, H., Loucaides, E. M., Matthews, D. A., Digard, P., and Hiscox, J. A. (2010) *Journal of Proteome Research* **9,** 5335-5345

69. Marko, M., Leichter, M., Patrinou-Georgoula, M., and Guialis, A. (2010) *Experimental Cell Research* **316,** 390-400

70. Landeras-Bueno, S., Jorba, N., Perez-Cidoncha, M., and Ortin, J. (2011) *Plos Pathogens* **7,**

71. Jorba, N., Juarez, S., Torreira, E., Gastaminza, P., Zamarreno, N., Albar, J. P., and Ortin, J. (2008) *Proteomics* **8,** 2077-2088

72. Arnold, H. K., Zhang, X. L., Daniel, C. J., Tibbitts, D., Escamilla-Powers, J., Farrell, A., Tokarz, S., Morgan, C., and Sears, R. C. (2009) *Embo Journal* **28,** 500-512

CHAPTER V

SUMMARY AND CONCLUSION

As one of the major unmet medical needs and public health priorities, ALI/ARDS is threatening the human lives of around 200,000 patients annually in US. Understanding the key hemostatic, inflammatory, and host defense response in ALI/ARDS is critical for continually reducing its mortality and mobility.

The emerging role of alveolar epithelium in the pathogenesis and resolution of ALI/ARDS has been increasingly appreciated. Loss of alveolar epithelium integrity leads to the increased permeability and influx of protein-rich edema fluid. However, a comprehensive understanding of the mechanism of alveolar epithelium injury involved in ALI/ARDS is still lacking. Developmental signaling such as Wnt/β-catenin signaling has been studied in the resolution and repair stage of ALI/ARDS and dysregulated matrix remodeling during pulmonary fibrosis. This is the first study which identified a new role of Wnt/β-catenin signaling in regulating alveolar epithelium injury in crosstalk with P2X7R-mediated purinergic signaling during the acute phase of ALI/ARDS.

Acute inflammation, thrombosis, and activation of coagulation cascade all contribute to the initiation and exacerbation of ALI/ARDS. However, the detail regulation of proinflammatory cells (neutrophils, monocytes, macrophages, and others) migration, and dysregulation of cells involved in hemostasis and thrombosis (platelets) are still not clear. Here we demonstrate a novel

regulation of neutrophil recruitment by alveolar epithelial cells, which are mediated by ICAM-1 and VCAM-1, controlled by Wnt/β-catenin signaling, and affected by platelets in acute inflammatory phase of ALI. We identified platelet-derived Dkk1 as a key modulator of Wnt/β-catenin signaling in alveolar epithelial cells. We also provided the proof-of-concept results of using Wnt3a or Dkk1 neutralization antibody to reduce neutrophil infiltration and acute inflammation in ALI/ARDS.

Viral lower respiratory tract infection is the most frequent cause of ALI/ARDS. Due to the high mutation rate of influenza virus, drug-resistant strains are continually emerging against conventional antivirals which target viral proteins. Identifying novel host factors with antiviral property can significantly benefit the development of new antiviral drug to limit future pandemic outbreaks. In this study, we reported for the first time that Axin1 boosted type I IFN response to influenza virus infection through the stimulation of JNK/c-Jun and Smad3 signaling. Axin1 and its chemical stabilizer, XAV939, successfully inhibited influenza virus replication and protected mice from influenza virus infection.

In summary, our study on crosstalk of P2X7R-mediated purinergic signaling and Wnt/β-catenin signaling in modulating alveolar epithelium integrity, and platelet-derived Wnt antagonist Dkk1 in ICAM-1/VCAM-1-mediated neutrophil infiltration open new fields in the ALI/ARDS research and provides insights for future drug development. We also identified Axin1 as a new member in the antiviral network of interferon. Novel antiviral approaches can be developed by targeting Axin1-mediated host defense response.

VITA

Yujie Guo

Candidate for the Degree of

Doctor of philosophy

Dissertation: DEVELOPMENTAL SIGNALING AND ACUTE LUNG INJURY

Major Field: Veterinary Biomedical Sciences (Physiology)

Biographical:

Education:

Bachelor of Science in Biosciences, University of Science and Technology of China (USTC), China, Sep. 2002- Jul. 2006

Bachelor of Laws, Southwestern University of Science and Technology, China, Apr. 2010- Jul. 2013

Master of Science in Entrepreneurship, Oklahoma State University (OSU), Jan. 2013- May. 2014

Ph.D: Completed the requirements for Doctor of Philosophy with major in Veterinary Biomedical Sciences (Physiology) at Oklahoma State University, Stillwater, Oklahoma in May, 2014.

Experience:

Junior Research Fellow, USTC, May. 2005- Jun. 2006
Graduate Research Associate, OSU, Aug. 2006- Dec. 2012
Clinical Operations Intern, Altheus Therapeutics, Jun. 2013-Aug. 2013
Intellectual Property Management Intern, OSU, Jan. 2013- present
General Manager, Respiron Therapeutics, Sep. 2013- present

Professional Memberships:

Society for Experimental Biology and Medicine (2009-2010)
American Physiological Society (2009-2011)
American Thoracic Society (2011-2013)
American Association for the Advancement of Science (2007-2013)
Licensing Executives Society (2013-present)
The International Society for Patent Information (2014-present)
The Honor Society of Phi Kappa Phi (2014-present)
The International Honor Society Beta Gamma Sigma (2014-present)